William & Mary
CHARTERED 1693

W&M ScholarWorks

Undergraduate Honors Theses

Theses, Dissertations, & Master Projects

4-2018

Kinematics of Brittle and Ductile Deformation in the Catoctin Formation near Rockfish Gap, Virginia

Katherine Lang

Follow this and additional works at: https://scholarworks.wm.edu/honorstheses

 Part of the Geology Commons, Sedimentology Commons, and the Tectonics and Structure Commons

Recommended Citation

Lang, Katherine, "Kinematics of Brittle and Ductile Deformation in the Catoctin Formation near Rockfish Gap, Virginia" (2018). *Undergraduate Honors Theses.* Paper 1206.
https://scholarworks.wm.edu/honorstheses/1206

This Honors Thesis is brought to you for free and open access by the Theses, Dissertations, & Master Projects at W&M ScholarWorks. It has been accepted for inclusion in Undergraduate Honors Theses by an authorized administrator of W&M ScholarWorks. For more information, please contact scholarworks@wm.edu.

Kinematics of Brittle and Ductile Deformation in the Catoctin Formation near Rockfish Gap, Virginia

A thesis submitted in partial fulfillment of the requirement
for the degree of Bachelor of Science in Geology from
The College of William and Mary

by

Katherine E. Lang

Accepted for Honors
(Honors, High Honors)

Christopher Bailey, Chair

Martin Gallivan

Rebecca Jíron

Williamsburg, VA
April 26, 2018

Kinematics of Brittle and Ductile Deformation in the Catoctin Formation near Rockfish Gap, Virginia

A thesis submitted in partial fulfillment of the requirement
for the degree of Bachelor of Science in Geology from
The College of William and Mary

by

Katherine E. Lang

Williamsburg, Virginia

Table of Contents

List of Figures……3

List of Tables……..5

Abstract……...6

Introduction……..…7
Historical Background……9
Geologic Background……...12

Methods……21
Field Work……..…21
Lab Work…….…..21

Results……...24
Rocks……24
Ductile Features……38
Brittle Features……..……..49
Petrographic Analysis……..52

Discussion……65
Rocks……65
Ductile Features……68
Brittle Features……...……..70
Petrographic Analysis…..……..71

Future Work……..80

Conclusions……...80

Acknowledgements……...82

References……84

List of Figures

Figure 1. Oblique aerial photo of Rockfish Gap……..……..……..……..8

Figure 2. Rockfish Gap Lidar Map……..……..……..……..……8

Figure 3. Virginia Central Railroad Map ……..……..……..……..……11

Figure 4. New and Old Bue Ridge Tunnel portals……..……..……..……11

Figure 5. Current extent map of Catoctin Formation……..……..……..17

Figure 6. Paleogeographic reconstruction of Laurentia……..……..……..18

Figure 7. Stratigraphic column of the western Blue Ridge……..……..……19

Figure 8. Paleogeographic reconstruction of the Catoctin Formation……..20

Figure 9. Oriented hand sample……..……..……..……..……..……..23

Figure 10. Geologic map of Rockfish Gap……..……..……..……..…….24

Figure 11. Generalized cross section of BRT and Scott Mountain……..……25

Figure 12. Sample locations……..……..……..……..……..……26

Figure 13. Geologic map of the Blue Ridge Tunnel……..……..……..……..27

Figure 14. Eastern BRT map……..……..……..……..……..……...28

Figure 15. Catoctin Formation greenstones……..……..……..……..……..29

Figure 16. Eastern portal bulkhead……..……..……..……..……..……30

Figure 17. Overturned bedding in BRT……..……..……..……..……30

Figure 18. Western BRT map……..……..……..……..……..…….32

Figure 19. Conglomerate contact……..……..……..……..……..……33

Figure 20. Bedrock exposure behind brick layers……..……..……..……..34

Figure 21. Purple phyllite in outcrop……..……..……..……..……35

Figure 22. U.S. 250 arksoic sandstone……..……..……..……..……36

Figure 23. U.S. 250 isoclinal fold..……..……..……..……..……..37

Figure 24. Stereogram of foliation……..……..……..……..……...39

Figure 25. Chlorite elongation lineations…….……..……..……..……..40

Figure 26. Flinn Diagram…….……..……..……..……..……41

Figure 27. Low angle shear zone…….……..……..……..……42

Figure 28. Boudinage in the Blue Ridge Tunnel…….……..……..……...43

Figure 29. Boudinage at the 250 outcrop……..……..……..……..……..47

Figure 30. P-t diagram…….……..……..……..……..……48

Figure 31. Rose diagram of fractures…….……..……..……..……50

Figure 32. High density fracture zone…….……..……..……..……...51

Figure 33. Plumose features…….……..……..……..……..……51

Figure 34. Thin sections of 17KL-03…….……..……..……..……53

Figure 35. Thin sections of 17KL-05…….……..……..……..……...55

Figure 36. Thin sections of 17BRT-2…….……..……..……..……..58

Figure 37. Thin sections of WP-10…….……..……..……..……..62

Figure 38. Catoctin flood basalt diagram…….……..……..……..……67

Figure 39. Folds map…….……..……..……..……..……..69

Figure 40. Atitaxial vein development…….……..……..……..……73

Figure 41. Schematic block diagram of Catoctin Formation…….……...74

Figure 42. Catoctin deformation timeline…….……..……..……..……75

Figure 43. Eastern portal entrance…….……..……..……..……...77

Figure 44. Brick test arch in the BRT…….……..……..……..……...78

Figure 45. Western portal limestone cover……..……..……..……...79

List of tables

Table 1. Sample locations, rock type, and density…….…….…….…….23

Abstract

Beneath Rockfish Gap, one of the lowest elevations along the crest of the Blue Ridge Mountains in Virginia, sits the historic 1858 Blue Ridge Tunnel (BRT). The BRT cuts directly through foliated metabasalts and metasedimentary rocks of the Ediacaran Catoctin Formation and provides a rare 3-dimensional exposure of the Blue Ridge cover sequence on the western limb of the Blue Ridge Anticlinorium. The purpose of this study is to characterize brittle and ductile deformation features in the Catoctin Formation in the BRT to determine their kinematic history. The Catoctin Formation includes a thick sequence of metabasaltic greenstone with thin layers of meta-arkose, sandstone, phyllite and conglomerates that formed between 570-550 Ma. In the arkoses and conglomerates, quartz and perthitic feldspars are the dominant clasts and are typically surrounded by a sericite matrix. Foliation strikes to the NE and dips moderately to the SE with down dip chlorite elongation lineations. Large (1 - 10 m) epidote-rich sandstone boudins typically display top-to-the NW asymmetry. Small, localized folds also occur in the sedimentary units and are tight, overturned NW-verging folds, consistent with NW-directed Neoacadian ductile deformation. Foliation in the greenstone is cut by low-angle top-to-the west shear zones that likely represent the later stages of deformation. Petrographic analysis reveals microstructures formed from dissolution, mass transfer, and volume loss processes under lower greenschist facies conditions. Mineral assemblages indicate that the Catoctin Formation at Rockfish Gap experienced temperatures between 300ºC - 400ºC. The Catoctin Formation is cut by two dominant fracture sets, a WNW-ESE set and NE-SW set that formed from two separate brittle deformation events; the former from the late Alleghanian Orogeny, and the latter from Atlantic rifting in the early Mesozoic.

Introduction (1)

Located at one of the lowest elevations along the crest of the Blue Ridge Mountains, Rockfish Gap is at the intersection of U.S Route 250, the Skyline Drive, and Interstate-64 (Figure 1). Underneath Rockfish Gap, the historic Blue Ridge Tunnel (BRT) from the mid-19th century cuts directly into the metabasalts of the Ediacaran Catoctin Formation. The tunnel is 1,302 m long and forms a straight NW-SE line from Nelson County and Augusta County in Virginia under Rockfish Gap (Figure 2). The BRT was labeled a Historic Civil Engineering Landmark in 1976, partly because it was the longest tunnel in America upon its completion in the late 1850s, but also because the BRT was a monumental engineering project for its time (Lyons, 2014).

Previous geologic research in the area conducted by Gathright et al. (1977) briefly mentions that the BRT is an excellent exposure of the Catoctin Formation. Other studies of the Rockfish Gap area (Dilliard et al., 1999) did not use the BRT as a study site to understand the rock types and geologic structures characteristic of the Catoctin Formation. While mostly greenstones, the Catoctin Formation lithology also includes metasedimentary units that were examined in the field and in thin section to better understand the structure of the Catoctin Formation in the study site. Because the BRT provides an unusual exposure of the formation, this study aims to identify and describe the geologic units, characterize both brittle and ductile deformation features, and interpret the local and regional kinematics, while illustrating the need for continued preservation of the BRT. Coupled with the lack of erosion and mass wasting inside the BRT and special access to the tunnel, this study was able to obtain structural measurements and collect samples otherwise unavailable to those who have investigated the Catoctin Formation before.

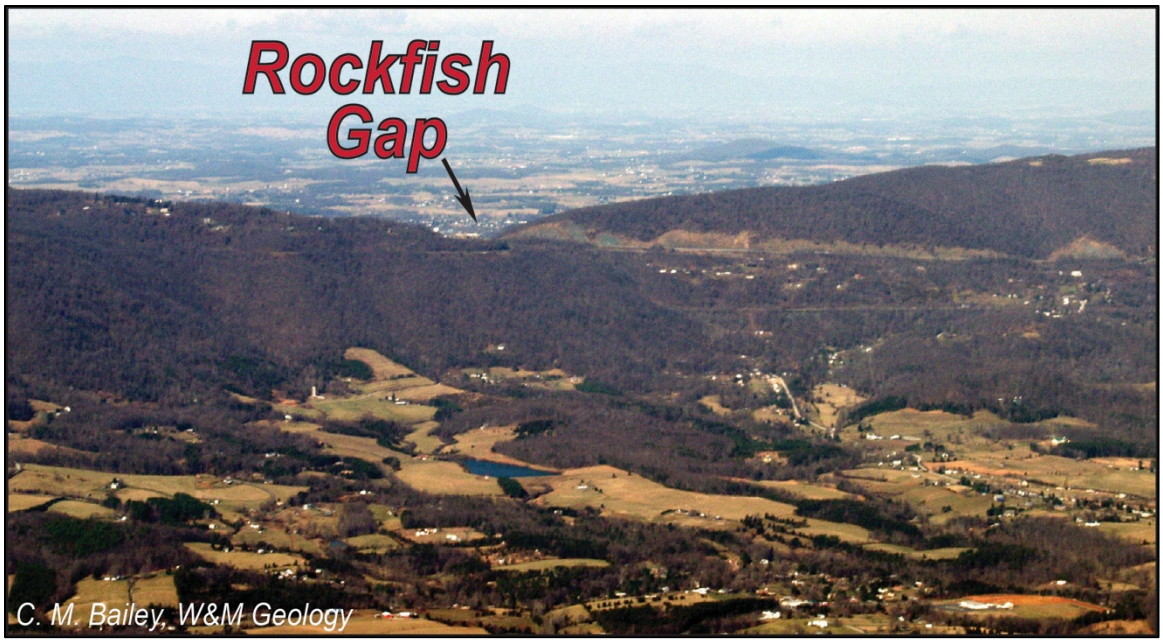

Figure 1. *Oblique aerial photograph of Rockfish Gap and the crest of the Blue Ridge Mountains as viewed from the south-southeast. Shenandoah Valley is in the background.*

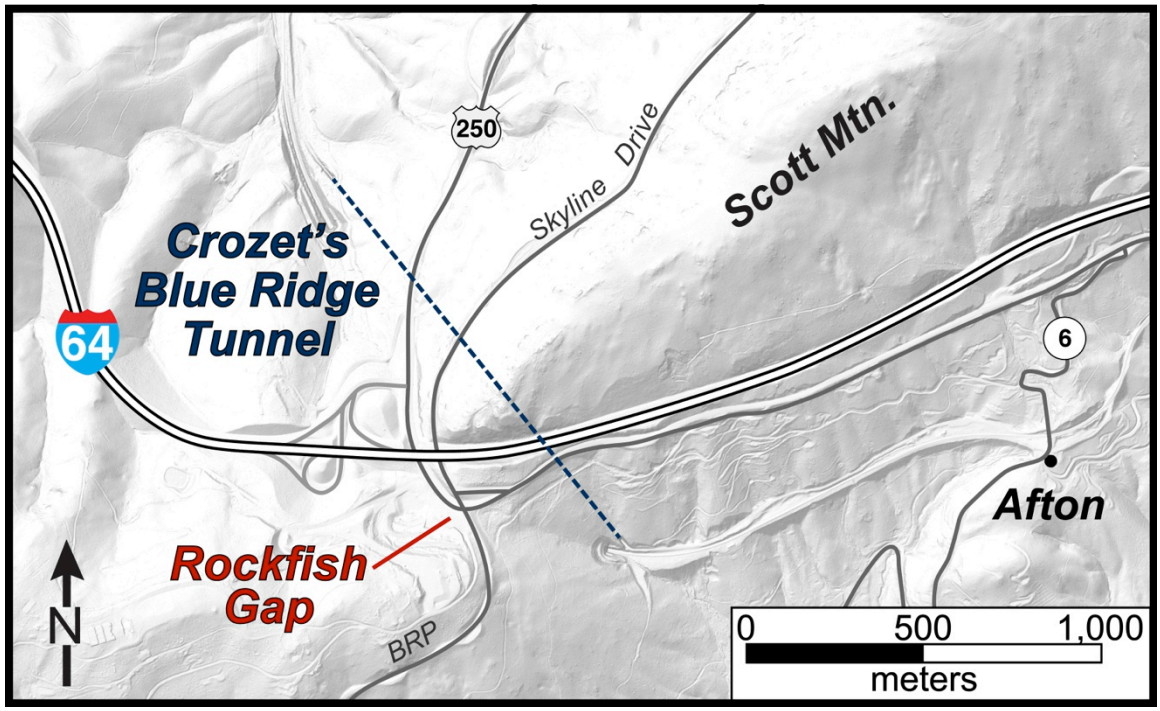

Figure 2. *Shaded relief map of Rockfish Gap based on LIDAR data. Pixel size is 0.75 m by 0.75 m. Illumination direction from the northwest.*

Historical Background (1.1)

Since the early 19th Century, Rockfish Gap has been a nexus for both people and goods crossing over the crest of the Blue Ridge Mountains. As early as 1818, there was a carriage road that crossed the gap. However, the state realized that in order to connect the western areas of the state to the east, a faster means of transportation was required. By the 1830s, it was clear that the Rockfish Gap area would provide an optimal place for a crossing; thus, the idea for a tunnel underneath the gap started to form.

Claudius Crozet was a Frenchman who was an engineering graduate of the École Polytechnique in Paris and was the engineer chosen by the Commonwealth of Virginia to work on the Virginia Central Railroad (eventually the Chesapeake and Ohio Railway) tunnel plans. As an advocate for the incipient railroad technology sweeping across the United States as early as the 1830s, Crozet was appointed as the Chief Engineer for Virginia's Board of Public Works (Blue Ridge Tunnel Foundation, 2017). However, it wasn't until 1850 that work on the BRT officially commenced. Immigrant Irish workers and a few African-American slaves were the main labor force that built this tunnel (Lyons, 2014). Construction was treacherous because the workers only had black powder and hand tools to blast away the hard rocks as the invention of dynamite would only come a few years after tunnel completion. Crozet expected the BRT to be completed by 1853, but due to the general hardness of these rocks, progress was slow, and lasted until 1858 (Blue Ridge Tunnel Foundation, 2017). This year, the BRT turned 160 years old and still retains its structural integrity.

The BRT was a crucial piece of the Virginia Central Railroad (Figure 3) that planned to provide railroad access from Richmond, Virginia, to the Ohio River (Blue

Ridge Tunnel Foundation, 2017). In the early to mid 19th century, the Ohio River was Virginia's westernmost boundary, so transporting goods across the hundreds of miles became more manageable with a rail line that could connect the entire state. In the early stages of the Civil War, Stonewall Jackson and his Confederate army eventually used the new Blue Ridge Tunnel to their advantage. During Jackson's famous 1862 Shenandoah Valley campaign, Jackson's forces boarded the Virginia Central Railroad at the Mechum's River Station and used the fledgling Blue Ridge Tunnel to emerge on the west side of the Blue Ridge Mountains en-route to the battle of McDowell in the Allegheny Mountains (Virginia Department of Historic Resources, 2016).

During World War II, the original Blue Ridge Tunnel was replaced by a new lower grade tunnel that was able to accommodate the longer, contemporary trains that the war demanded (the original BRT has a grade of 21m/km) (Figure 4). In the 1950s, plans were made to store natural gas in the out-of-use BRT, and two concrete bulkheads were fashioned to create storage space in the center of the tunnel; however, natural gas was never stored in the tunnel despite the bulkheads. These concrete slabs enclose over ⅓ of the BRT, and this central section is only accessible through two 2½ foot wide by 20 ft long metal tubes on both sides. Currently, Nelson and Augusta counties are endeavoring to turn the abandoned BRT underneath Rockfish Gap into a public recreational trail such that future generations can enjoy this historic site. Yet due to this tunnel revitalization, concrete may be poured onto the walls of the BRT in order to facilitate development of a public trail. This study aims to illustrate the geologic features and describe the integrity of the BRT in order to prevent the loss of geologic capital for future generations of geologists and historians.

Figure 3. *Map of the Virginia Central Railroad from the 1850s illustrating the route connecting Virginia to western Virginia. Image from the Library of Congress archives: https://www.loc.gov/resource/g3881p.rr006010/.*

Figure 4. *Eastern portals of the new and old Blue Ridge Tunnels, respectively. Photograph from 1968. Image from the Library of Congress archives: https://www.loc.gov/item/va0254/.*

Geologic Background (1.2)

The Catoctin Formation is a widespread unit in the central Appalachians (Figure 5), and comprises part of the Blue Ridge Anticlinorium, a regional scale fold breached by erosion (Reed, 1955; Gathright et al., 1977). A suite of Grenvillian granitoids of the basement complex are exposed at the center of the anticlinorium (Badger and Sinha, 1988; Johnson et al., 2014) and the rocks of the Catoctin Formation are exposed on the outside of the granitic interior, as they are younger than the Mesoproterozoic basement complex. In the stratigraphic sequences on both the eastern and western limbs of the anticlinorium, the Catoctin Formation serves as a time-marker unit due to its characteristic green color throughout its large lateral extent (Bailey et al., 2017a). The formation extends from Pennsylvania to Virginia and was first described by Keith (1894) from exposures on Catoctin Mountain in Maryland. Effectively, the Blue Ridge province forms a large basement massif at the hinterland edge of the foreland fold-and-thrust belt (Bailey et al., 2007).

Eastern Laurentia experienced two distinct phases of Neoproterozoic rifting: the first, an unsuccessful event in the Cryogenian period between 680 Ma to 765 Ma (Aleinikoff et al., 1995; Tollo et al., 2004) and a later, second event from 550 Ma to 570 Ma that led to the opening of the Iapetus Ocean and the breakup of the Rodinian supercontinent (Rankin, 1975; Badger and Sinha, 1988; Simpson and Eriksson, 1989; Aleinikoff et al., 1995; Tollo and Aleinikoff, 1996; Dilliard et al., 1999; Laskowski, 2010). This development of Ediacaran rifting created a southeast-facing passive margin (Badger and Sinha, 1988; Aleinikoff et al., 1995; Simpson and Eriksson 1989). Thus, the Catoctin Formation formed either as a series of continental flood basalts associated with the second rifting event or as a result of a mantle plume emplacing

large amounts of basalt onto the surface (Johnson and Bailey, 2013). During this period of rifting, the basalt of the Catoctin Formation was extruded on the Laurentian margin in both subaerial and subaqueous settings (Figure 6) (Reed 1955; Badger, 1986).

Previous geochronologic studies further confirm that these flood basalts were extruded during the Ediacaran period. Badger and Sinha (1988) report a Rb-Sr age of 570 ± 36 Ma, whereas the U-Pb zircon ages from Aleinikoff et al. (1995) reported a 564 ± 9 Ma date with far more precision than Badger and Sinha's Rb-Sr values. Southworth et al. (2009) obtained 3 U-Pb zircon ages to further that age of the Catoctin Formation. The uncertainty decreased for these three most recent U-Pb zircon ages and reported 568 ± 4 Ma, 559 ± 5 Ma, and 555 ± 4 Ma (Southworth et al., 2009).

The basaltic rocks of the Catoctin Formation are a series of volcanic flows, and have been separated into individual flow events (Badger et al., 2010). The basalts were extruded over an area of (>30,000 km^2) and were created from mantle-derived tholeiitic magmas (Badger and Sinha 2004, Johnson et al., 2013; Johnson et al., 2014). The original thickness of the formation was estimated to be 3 km on the eastern Blue Ridge, whereas in the western Blue Ridge it ranges from 400 to 900 m thick as it thins towards the west and southwest (King, 1950; Gathright, 1976; Espenshade, 1986; Reed and Clarke 1989; Johnson et al., 2014). Intrusions of metadiabse dikes of similar composition to the metavolcanics of the Catoctin Formation likely acted as feeder dikes for the overlying Catoctin strata (Figure 7) (Marshall et al., 2014; Bailey et al., 2017b). A paleogeographic reconstruction by Johnson and Bailey (2013) proposes that these basalts were extruded tens of km to the east of where they currently crop out, making the current Catoctin Formation allochthonous (Figure 8). This reconstruction was designed by recreating the original thickness and returning the folded and faulted

units to a horizontal and non-transported position.

The Catoctin Formation is interlayered with clastic rocks at many locations, and displays contact geometry that is consistent with a coeval relationship of the underlying Neoproterozoic Swift Run Formation and the lower member of the Catoctin Formation (King, 1950; Gattuso et al., 2009). The siliciclastic Cambrian Chilhowee Group unconformably overlies these metabasalts (Gathright et al, 1977; Bailey et al., 2017b). Layers of metasedimentary rocks such as phyllite, quartzite, and marble, along with volcanic breccia occur within the Catoctin Formation (Gathright, 1976; Dilliard et al., 1999; Southworth et al., 2009). The dominant lithology of this formation ranges from chlorite-epidote-albite greenstone to actinolite-epidote-chlorite-albite greenstone (Gathright et al., 1977).

Dilliard et al. (1999) examined the metasedimentary layers of the Catoctin Formation on the western Blue Ridge near Rockfish Gap and found that the sedimentary member subdivided the Catoctin Formation into lower and upper members. The lower member consists mostly of basalt and some clastic sedimentary rocks, while the upper member is mostly dominated by just basalts (Dilliard et al., 1999). The two unit members record hyperconcentrated flow deposits: sheet elements (SE) and channel elements (CE). From these sedimentary elements, the Catoctin rift basin was originally filled in by three separate phases, which include: 1) lower Catoctin Formation - basalt encasing channel elements; 2) middle sedimentary member - sheet elements with interbedded minor basalts followed by; 3) upper Catoctin Formation - basalt with little or no sediments interbedded (Dilliard et al., 1999). According to their study, these three phases were controlled by the effect of variations in effusive rate, clastic supply, and subsidence. Massive sandstones and conglomerates represent the dominant facies of the hyperconcentrated flows, while

other additional facies are the byproduct of normal stream flows and thus the subsiding of the hyperconcentrated flows (Dilliard et al., 1999). However, Dilliard et al. (1999) failed to discuss the source or provenance of the sedimentary layers, which is vital in understanding the significance of the sedimentary units in a kinematic context.

The timing of metamorphism and deformation for the Catoctin Formation has long been contested. Previous studies have argued that metamorphism of the basalts into greenstones occurred during the mid-to-late Paleozoic, or during the Carboniferous (Sinha and Zeitz, 1982; Badger and Sinha, 1988). However, more recent work has refined these early attempts. Regional deformation and metamorphism in the western Blue Ridge occured prior to the Alleghanian Orogeny (330-275 Ma) (Bailey et al., 2006; Baliey et al., 2007). White mica 40Ar/39Ar cooling ages for the western Blue Ridge rocks range from 355 to 315 Ma, and reflects Acadian to Neoacadian regional deformation and metamorphism (Wooten et al., 2005; Bailey et al., 2007; Jenkins et al., 2012). The Neoproterozoic and Cambrian cover sequence of the western Blue Ridge never reached temperatures over 400º C, and further evaluation of metamorphic mineral assemblages, geothermometry, and diagnostic microstructures indicate that the penetrative foliations and folds developed during the later Devonian to the Pennsylvanian (Bailey et al., 2007). Deformation from this event produced the penetrative and prominent SE dipping foliation in all Blue Ridge rocks (Wooten et al., 2005; Bailey et al., 2007; Jenkins et al., 2012; Burton et al., 2015). The mineral assemblages in the Catoctin greenstones are evidence of greenschist facies metamorphism (Badger and Sinha, 1988; Reed and Clarke, 1989; Evans, 1994; Wooten et al., 2005). A kinematic analysis of nearby mylonites in the Blue Ridge determined that the region experienced a top-to-the-NW ductile shear during regional

NW-to-SE crustal shortening (Bailey and Simpson, 1993).

The regional scale structure of the Blue Ridge Anticlinorium was developed during the later stages of the Neoacadian Orogeny, with much of the Blue Ridge sequence being thrust up a tectonic ramp from east to west over the Cambrian and Ordovician sedimentary rocks of what is now the Valley and Ridge during the Paleozoic (Evans, 1989). This tectonic transport of the Blue Ridge massif emplacement over the sedimentary rocks of the Valley and Ridge province along a brittle fault system that over cuts the ductile penetrative fabrics likely occurred during the late Alleghanian (305- 280 Ma) (Aleinikoff et al., 1995; Bailey et al., 2007).

In the Triassic, at the onset of the Atlantic rifting, normal faulting occurred approximately from 200-180 Ma during the early Mesozoic, and several half-graben complexes or rift basins developed east of the western Blue Ridge (Southworth et al., 2009). The intrusion of the diabase dikes in the Triassic is also associated with this Atlantic rifting (Southworth et al., 2009; Bailey et al., 2017b). Towards the end of the Mesozoic and beginning of the Cenozoic, there was thermal subsidence and the entire area became the passive margin that characterizes the area today as the Atlantic Ocean was created (Bailey et al., 2017b).

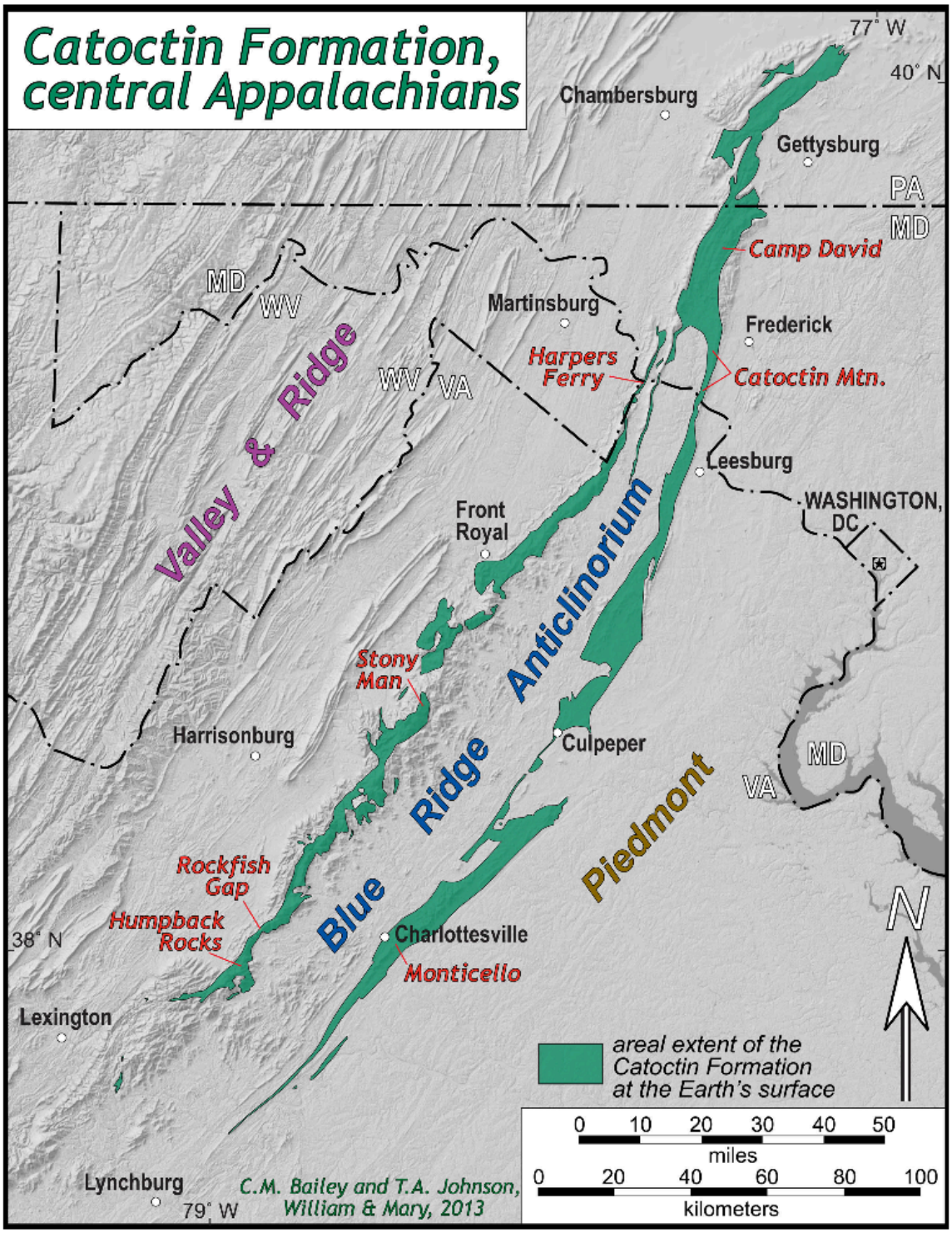

Figure 5. *Geologic map of the Catoctin Formation in the central Appalachians. Green areas show the distribution of the formation compared to the older granitic basement complex in the center of the Blue Ridge Anticlinorium. Area of interest for this study is at Rockfish Gap. From Bailey and Johnson (2013).*

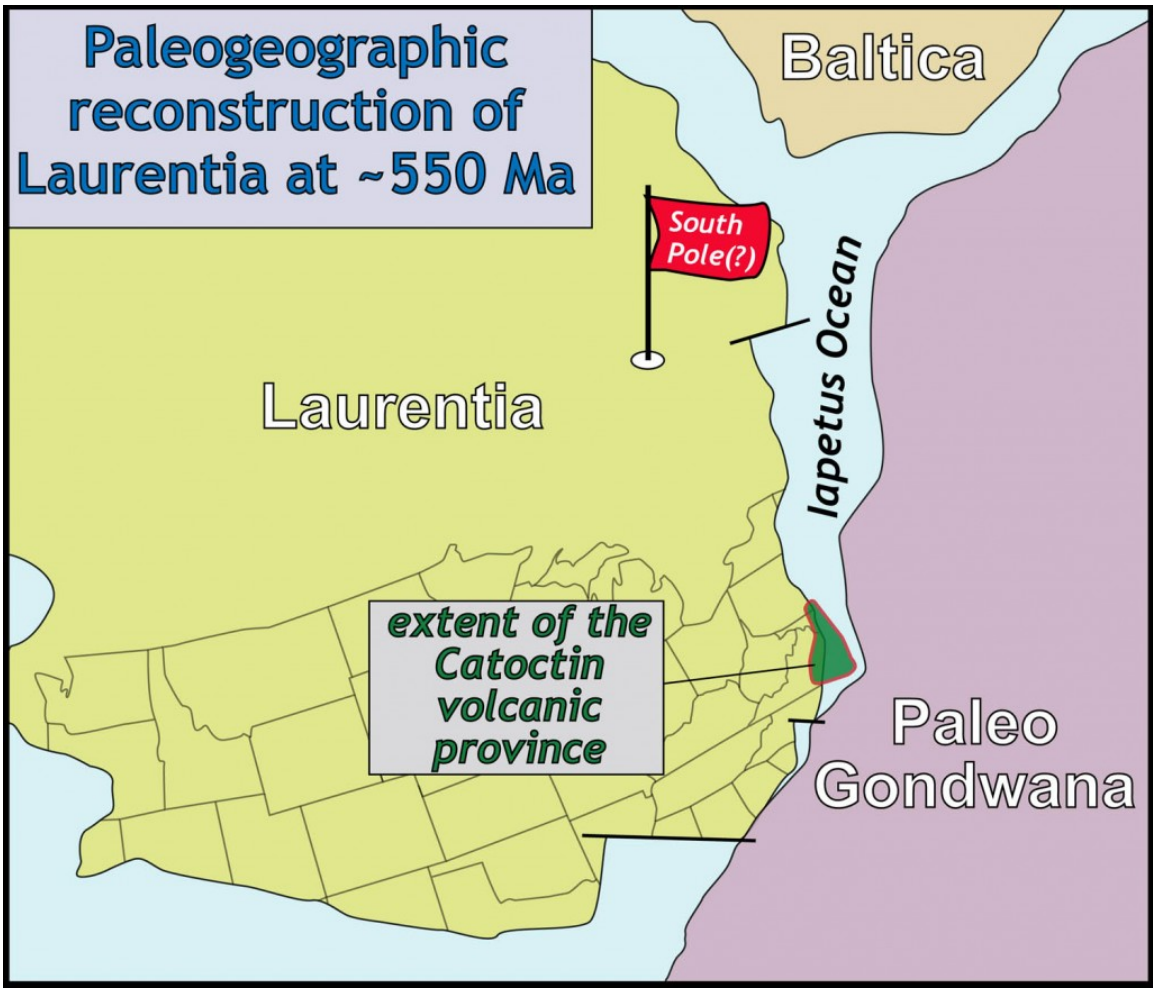

Figure 6. *Paleogeographic reconstruction of Laurentia around 550 Ma from Bailey and Johnson (2013).*

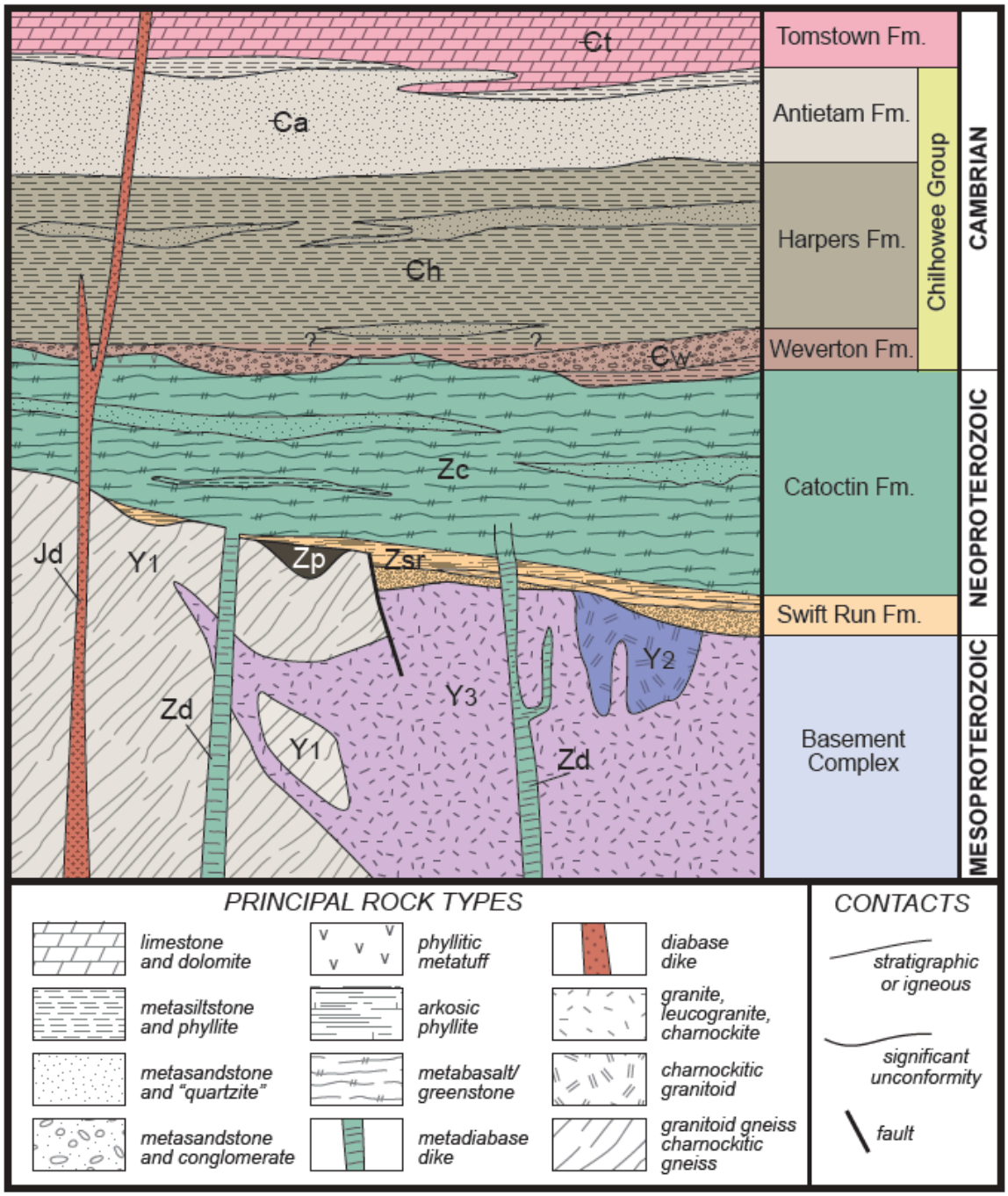

Figure 7. *Stratigraphic column of the western Blue Ridge which illustrates the basement complex, Neoproterozoic, and Cambrain cover sequences of the classic rift-to-drift sequence from the Ediacaran period. Note the Catoctin Formation feeder dikes that intrude both the younger suite of Grenvillian granites and the older suite of granitoids. From Southworth et al. (2009).*

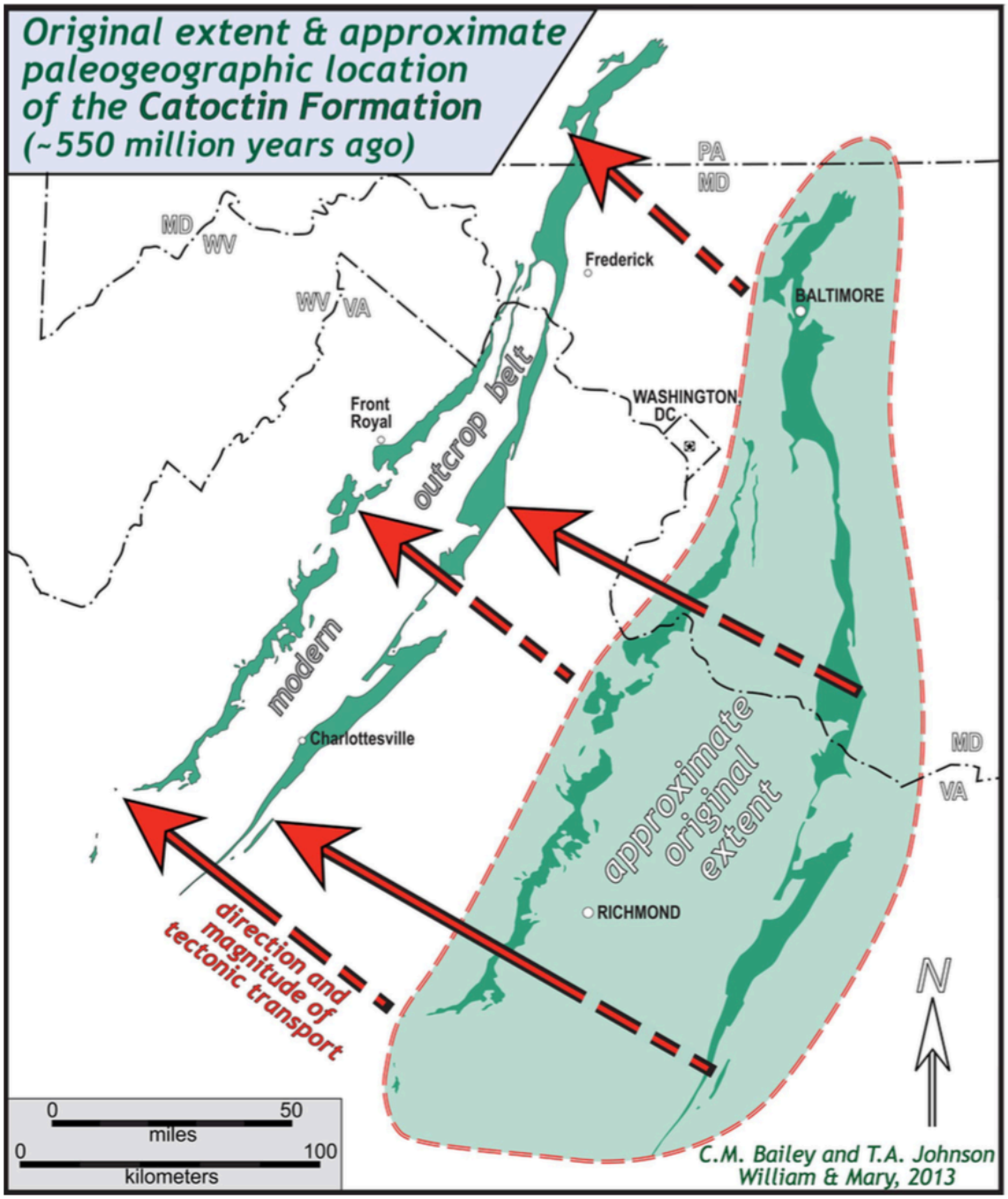

Figure 8. *Extent and paleogeographic location of the Catoctin Formation upon extrusion at ~550 Ma superimposed onto modern topography. Tectonic transport direction to the northwest.*

Methods (2)

This study utilized both field and laboratory methods, including field mapping at multiple scales, field observations, petrological analysis, and structural measurements to answer the kinematic research questions. Two main areas were the focus of this study: 1) Rockfish Gap at road cuts along U.S. Route 250, and 2) in and near the Blue Ridge Tunnel underneath Scott Mountain and Rockfish Gap. Sections outside the tunnel along the expanse of the original and modern railroad tracks were utilized to bolster the data, as well as to record orientation of the fractures, foliation, and elongation lineations in multiple areas. Geologic field mapping was conducted in detail in order to delineate the contacts between the metasedimentary units and the metabasalts of the Catoctin Formation. Field data were taken over multiple trips to the study sites. Rock type, primary and secondary rock structures, and relative location were noted while in the field. The lithology was determined by color, mineralogy, grain size, texture, and weathering. Structural measurements include the orientation of fractures, foliation, elongation lineations, and bedding indicators in addition to shear zones and boudinage as kinematic indicators.

Field Work (2.1)

A total of 8 oriented and non-oriented samples were collected during field work: from the western portal of the BRT, from the inside the concrete bulkheads of the BRT, from the Eastern Portal of the BRT, and the roadcut along U.S. Route 250 (Figure 9). All samples except 17BRT-2 were oriented in the field.

Lab Work (2.2)

Four samples (17BRT-2, WP-10, 17KL-03, and 17KL-05) were prepared for cutting, and a single thin section chip was created to examine the mineralogy for each sample.

Sections were cut in three orientations: foliation-parallel lineation-parallel, foliation-normal lineation-normal, and foliation-normal and lineation-parallel. Sample 17BRT-5 was the only sample to be cut in the three directions, while the other samples varied in the orientation of cuts. All thin sections had coverslips applied for standard petrographic analysis. Density measurements of samples were also conducted in order to determine the differences between the metasedimentary units within the Catoctin Formation for five of the eight samples.

After preparation, thin sections were analyzed for mineralogy using the Olympus BH-2 petrographic microscope. Mineralogy and texture were determined first, as well as mineral shape. Microstructures such as undulose extinction, albite twinning, pressure shadows, and stylolites were closely noted to infer metamorphic conditions, as well as the mineral assemblages of each sample. Digital images of entire thin sections were created using the Nikon Super Coolscan 4000, with each section in XPL and PPL.

Over 150 structural measurements were collected in the field from fractures, foliations, elongation lineations, slickenlines, and faults. I utilized Stereonet (Version 9.9.5) to create stereographic representations of the orientation measurements for the foliation, fractures, and elongation lineations. Foliation orientation data was represented using poles to the foliation, and contoured using a Kamb contour based upon standard deviations. A mean vector for the poles was used to calculate the mean foliation and fracture orientations for the rocks at Rockfish Gap and the BRT. Down-dip elongation lineations of chlorite blebs were plotted onto the foliation stereogram. Aspect ratios from the lineations were measured and plotted upon a Flinn Diagram to determine the type of strain the rocks underwent. Fracture orientations were also plotted onto the Stereonet program, but I represented fractures on both a stereogram,

illustrating poles to the fracture plane, as well as a rose diagram. The data were separated by 10º bins on the rose diagram and a total area circle outline was added to illustrate the dispersal of data on the plot. Faultkin (Version 7.7.1) was used to identify P and T axes and slip direction for the faults in one of the epoditized boudins at the U.S Route 250 outcrop.

Figure 9. *Oriented hand sample 17KL-03 from the road cut along U.S. Route 250.*

Sample Name	Sample Location (UTM Zone 17S)	Rock Type	Density (g/cm^3)
17BRT-2	687732 E 4212014 N	Meta arkosic wacke with feldspar, quartz veins and slickenlines	2.7
17KL-03	687839 E 4211690 N	Meta-arkose with thinly laminated beds of opaque minerals, feldspar, quartz veins	2.6
17KL-05	687553 E 4212390 N	Schistose phyllite with large amounts of opaques and purple hematite staining	3.0
WP-10	687713 E 4212342 N	Metabasalt from a low angle shear zone with elongated chlorite blebs and epidote	2.7

Table 1. *Table showing sample locations, rock type, and density of the four samples that also have thin sections.*

Results (3)

Rocks (3.1)

A geologic map of the Rockfish Gap area was produced by this study in order to identify the rock types within the BRT and at the U.S. 250 road cut (Figure 10). Based off of the Gathright et al. (1977) Waynesboro East 7.5 Quadrangle map, this study includes the Chesapeake and Ohio Railway tracks that delineate the path of the BRT tracks. Because the BRT is cut into Scott Mountain (Figure 11), this study was better able to understand the geology and kinematics of the Catoctin Formation.

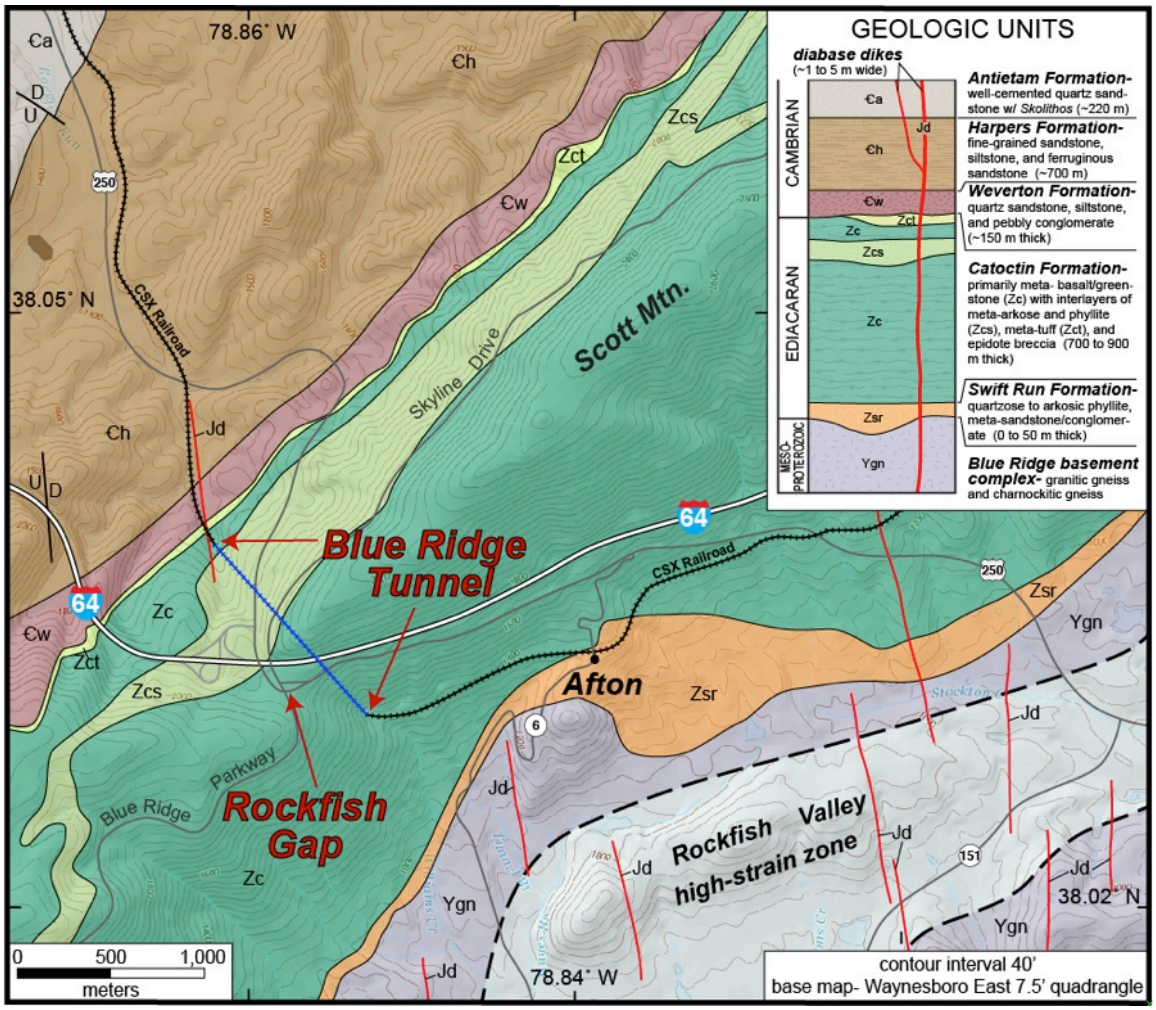

Figure 10. *Geologic map of the Rockfish Gap area. Red arrows show the entrances to the BRT, while the blue line represents the path of the tunnel. Note the metabasalts (Zc) crop out on the eastern portal entrance, while the meta-arkose and phyllite (Zcs) crop out at the western portal entrance. Modified from Gathright et al. (1977) and Bailey et al. (2017a).*

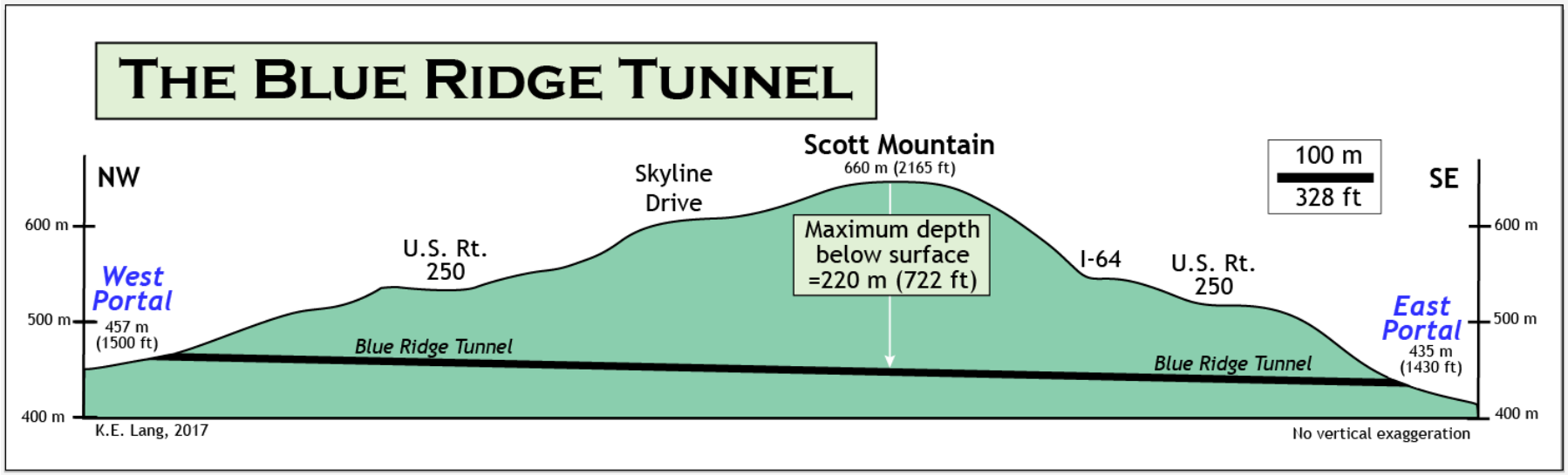

Figure 11. *Generalized cross section of Scott Mountain including the Blue Ridge Tunnel. Note slight grade of the tunnel path (70 ft/mi or 20 m/1.6 km).*

The samples collected for this study were collected from where the Catoctin Formation was exposed near the Rockfish Gap area. Locations for the 8 individual samples collected during field work and their position within the metasedimentary units (Zcs, Zct) or the metabasalt unit (Zc) were placed onto a location map (Figure 12). For a more in depth look at the BRT and the geology within this landmark, I created a separate map that plots sample locations, lithology, structural features, and brick layers inside the main section of the BRT (Figure 13).

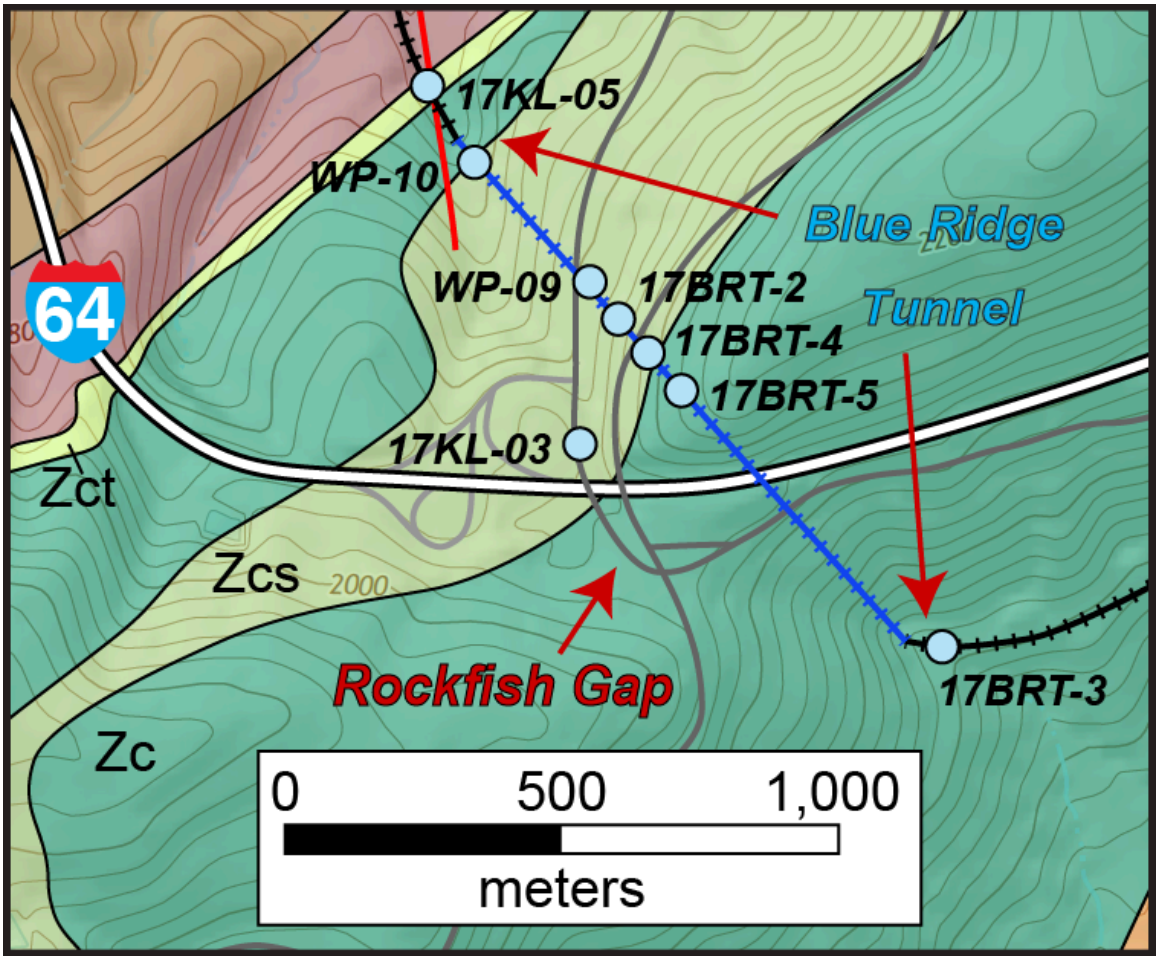

Figure 12. *Sample locations for this study in the Rockfish Gap area; all samples except for 17BRT-3 and 17BRT-5 were collected from within the metasedimentary layers (Zcs and Zct). Map is modified off of the Gathright et al. (1977) Waynesboro East 7.5' quadrangle, but adapted from Bailey et al. (2017b).*

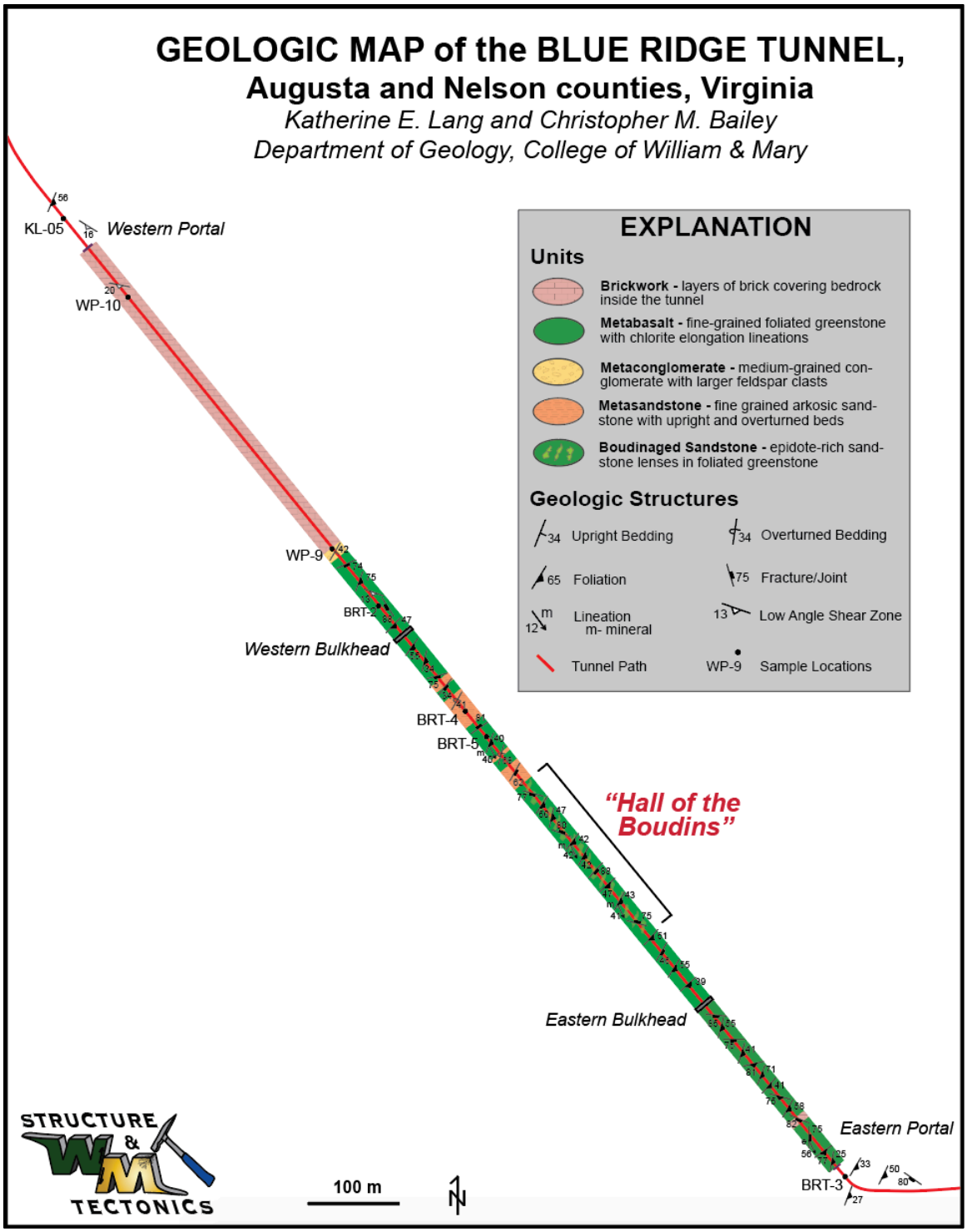

Figure 13. Detailed geologic map of the BRT. Structure symbols and lithology are delineated down to 2 m of resolution. Pale red areas represent the places where bricks are covering the bedrock walls. Base plan of tunnel path (represented by red line) was from a current engineering plan of the BRT.

Samples 17BRT-3 and 17BRT-5 from the eastern side of the BRT (Figure 14) are typical of the greenstone lithology of the Catoctin Formation. Both are denser, well-foliated, dark green fine-grained metabasalts (Table 1) (Figure 15). Elongated chlorite lineations trend down dip of the foliation. Hand sample 17BRT-3 came from a fault surface just before the entrance to the eastern portal, is less foliated, and contains fewer chlorite blebs in the overall sample in comparison to 17BRT-5. Rare clasts of large potassium feldspar and jasper grains do occur in 17BRT-5.

Both 17BRT-5 and 17BRT-4 are located inside the concrete bulkheads that encase about ⅓ of the BRT (Figure 16). BRT-4 is a dark gray, fine-to medium grained meta-arkosic wacke with darker clasts of rock that are visible in hand sample. Bedding indicators from the sedimentary layer in which BRT-4 originates from suggests that this layer is stratigraphically overturned. The overturned bedding layers from this particular sedimentary section dip 41° to the SE. The thinner, overturned sedimentary section to the southeast dips more steeply at 68° and is finer grained than the section of BRT-4 (Figure 17).

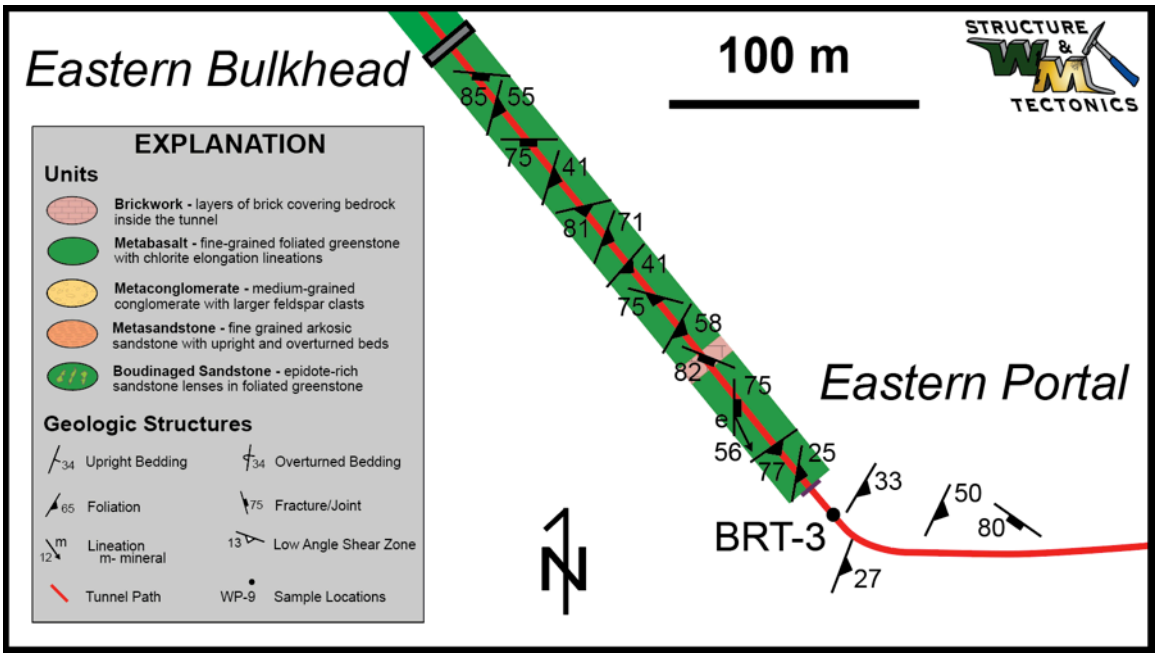

Figure 14. Zoomed in figure of the eastern portal. Red line shows the path of the old BRT train tracks. Lithology is horizontally extended out for visual representation.

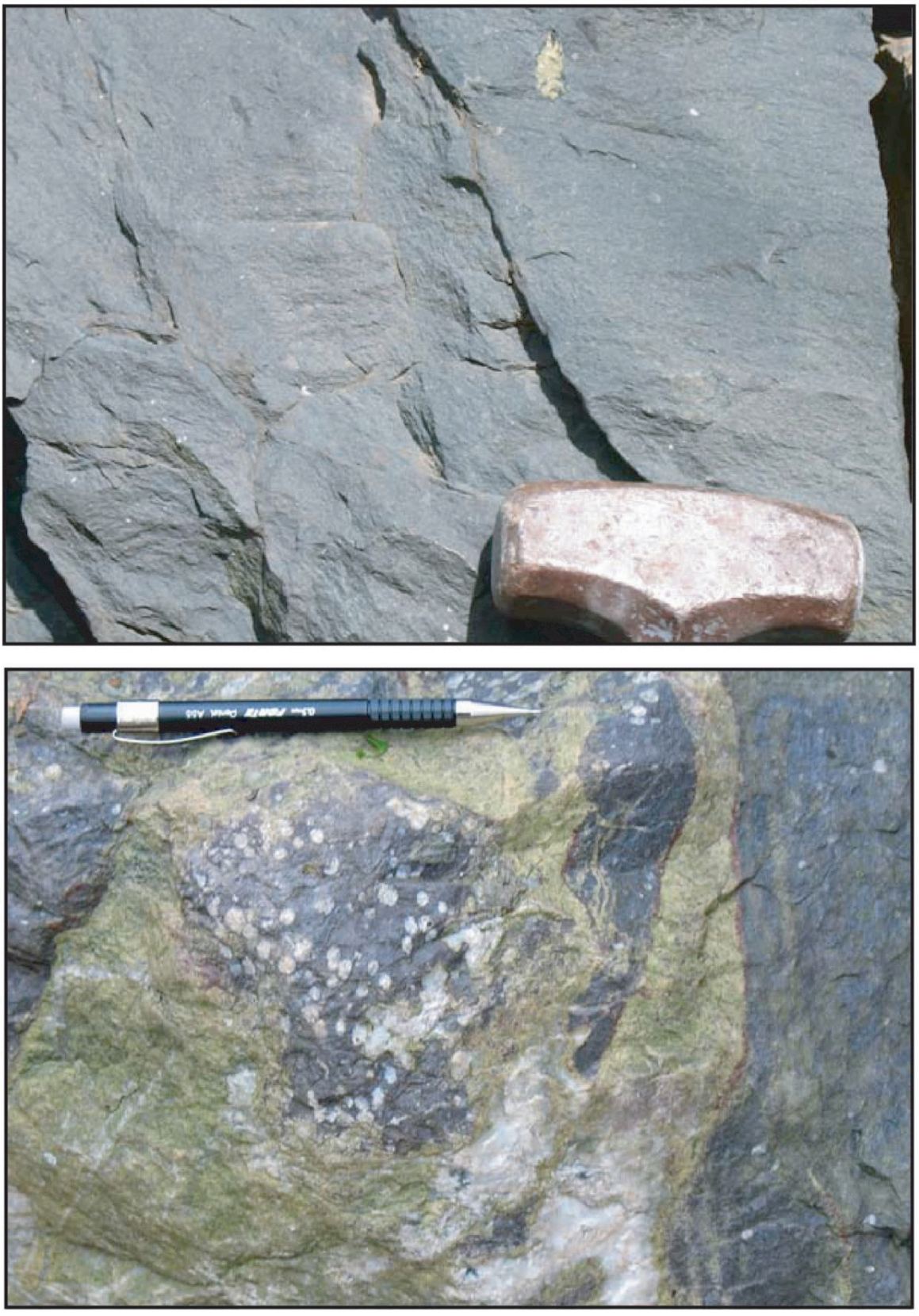

Figure 15. *Typical rocks in the Catoctin Formation. Above, a typical fine-grained, foliated metabasalt. Below, epidote and quartz veins in the greenstone, with amygdules.*

Figure 16. *View from the eastern portal of the Blue Ridge Tunnel looking towards the concrete bulkhead 750 feet (230 m) inside the entrance. Note the water on the tunnel floor and the tube that provides the only access to the middle of the tunnel.*

Figure 17. *Overturned bedding in the metasandstone south-east of sample 17BRT-4 in the center of the BRT. Right way up illustrated by white arrow. Hand for scale.*

On the western portal side, sample 17BRT-2 lacks context because it was not in its original position within the formation, but rather was lying on the floor of the BRT. Despite this lack of spatial data, the sample itself is a fine-grained meta-arkosic wacke, and is light green to gray-green in color. Cut by two K-feldspar veins that trend parallel to one another, clasts of quartz and perthitic-feldspar are surrounded by a sericite matrix. A secondary feature of this rock includes slickenlines on the outer surface of the hand sample.

Further on the western side, much of the BRT is sheathed in 3 to 4 layers of a brick facade (Figure 18). This bricked section correlates to a section of the thicker sequence of meta-sedimentary units (Zcs) of the Catoctin Formation on the Gathright et al. (1977) map. Sample WP-9 was collected on the boundary where the 300 m (1,000 ft) brick arch begins and extends to the opening of the western portal (Figure 19). Gray-blue to green to purple in color, sample WP-9 has 3 separate stratigraphic layers; the bottom and top layers are thinly-laminated green and purple layers of fine-grained arkosic sandstone, whereas the middle layer is a medium- to coarse-grained conglomerate with large blue and gray quartz clasts and pink potassium feldspar clasts.

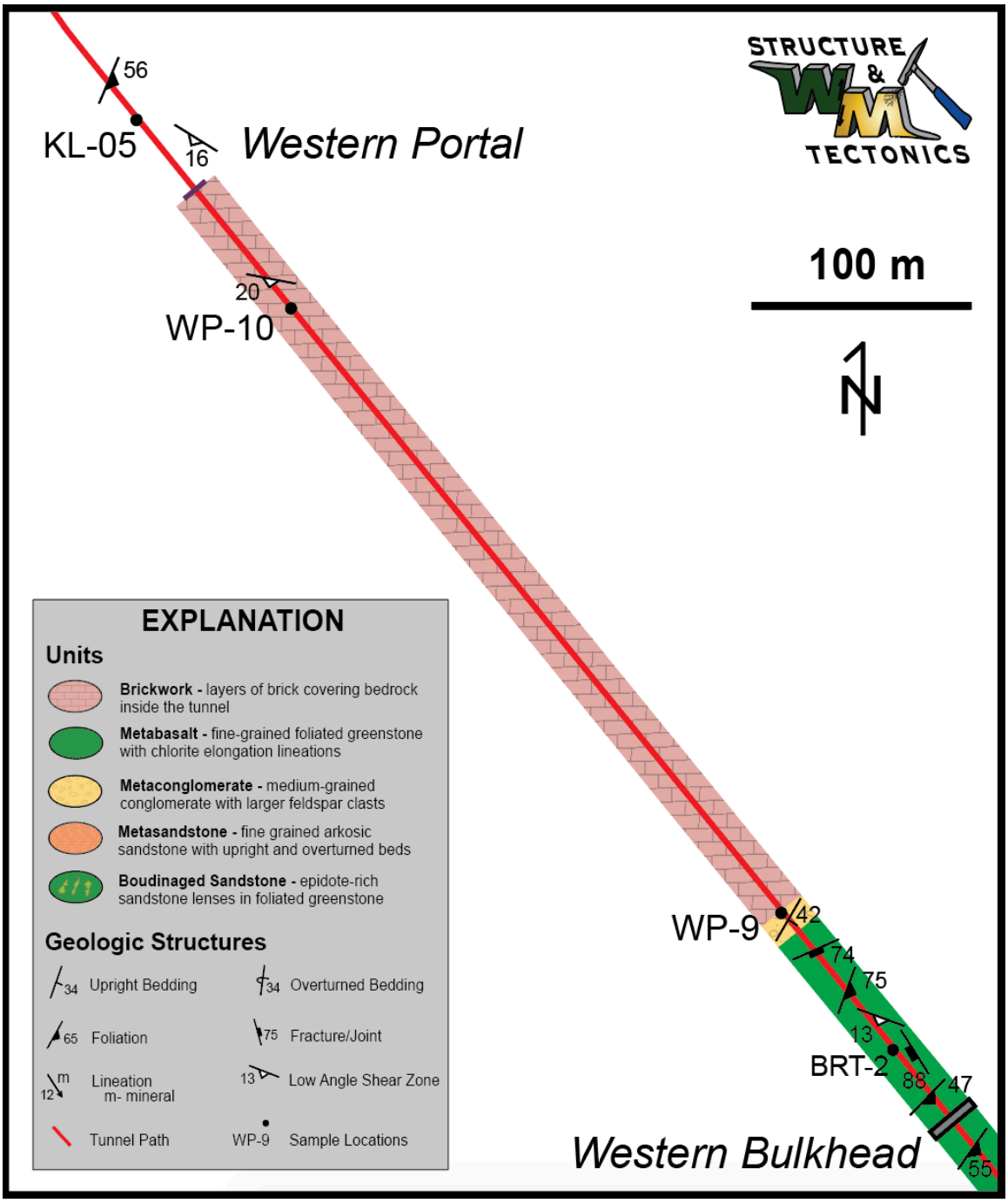

Figure 18. *Western side of the Blue Ridge Tunnel geologic map. Pale red area shows where the length of the brick arch that covers the bedrock of the tunnel is located. Gray bars represent the concrete bulkheads that block off the central section of the tunnel by the 2 and a half-foot wide tubes.*

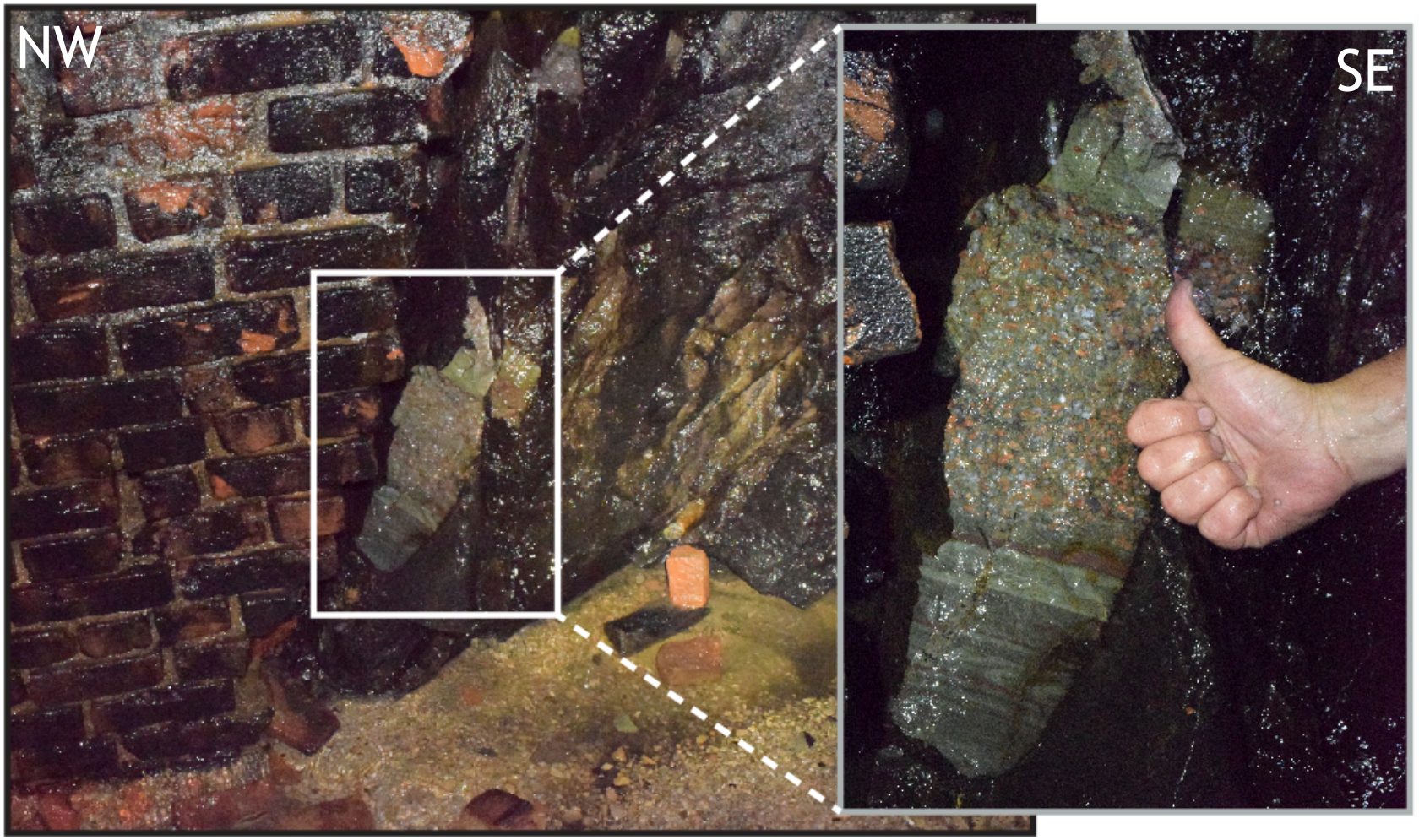

Figure 19. Contact between the brick layer (left) and the metaconglomerate and metasandstone layers, showing where sample WP-9 was collected. Note the repeating sandstone layers and the arkosic conglomerate in between.

Approximately 76 m (250 ft) from the western portal entrance, there is an exposure where the layers of brick have crumbled away to reveal the bedrock behind the facade. This area of exposed bedrock is a perfect example of a localized, low angle shear zone in the metabasalt (Figure 20). The foliation around this low angle shear zone is deflected into the area, and is not steeply dipping. Sample WP-10 was collected from this sheared zone in the greenish-gray fine-grained metabasalt. Chlorite elongation lineations became more common in the sample closer to the proposed zone of shearing. In addition, there is at least one other contact between the conglomerate and sandstone layers from WP-9 to hundreds of feet down the tunnel path to the WP-10 exposure. Yet because the bedrock is sheathed in layers of brick, the exact contact is not identifiable in this section of the tunnel.

Figure 20. *The low angle shear zone from the western portal that has been exposed from recent brickfall, and the area where sample WP-10 was collected.*

About 60 m from the western portal entrance, sample 17KL-05 (Figure 18) was collected from the layer interpreted by Gathright et al. (1977) to be the meta-tuff layer (Zct on map). This sample is a very fine-grained, purple to brown phyllite with hematite staining and a large quantity of opaque minerals. The extent of the purple phyllite layer was approximately 12 m thick in outcrop and varied in intensity of foliation throughout the section (Figure 21).

Figure 21. *Outcrop picture of the purple phyllite covered with moss. Hand for scale.*

Hand sample 17KL-03 was the only sample collected from the road cut along U.S. 250 (Figure 9). The sample is a fine- to medium-grained feldspathic sandstone and is greenish-brown in color. Thin bedding layers of opaque minerals are visible in both hand sample and thin section, and are mostly comprised of boxy-shaped opaque minerals that are likely magnetite. Based off of primary bedding indicators, this area of the sedimentary section preserved at the outcrop is stratigraphically upright as the sequences fines upwards (Figure 22). However, the exposure at U.S. Route 250 has a sequence of upright and overturned beds from the localized isoclinal, NW-verging folds (Figure 23).

Figure 22. *Metamorphosed feldspathic sandstone at the U.S Route 250 road cut. Note the fining upwards sedimentary structure, and dark beds of opque minerals. White arrow shows upright direction.*

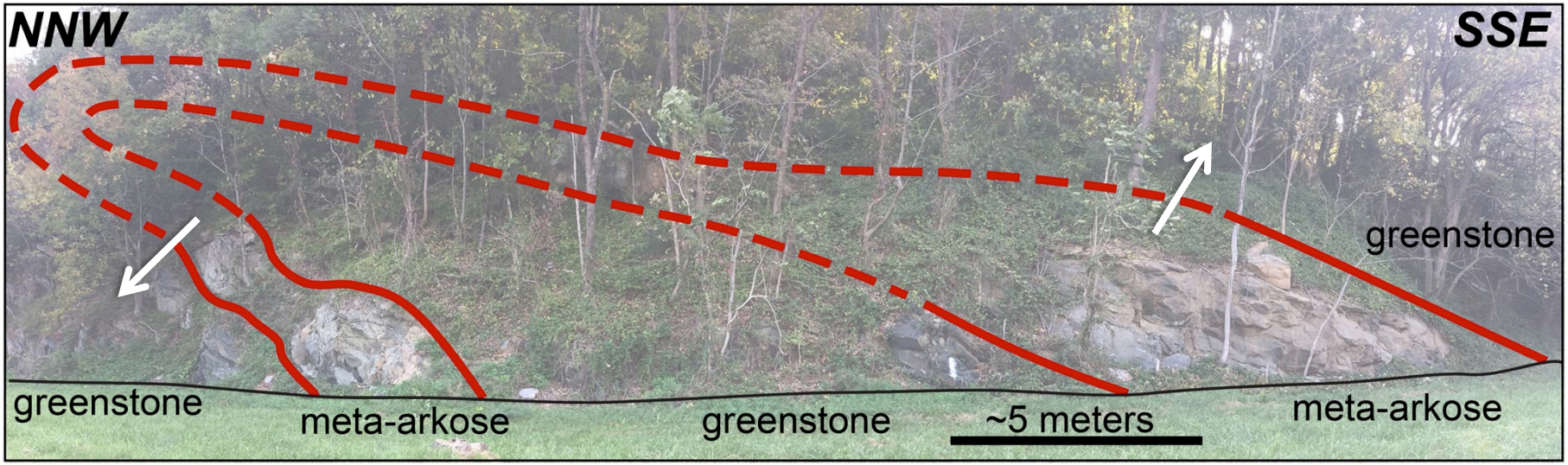

Figure 23. *Outcrop sketch of the U.S. Route 250 roadcut on the east side of Rockfish Gap. The fold verges to the NW, and displays close to isoclinal fold geometry. White arrows show the upright direction of the stratigraphic layers.*

Ductile Features (3.2)

The axial planar foliation (cleavage) of the greenstones of the BRT and U.S. 250 road cut are characteristic of the Catoctin Formation on both the western and eastern limbs of the Blue Ridge Anticlinorium (Cloos, 1971). A total of 69 foliations were measured from the two study sites (Figure 24). Poles to the foliation cluster very tightly in the NW area of the stereogram, and represent a mean foliation of 035º 49º dipping to the SE. Only one foliation measurement from inside the BRT dipped to the W (measurement 005º 32º W). The foliation is more gently dipping to the SE than the bedding, which suggests that the bedding is overturned from their original depositional position (Gathright et al., 1977). Thus, the orientation of the foliation helped this study infer the stratigraphic upright or overturned direction of the sedimentary sections within the Catoctin Formation at these study sites. Chlorite elongation lineation aspect ratios were measured from three planes on a greenstone sample (Figure 25), and Flinn Diagram values record apparent flattening strain (Figure 26). Low angle shear zones deflect the main foliation, but also display a top-to-the-NW sense of ductile shear (Figure 27).

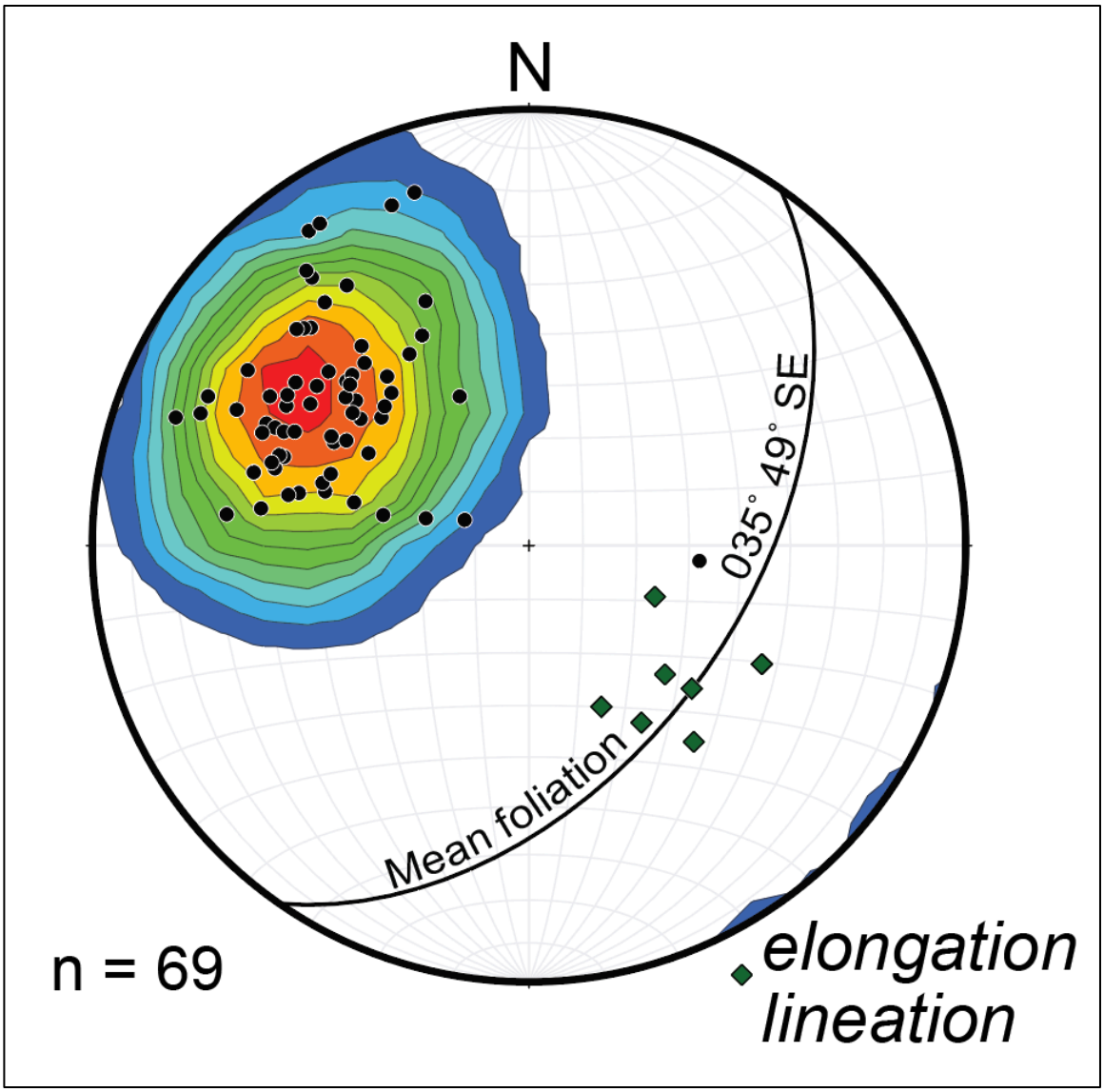

Figure 24. *Stereogram of poles to the foliation and elongation lineations (green diamonds) in the study areas. Contoured with a Kamb contour of single standard deviations. Foliation strikes to the northeast and dips moderately to the southeast. Elongation lineations plunge down dip.*

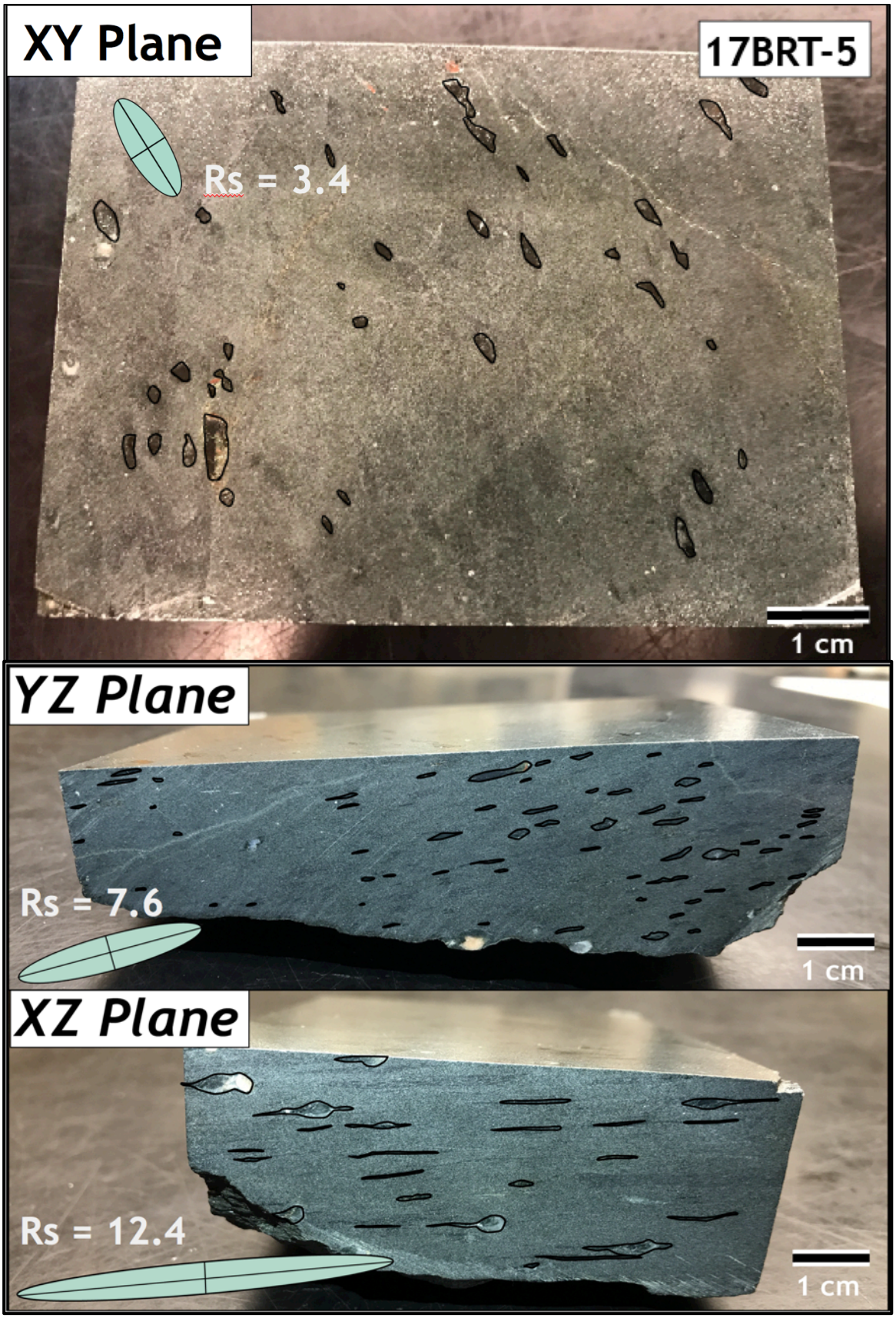

Figure 25. *Chlorite amygdules outlined in black for the XY, YZ, and XZ planes. Aspect ratios and strain ellipses are drawn in pale green.*

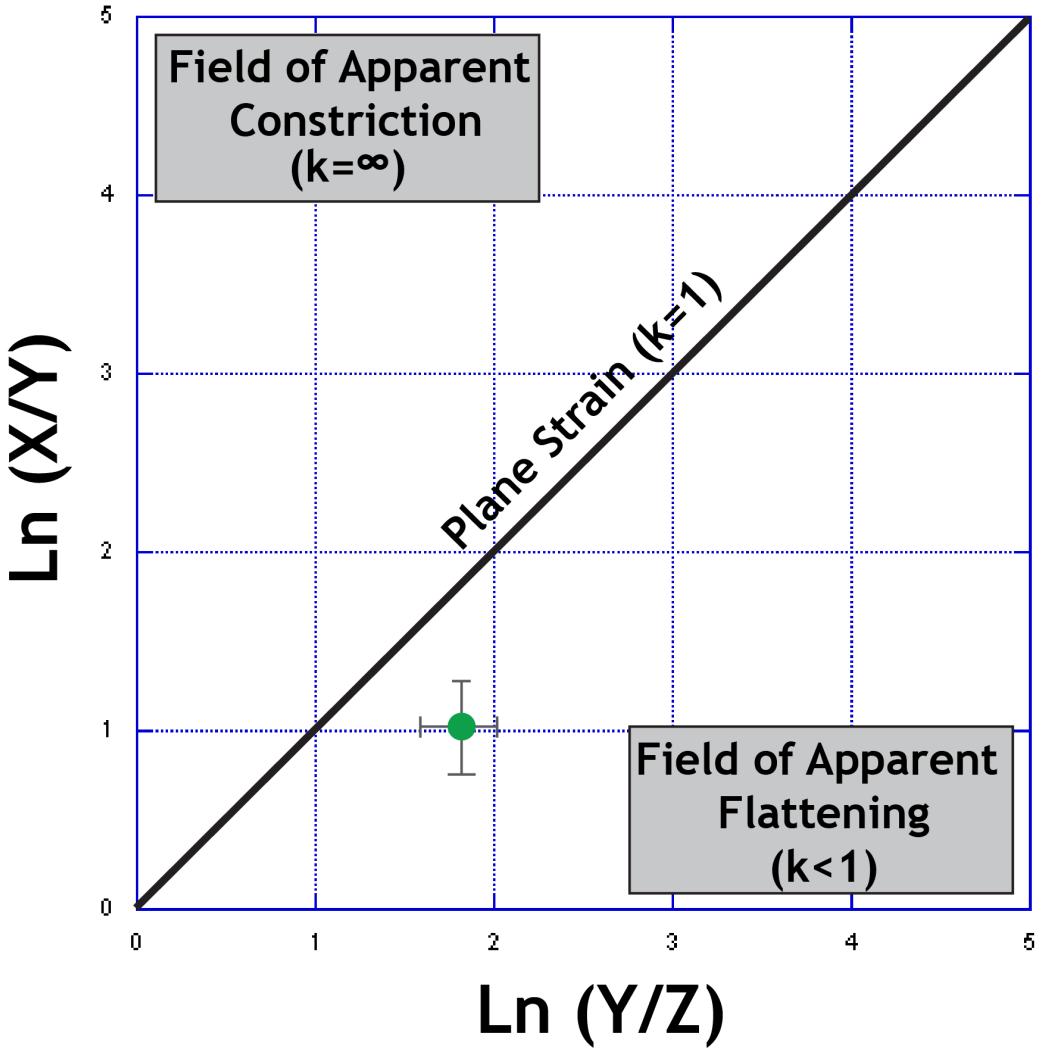

Figure 26. *Flinn Diagram of the chlorite elongation lineation k-value. Gray lines on the green dot represent the degree of uncertainty.*

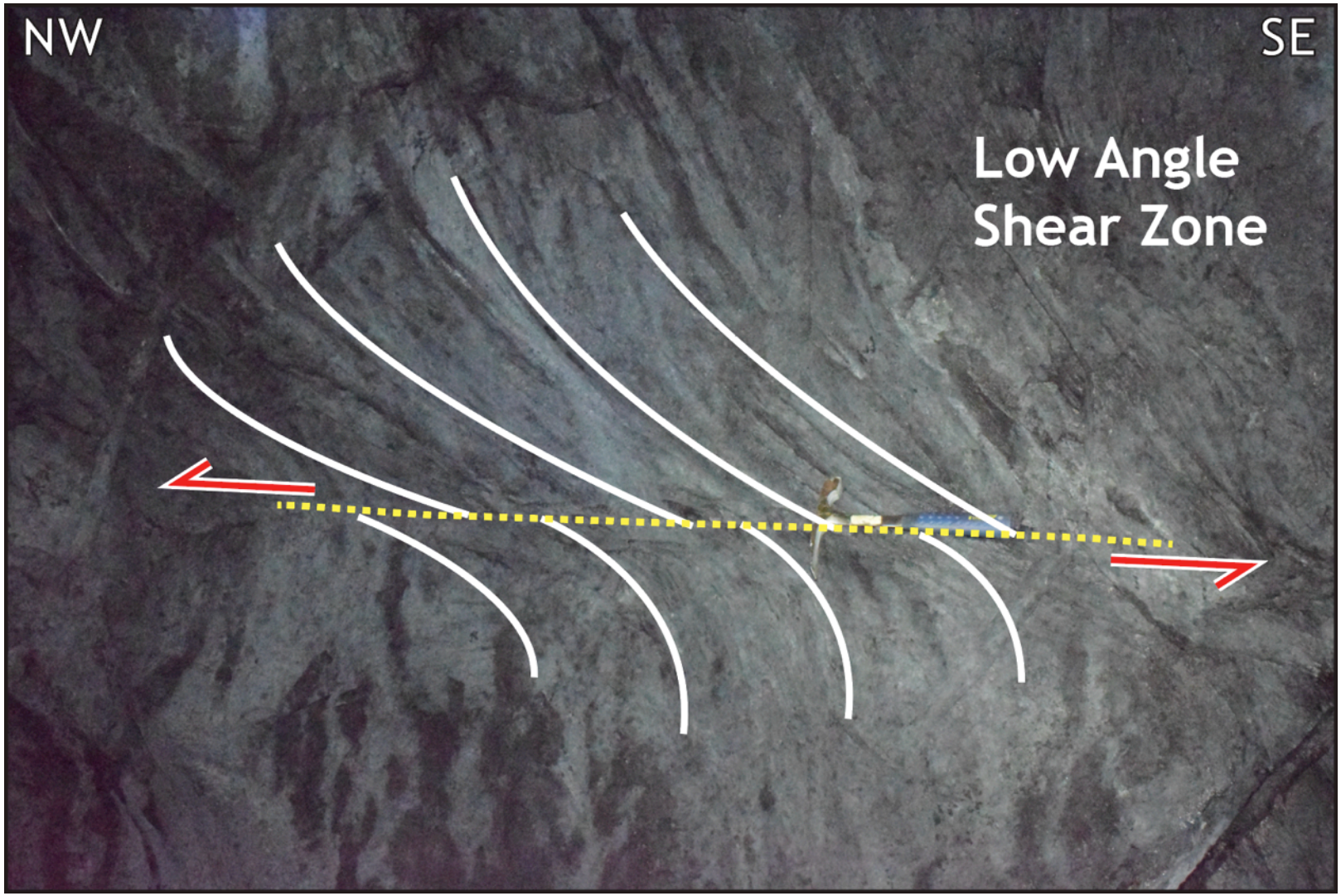

Figure 27. *Low angle shear zone 2660 ft (810 m) from the eastern portal entrance. The sense of shear is top-to-the-NW.*

Large, asymmetric epidote-rich sandstone boudins crop out in a 220 m (700 ft) section inside the two tunnel bulkheads, an area of the BRT in which the study has named the "Hall of the Boudins" (Figure 13). The geometry of the boudinaged sandstone lenses display varying levels of complexity at multiple scales (Figure 28a-f), but all record top-to-the-NW ductile sense of shear. Zones of epidote breccia and quartz veins are commonly included within the boudins and at their margins (Figure 28a, 28f) which is indicative of complex internal boudin deformation within the more competent sandstone layer. The main foliation is also deflected around the boudins, and are concomitant to one another.

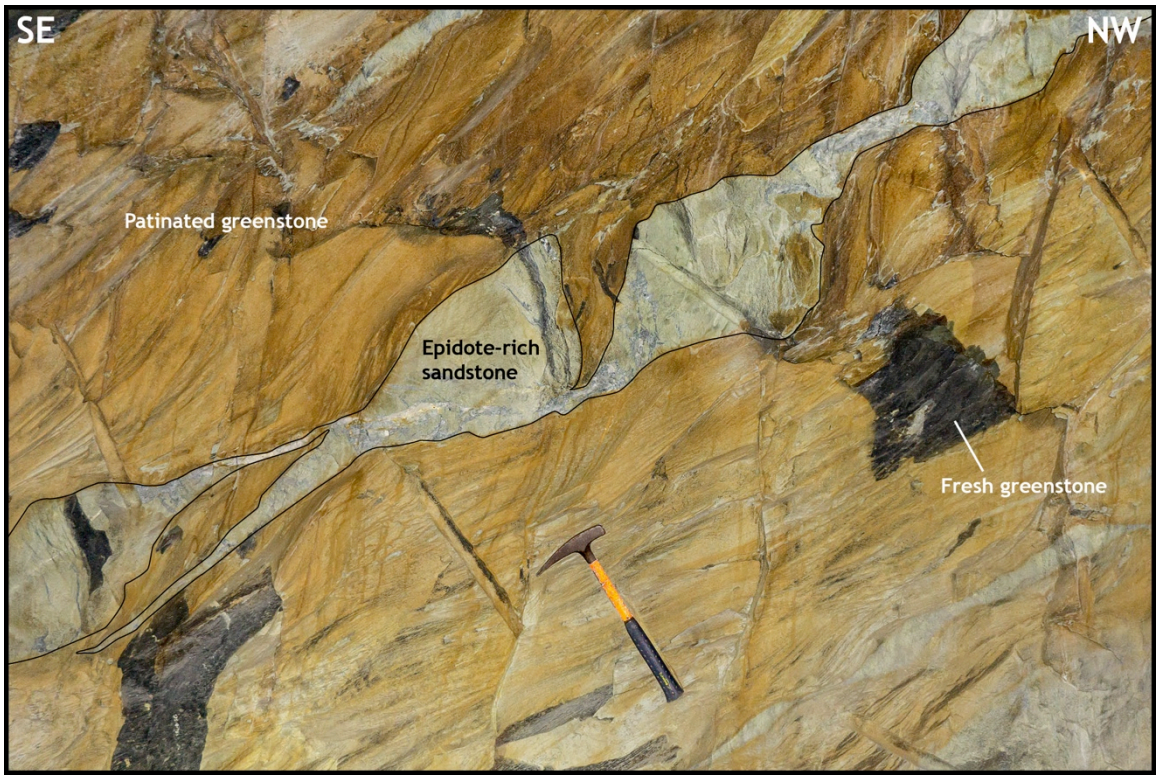

Figure 28a. *This epidote-rich sandstone boudin shows a ductile top-to-the-NW sense of shear. Zones of breccia and quartz veins are visible inside the sandstone. Note the fresh surface of greenstone versus the patinated surface likely from the spraying of gas inside the BRT in the 1950s. Hammer for scale.*

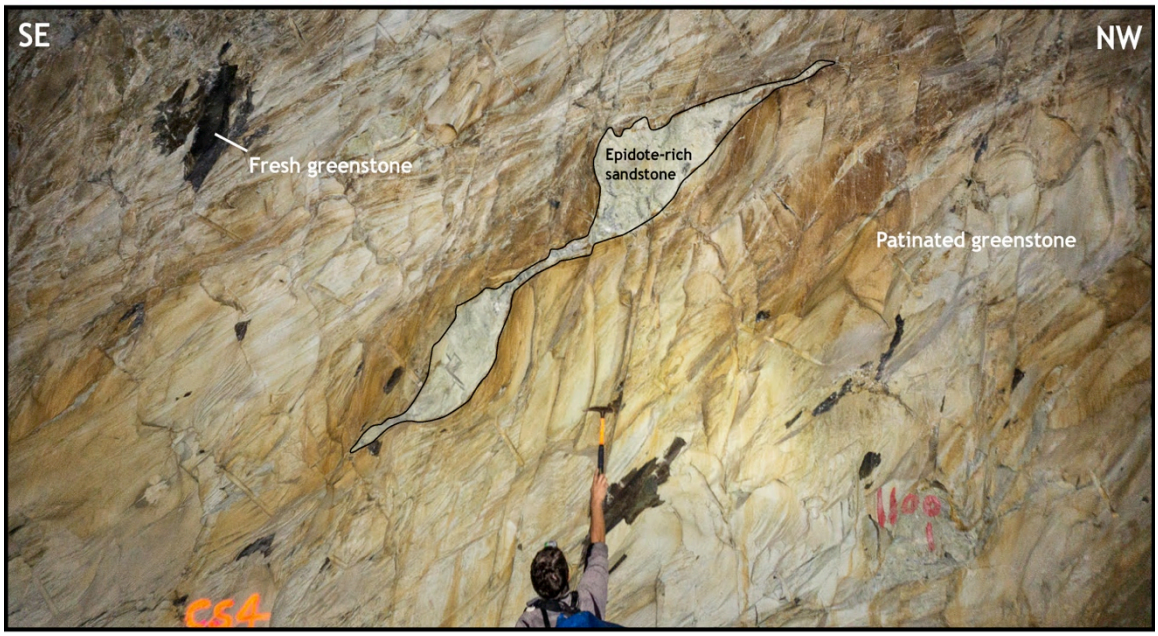

Figure 28b. *This epidote-rich sandstone boudin also shows a ductile top-to-the-NW sense of shear, but the foliation seemingly is deflected around the more competent sandstone. C.M.B. for scale.*

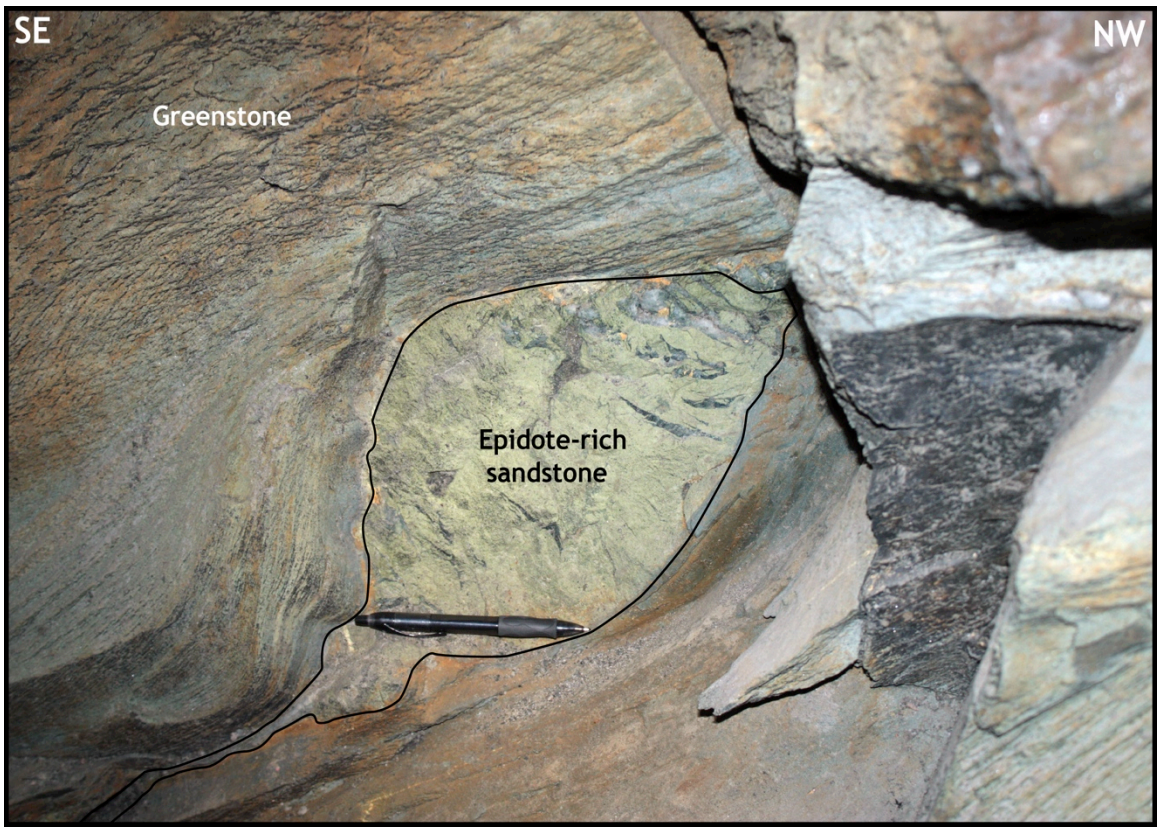

Figure 28c. *View is looking down upon the plane of foliation. This epidote-rich sandstone boudin shows a ductile top-to-the-NW sense of shear. Zones of breccia and quartz veins are visible inside the sandstone in the NW corner. Pen for scale.*

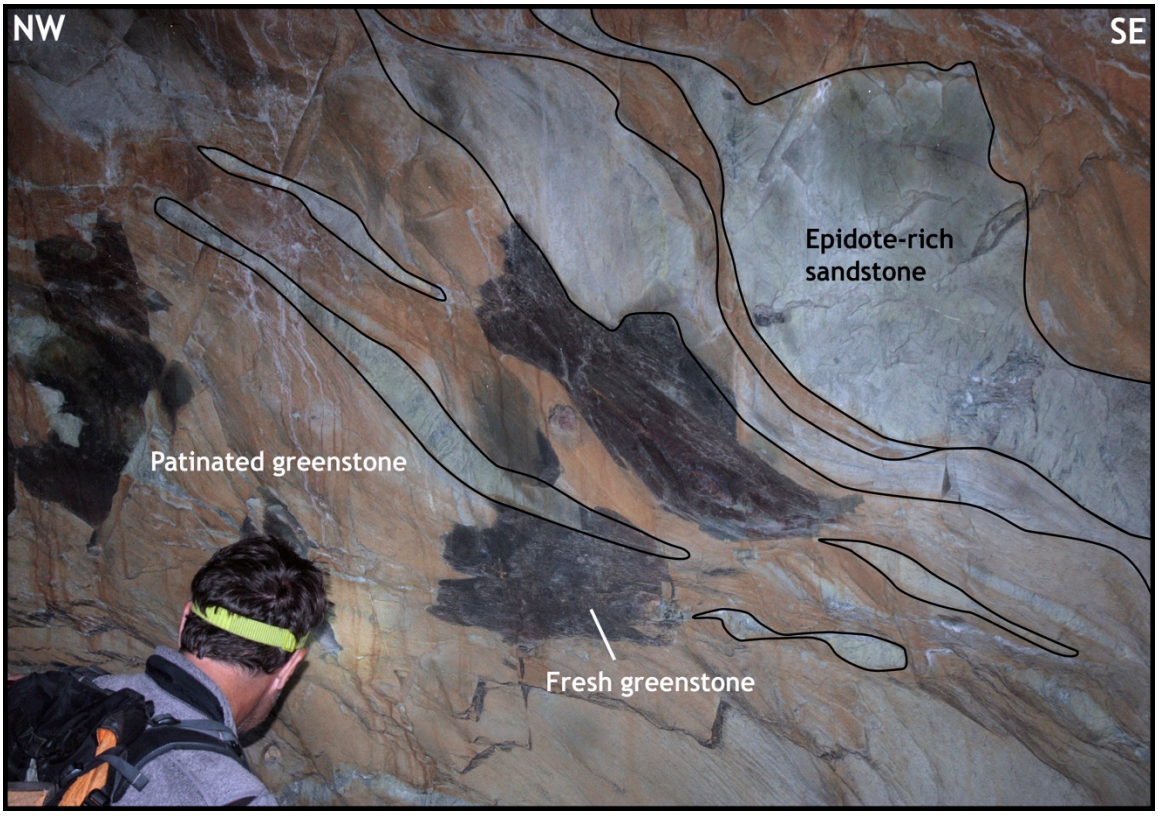

Figure 28d. *This area inside the Hall of the Boudins shows a complex geometry in a larger network of sandstone lenses. The ductile NW-directed shear is also noted in each of the smaller boudins.*

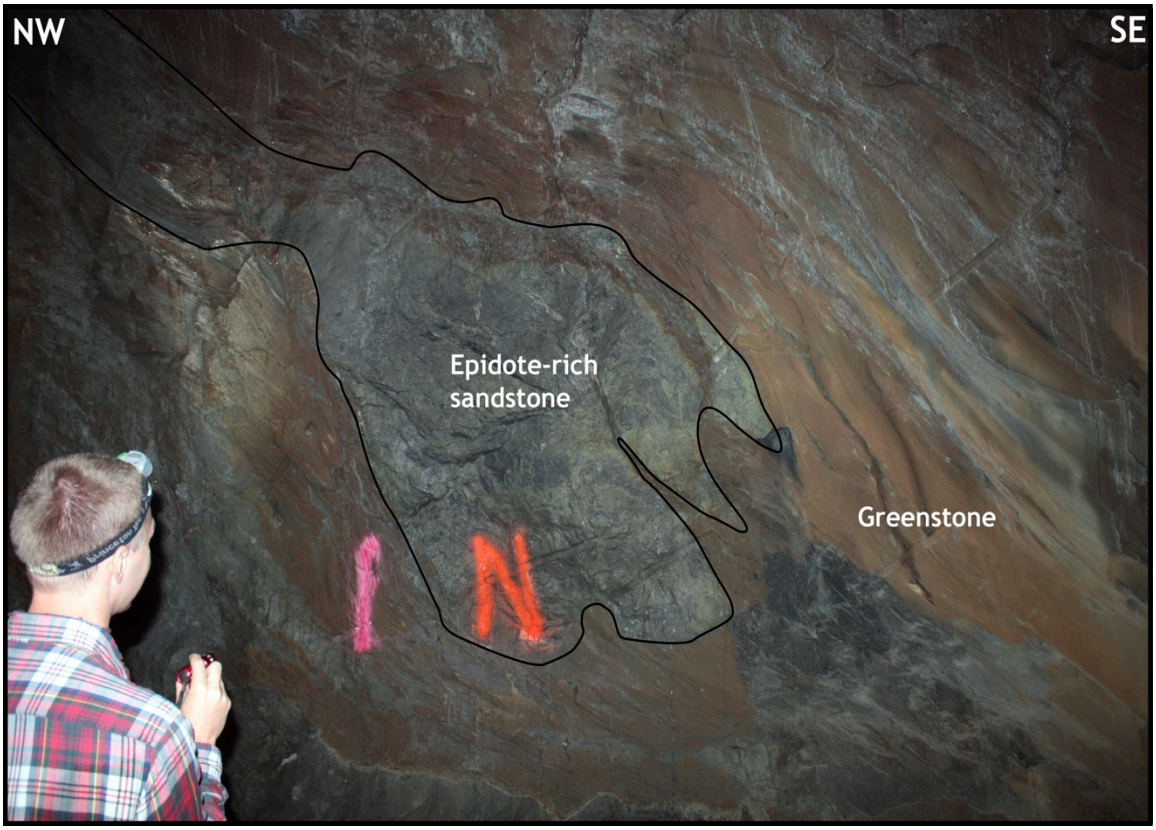

Figure 28e. *This epidote-rich sandstone boudin shows a convoluted end pattern as the less competent matrix flows around the harder sandstone.*

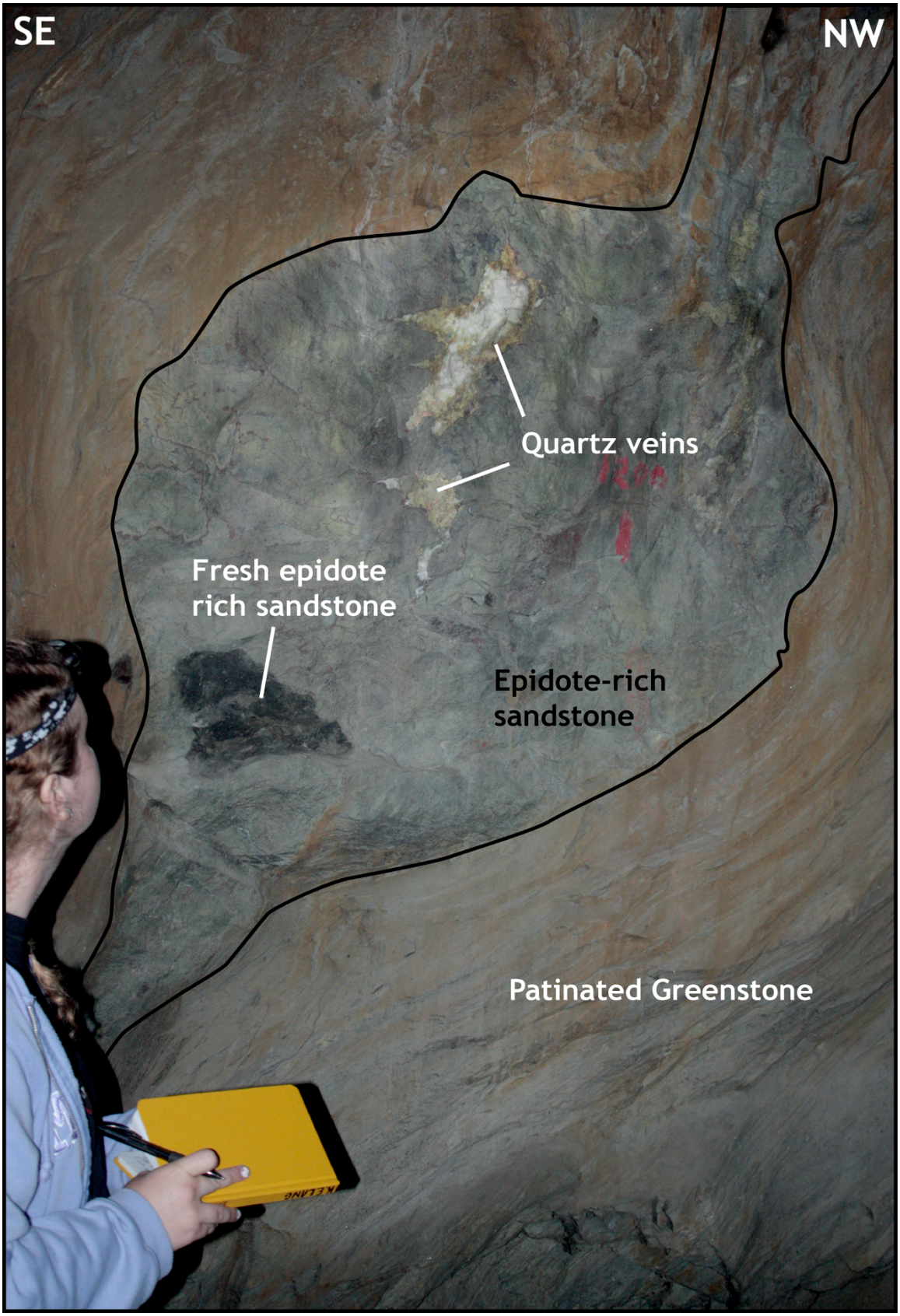

Figure 28f. *Quartz veins and epidote rims are found within the epidote rich sandstone boudin. Note the strong deflection of the foliation direction around the exterior of the ductile feature. A top-to-NW sense of shear is apparent in this image.*

A localized example of a fold within the metasedimentary units of the Catoctin Formation is present at the Route 250 road cut study site (Figure 23). The axis of the fold strikes to the NW, and displays isoclinal fold geometry from observations of upright and overturned limbs. In the overturned section of the meta-arkose, the thickness of the fold limb changes to accommodate a boudinaged section of epidote-rich arkose. From field observations, it is clear that this section of rock became a more competent layer as this section underwent the process of boudinage. The internal deformation within the epidote-rich sandstone layer was likely complex due to its competent physical properties. As a result, an array of quartz veins within the boudinaged area (Figure 29) attests to the processes of stress that changed the competent layer. Additionally, sets of slickenlines from within the boudin at the Route 250 outcrop were plotted onto a P-t stereogram (Figure 30).

Figure 29. *Close up image of the U.S. Route 250 boudin within the overturned section of an isoclinal fold. The white quartz veins show the internal boudinage extensional direction (black arrows). The yellow arrow indicates the sedimentary fining sequence which is overturned at this outcrop.*

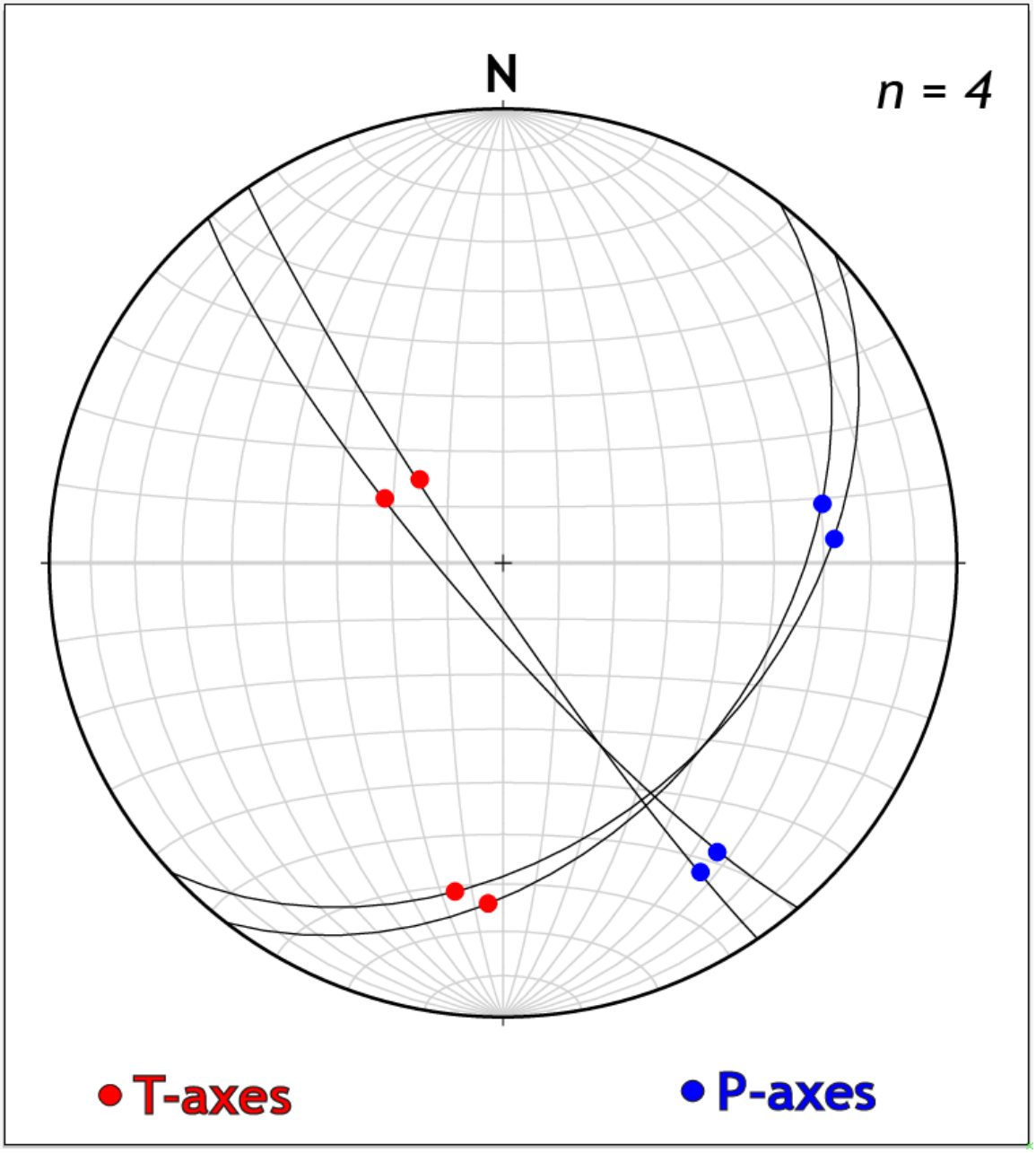

Figure 30. *The P-t diagram of the slickenlines. Data from within the boudin on the overturned limb of the fold at the U.S. 250 outcrop. P axes represent the area of Pressure and t axes represent areas of tension.*

Brittle Features (3.3)

A total of 89 fractures were measured at the two study sites. The data is represented by a rose diagram which allows this study to infer the relative percentages of the orientations in relation to the rest of the data as well as a stereogram with poles to the fractures plotted (Figure 31). Two dominant sets are apparent in the diagram: the first major orientation of the fracture sets strike from a range of 290º-320º (WNW-ESE), whereas the second major set strikes from 030º-050º (NE-SW). However, there is a 50º range in the WNW set, and a majority of the fractures from this first set broadly strike to the NW-SE as a whole.

A high-density fracture zone is located 50 m (165 ft) from the Eastern portal entrance of the BRT (Figure 32). This area along the BRT path of the Catoctin Formation is significantly more fractured than the other surrounding areas. The metabasalts in this area have been uncovered by recent BRT construction, and are more highly weathered and eroded than the surrounding metabasalts closer to the eastern portal entrance. Small chunks of greenstone have broken away from the outcrop along this 15 m (50 ft) section of highly fractured rock, and some pieces have elongation lineations. Inside the BRT on the eastern portal, extensional fractures were also measured, with a minor few fractures displaying plumose features such as hackles and arrest lines (Figure 33).

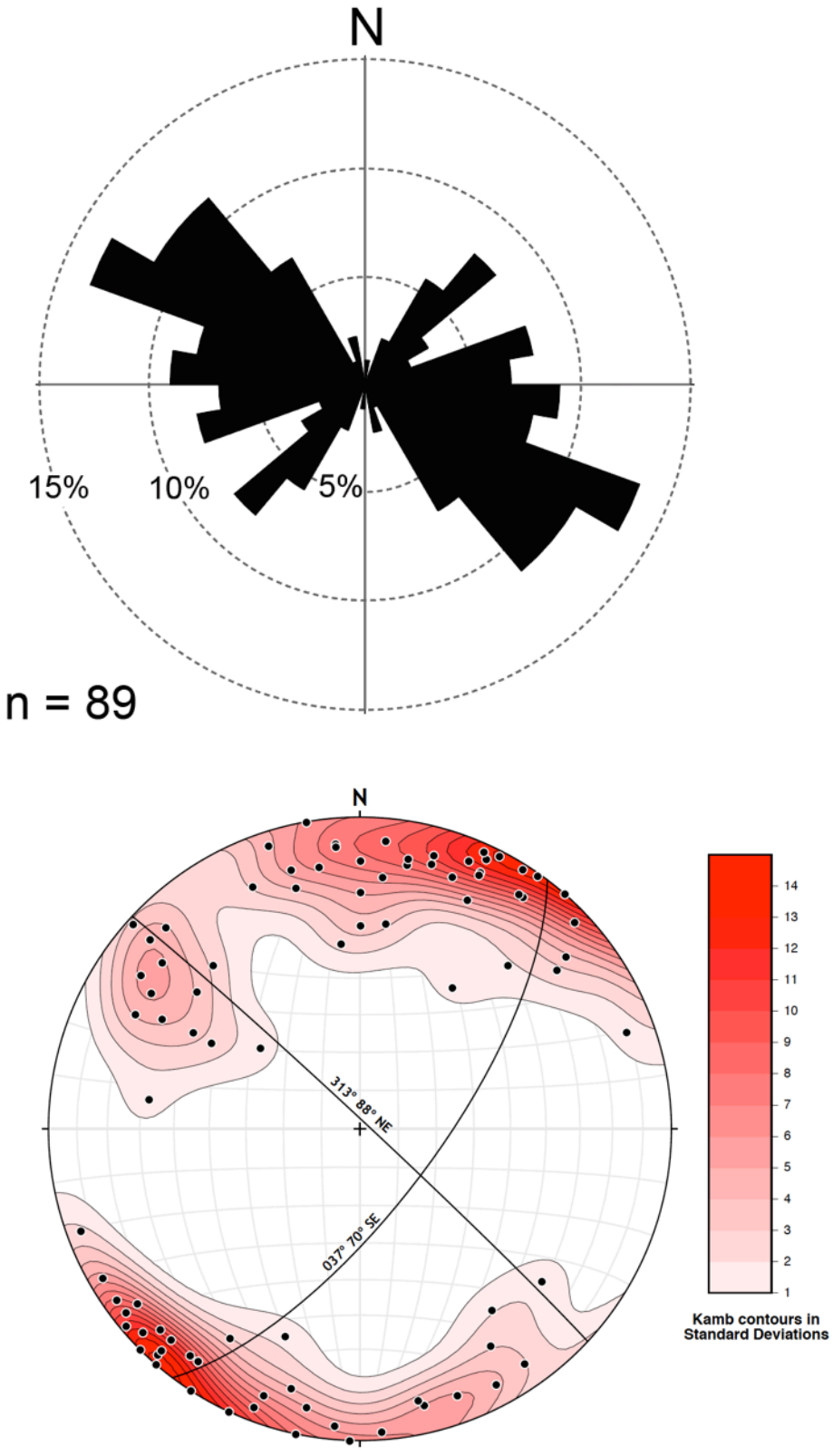

Figure 31. *Rose diagram of fracture strikes and stereogram of the poles to the two fracture sets. The black great circles of the stereogram represent the average fracture orientation and dip angle. The Kamb contours are in standard deviations.*

Figure 32. *The high density fracture zone near the eastern portal entrance of the Blue Ridge Tunnel, with a majority of the fractures striking to the NW. The greenstones here are highly weathered, hence the tan to red color.*

Figure 33. *An extensional fracture in the BRT with typical plumose structures: hackles and arrest lines.*

Petrographic Analysis (3.4)

Four thin sections from the eight hand samples were analyzed for mineralogy, texture, and microstructures. Of the four thin sections, three were from metasedimentary units within the Catoctin Formation at Rockfish Gap and the BRT. The thin section from hand sample 17KL-03 was cut normal to the bedding in order to identify stratigraphic properties and bedding direction at the microscale to complement field observations (Figure 34a). The matrix of the sample was mostly that of sericite or the fine-grained white mica that is common in greenstones and their sedimentary counterparts. Larger grains of quartz, perthitic potassium feldspar, or other rock clasts of the granite basement complex (Figure 34b) are situated in the finer the matrix. The minerals perthite, microcline, and albite make up the remaining mineralogy of this sample (Figure 34c). Thin, uneven layers of opaque minerals provide clues about the facing direction (Figure 34d). The least deformed of the four, 17KL-03 preserves primary sedimentary features of the bedding layers. Microstructures such as stylolites and strain shadows are common in the sample matrix.

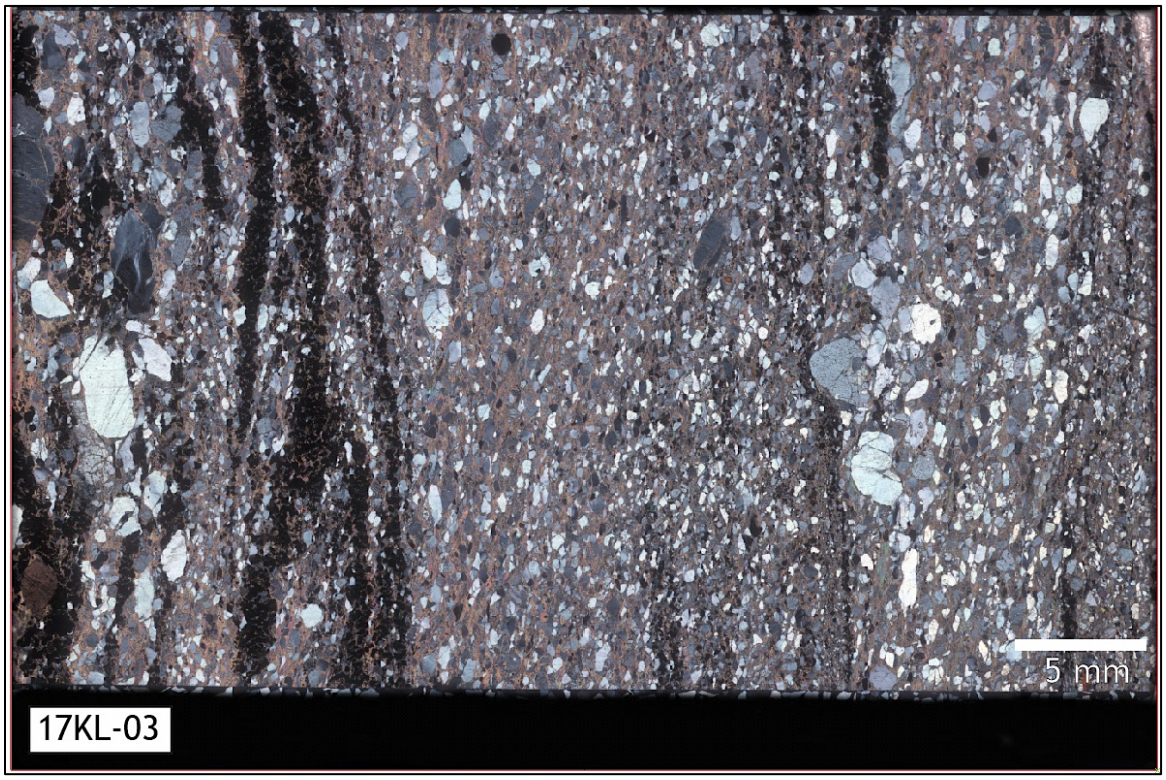

Figure 34a. *XPL Scan of the meta-arkosic wacke in thin section with primary structures (bedding). Note the black layers of opaque minerals, and the variability in grain size up and down the thin section.*

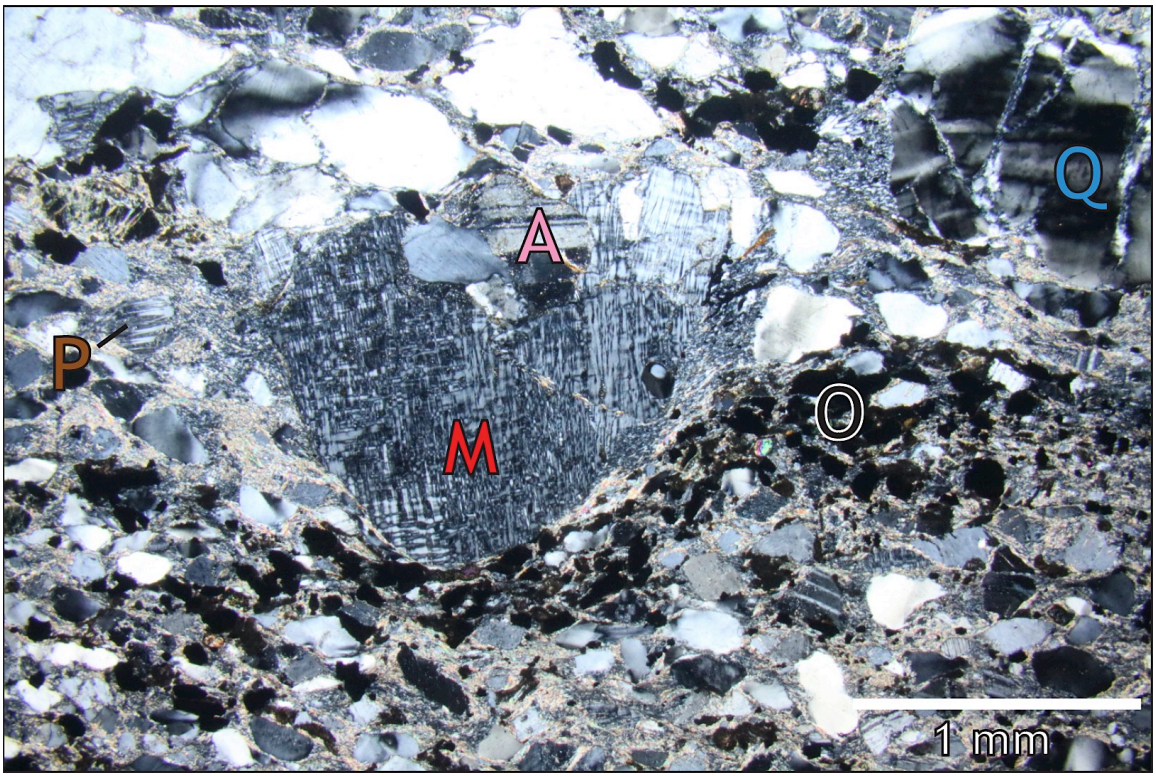

Figure 34b. *A granitic rock fragment containing microcline (M), albite (A), and quartz (Q) with a layer of opaque minerals underneath (O). Quartz displays particularly well-developed undulose extinction in the upper right corner.*

Figure 34c. *A large quartz grain with undulose extinction and small fractures.*

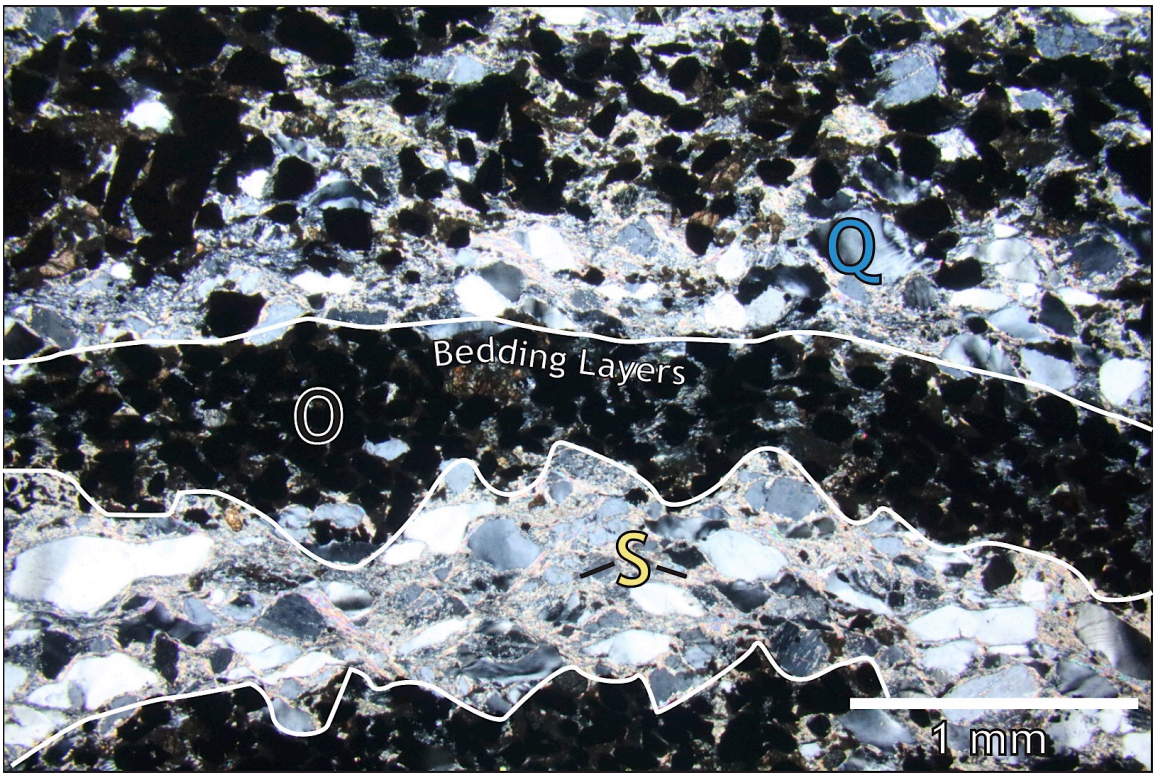

Figure 34d. *Thin layers of opaque minerals with quartz and sericite in between them. The opaque layers seen in thin section are also visible in hand sample 17KL-03.*

Thin section 17KL-05 was the sample previously interpreted to be tuffaceous in origin (Gathright, 1976; Gathright et al., 1977), and was sampled from 60 m outside the western portal of the BRT (Figure 35a). On the right side of the thin section scan, there is a contact between the purple-brown phyllite layer and a coarser-grained metasandstone (Figure 35b). The mineralogy of the purple phyllite consists of a very fine-grained matrix (100 um) of plagioclase and opaque minerals (Figure 35c), hematite, quartz, sericite, potassium feldspar, and rare grains of epidote. Stylolites (Figure 35d) and pressure shadows (Figure 35e) are equally prevalent in the sericite matrix of the metasandstone.

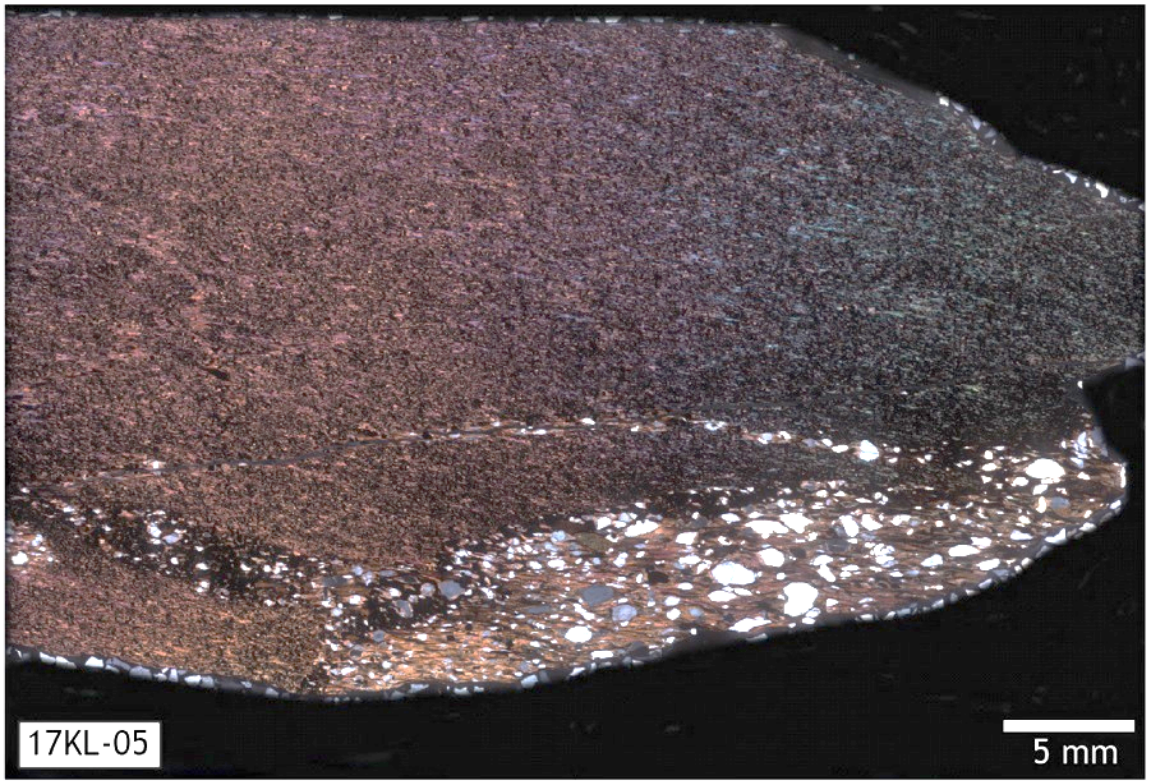

Figure 35a. *XPL Scan of purple phyllite thin section 17KL-05. Note the contact between the purple phyllite and the metasandstone layer in the lower right corner.*

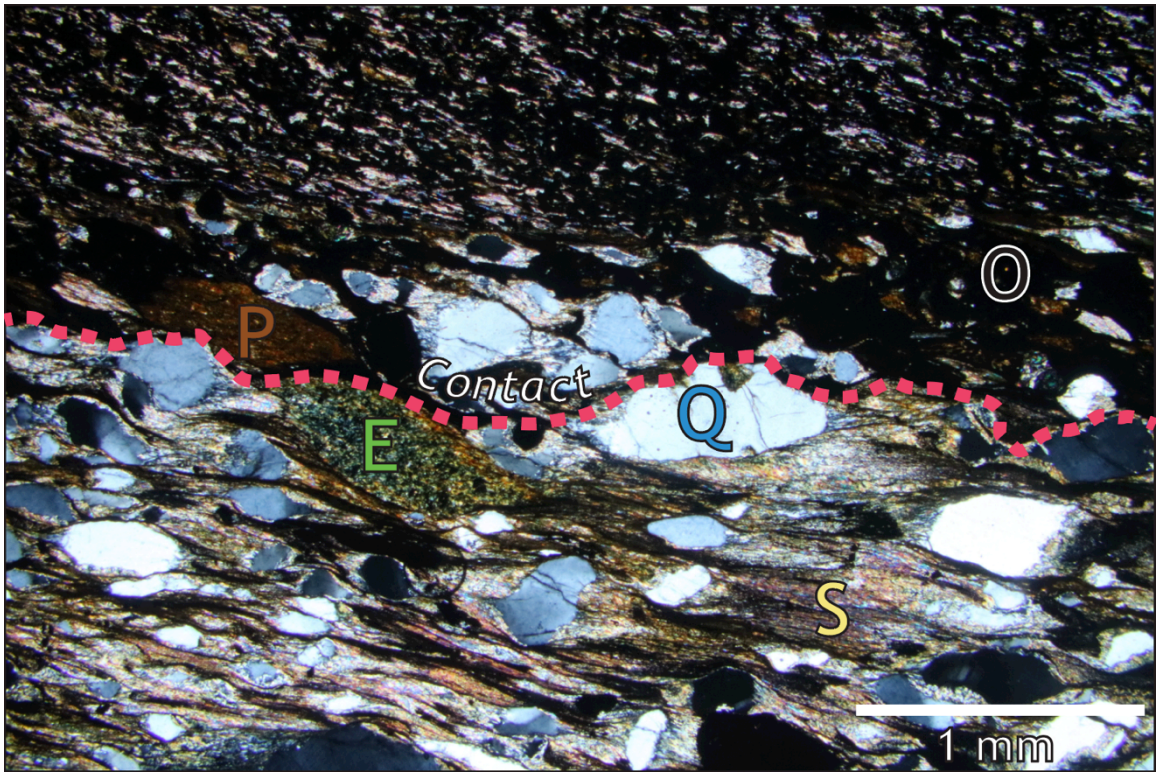

Figure 35b. *Localized area of opaque (O) mineral concentration. Epidote (E) grains are elongated, and halos of sericite (S) surround the quartz (Q) grains. The beginnings of pressure shadows appear around the quartz, as well, and there is a contact with the more plagioclase-rich fine-grained purple phyllite.*

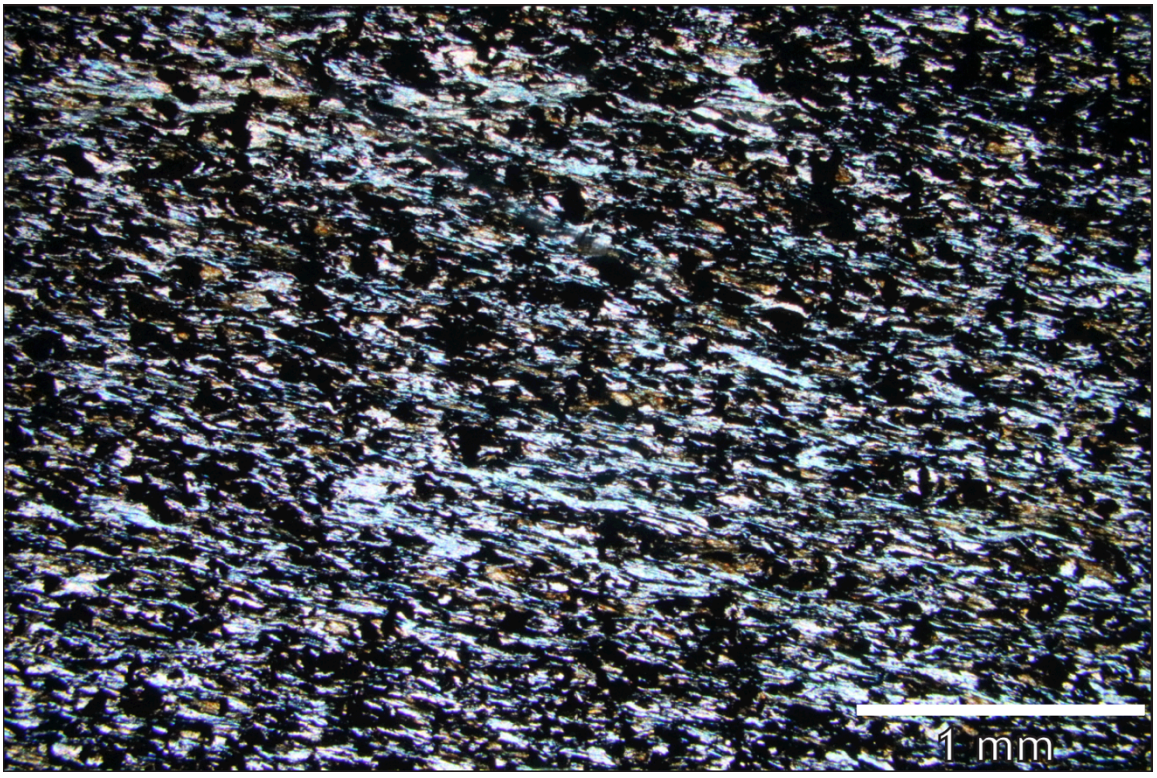

Figure 35c. *Fine-grained matrix of sample 17KL-05, with large amounts of elongate opaque minerals.*

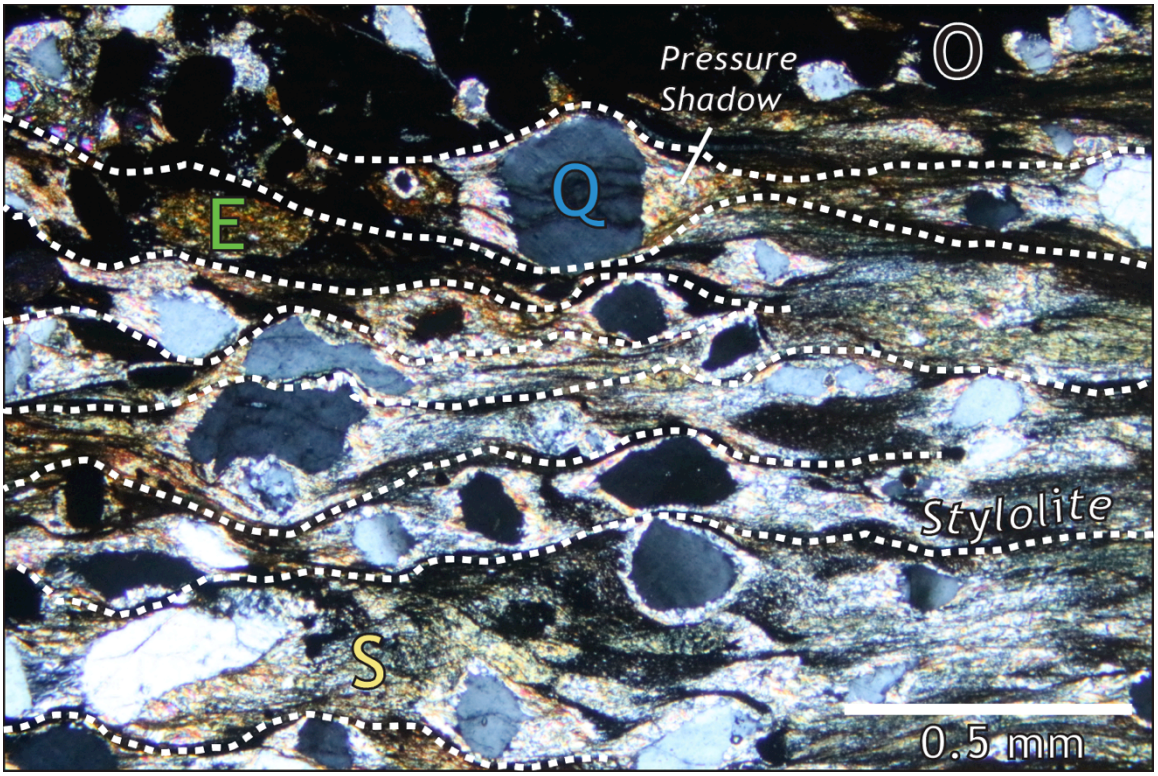

Figure 35d. *White lines show stylolites formed from dissolution and mass transfer in the purple phyllite layer.*

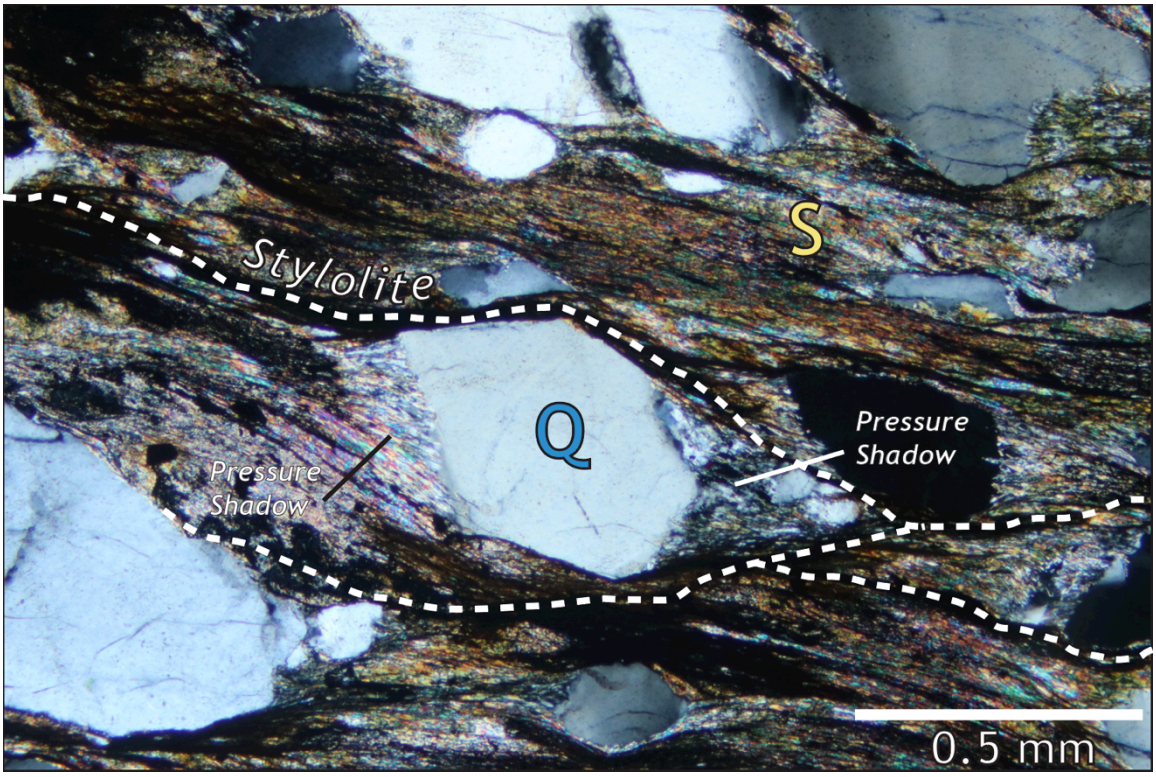

Figure 35e. *Pressure shadows on either side of the central quartz vein show asymmetric shear indicators. White lines also are stylolites formed from dissolution and mass transfer in the purple phyllite layer.*

Although 17BRT-2 is the only sample that was not oriented in the field, it presents a revealing picture in thin section (Figure 36a). Two fibrous antitaxial veins of potassium feldspar and quartz veins cut across the hand sample (Figure 36b/c) (Ramsay and Huber, 1983; Passchier and Trouw; 1998). Strain shadows appear around larger feldspar grains (Figure 36d) within the sericite matrix and quartz veins separating the original grain are common (Figure 36e). Over the entire thin section, both quartz and potassium feldspar grains are slightly cracked, with sericite forming at the newly formed crack edges (Figure 36f). A penetrative foliation is also apparent under the thin section scan in the meta-arkosic wacke (Figure 36g).

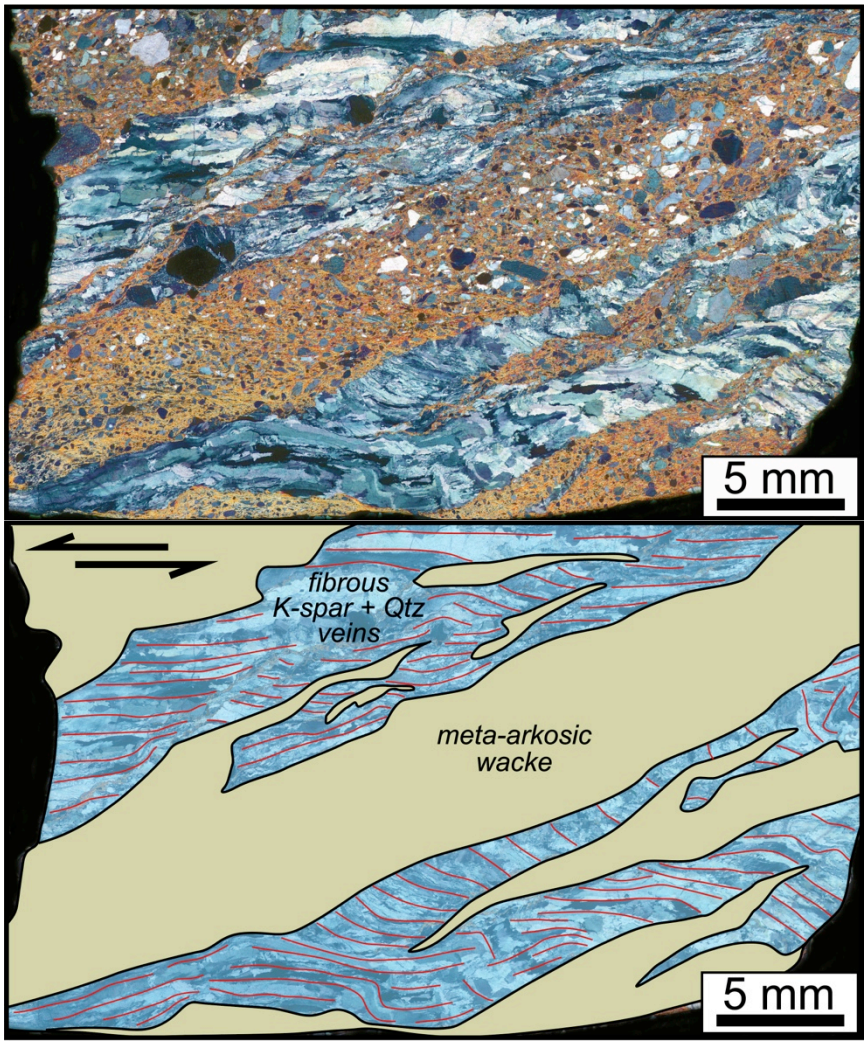

Figure 36a. *XPL Scan of the meta-arkosic wacke thin section 17BRT-2. Below, a schematic of the veins intruding the meta-arkosic wacke host rock showing a top-to-left sense of shear.*

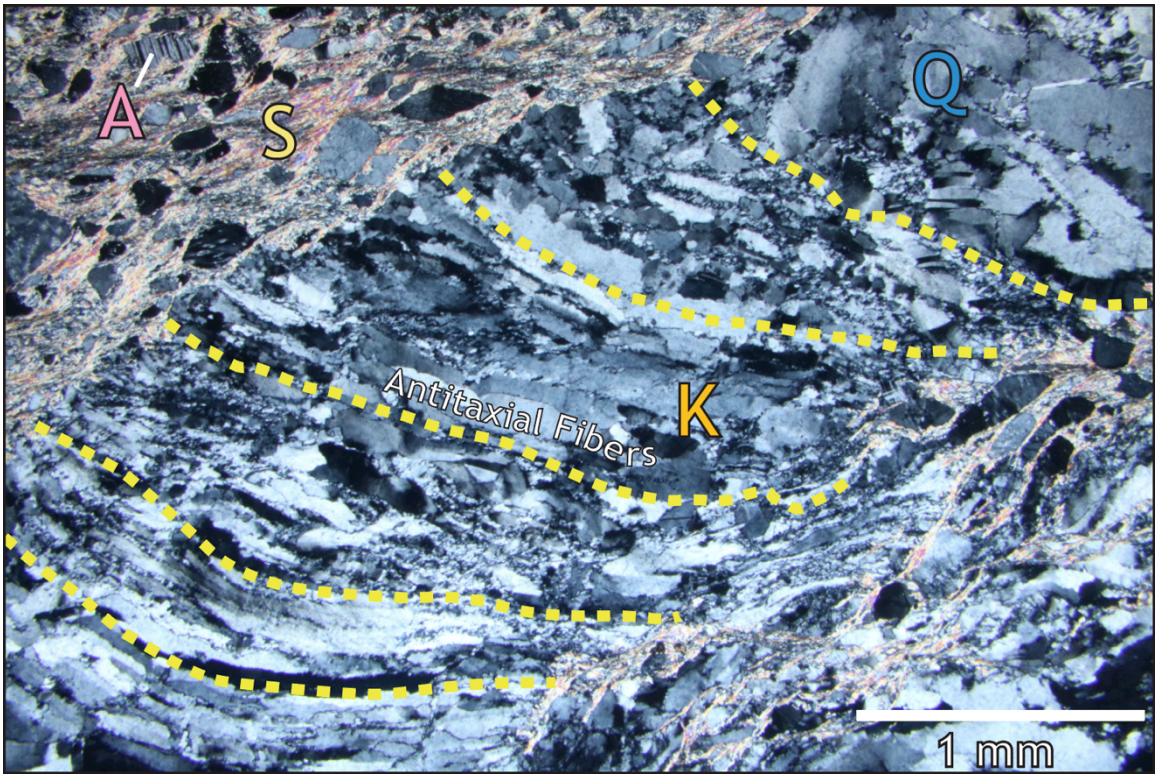

Figure 37b. *Antitaxial fibrous vein of quartz (Q) and potassium feldspar (K). Yellow lines delineate direction of the fibers.*

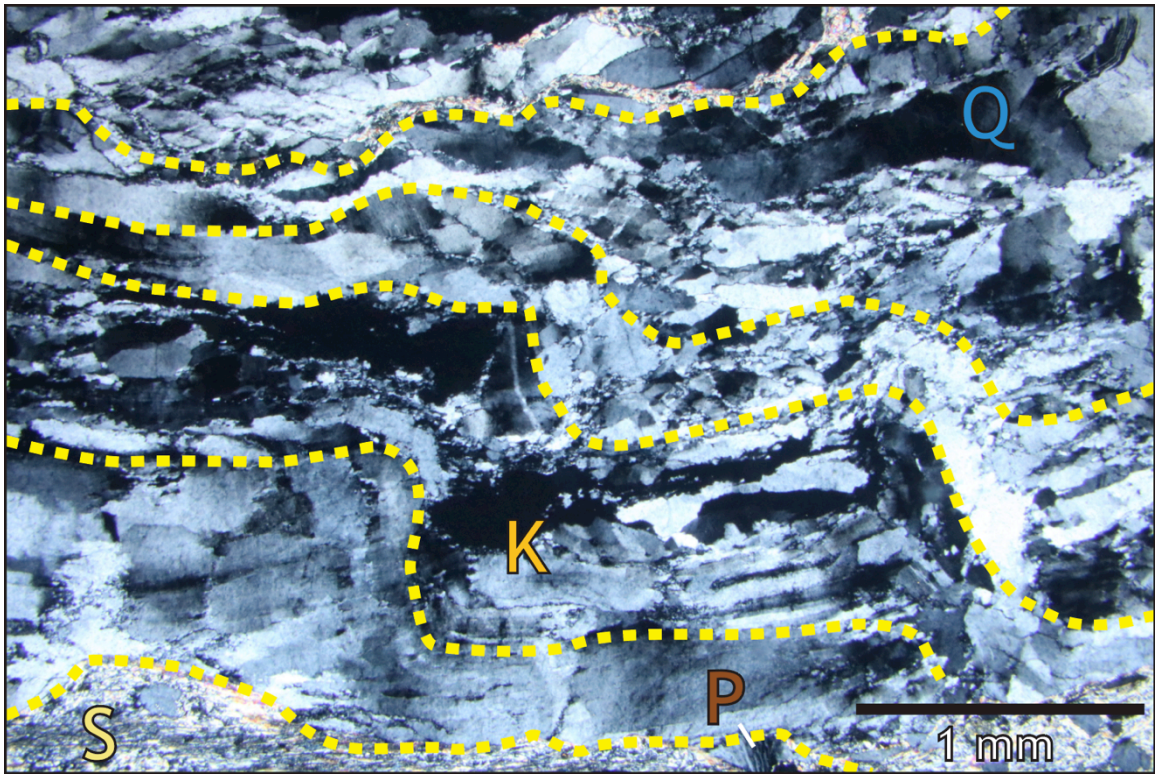

Figure 37c. *Antitaxial vein with kinked fibers that likely reflects a change in the instantaneous stretching axis (ISA).*

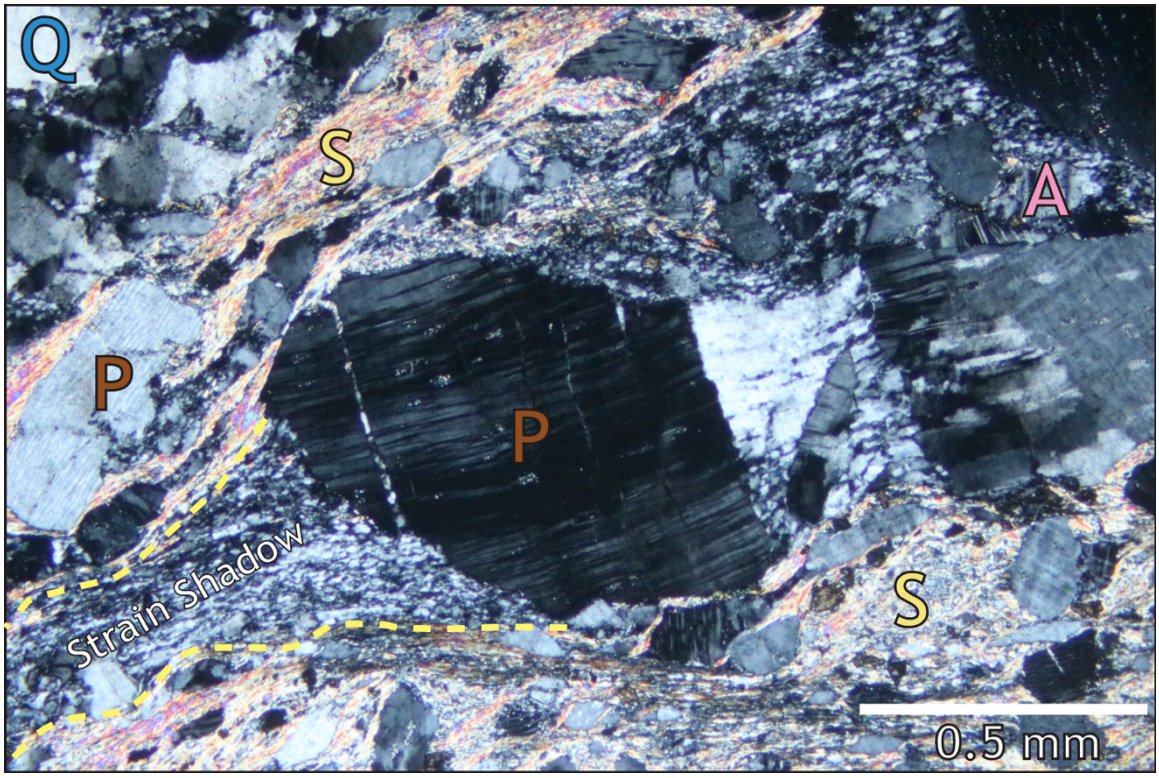

Figure 36d. *Perthitic grain (P) with tiny grains of quartz (Q) in the strain fringes and pressure shadows.*

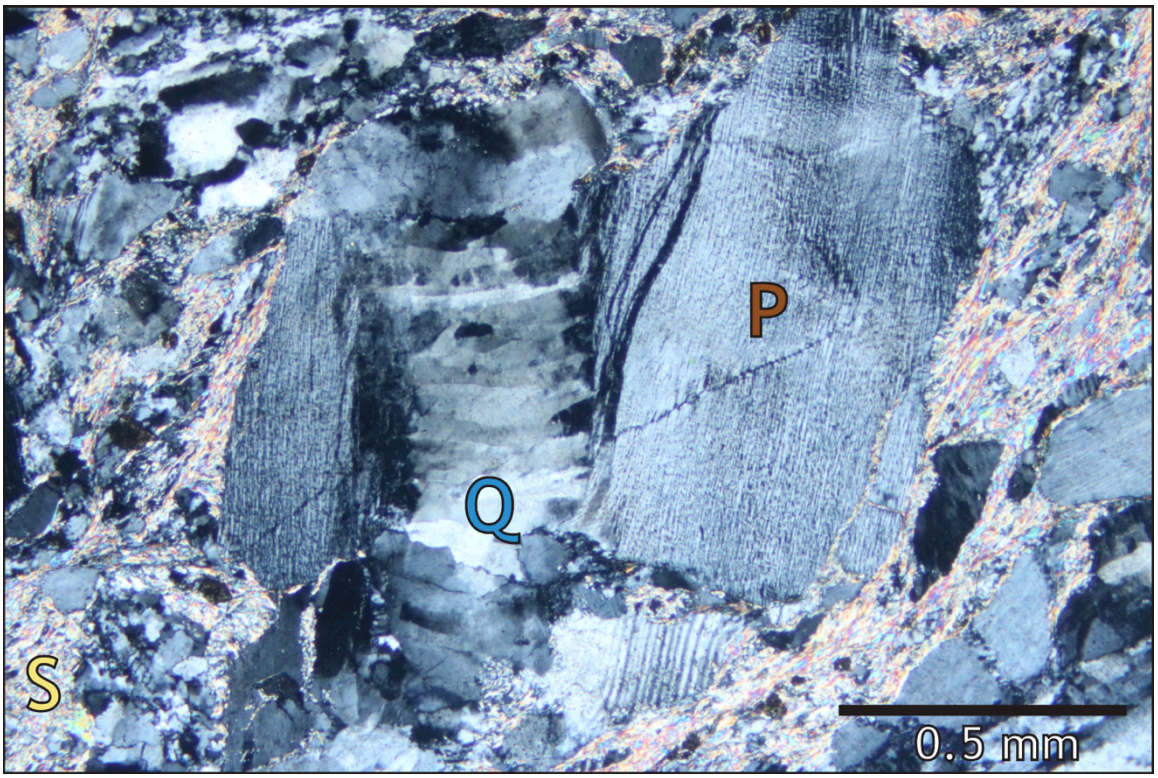

Figure 36e. *A fibrous quartz grain (Q) stretching a large perthitic grain (P) in half.*

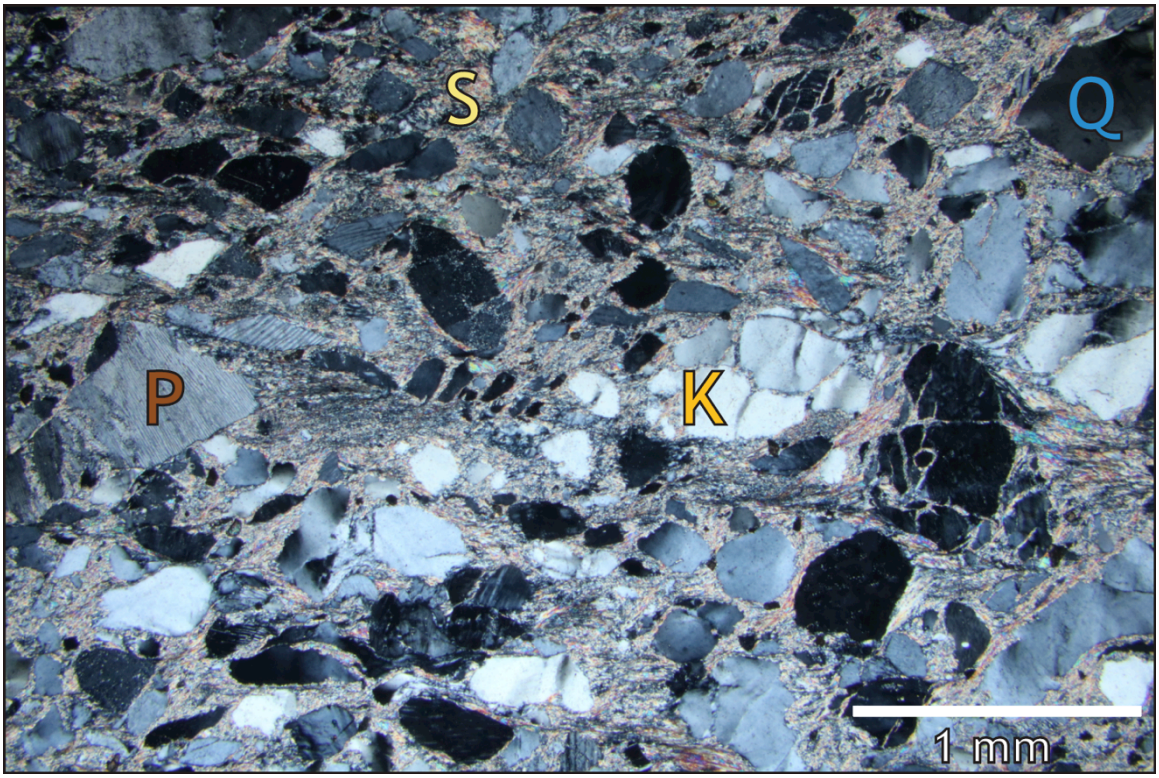

Figure 36f. *Feldspars are cracked by cataclastic processes that were helped along by the dissolution of feldspars.*

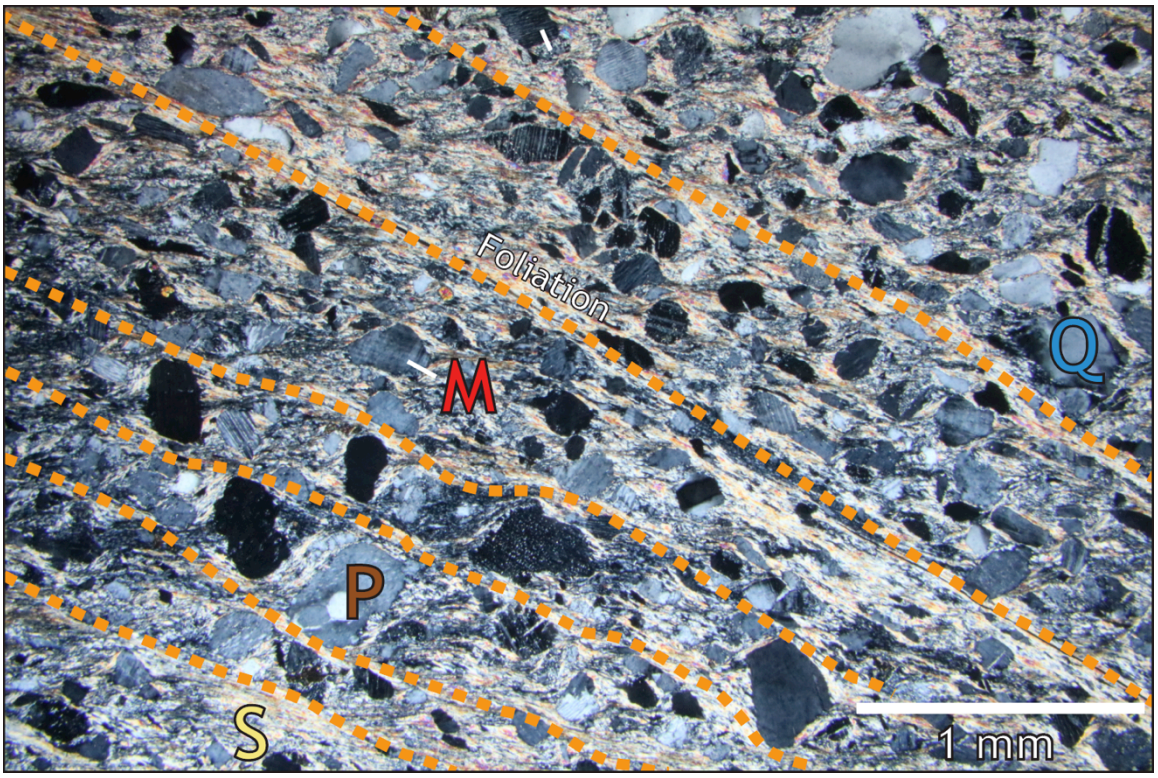

Figure 36g. *Penetrative foliation in a sericite (S) matrix.*

Exposed behind fallen layers of brick, the thin section from sample WP-10 was cut in order to show the character of the low angle shear zone, and is similar to what the typical fine-grained metabasalts look like in thin section (Figure 37a). Under the highest magnification, the fine-grained minerals are difficult to distinguish from one another. However, there are certain areas that have elongated chlorite blebs (Figure 37b) that began as amygdules in the basalt and are distinguishable when compared to the sericite and opaque minerals that make up the matrix. Within the areas that contain chlorite, epidote appears in a generally elongated form (Figure 37c). Two particular areas have large perthitic and feldspar grains that have been cracked and pulled apart from cataclastic mechanisms, compared to the fine-grained matrix (Figure 37d).

Figure 37a. *PPL Scan of the metabasalt thin section WP-10.*

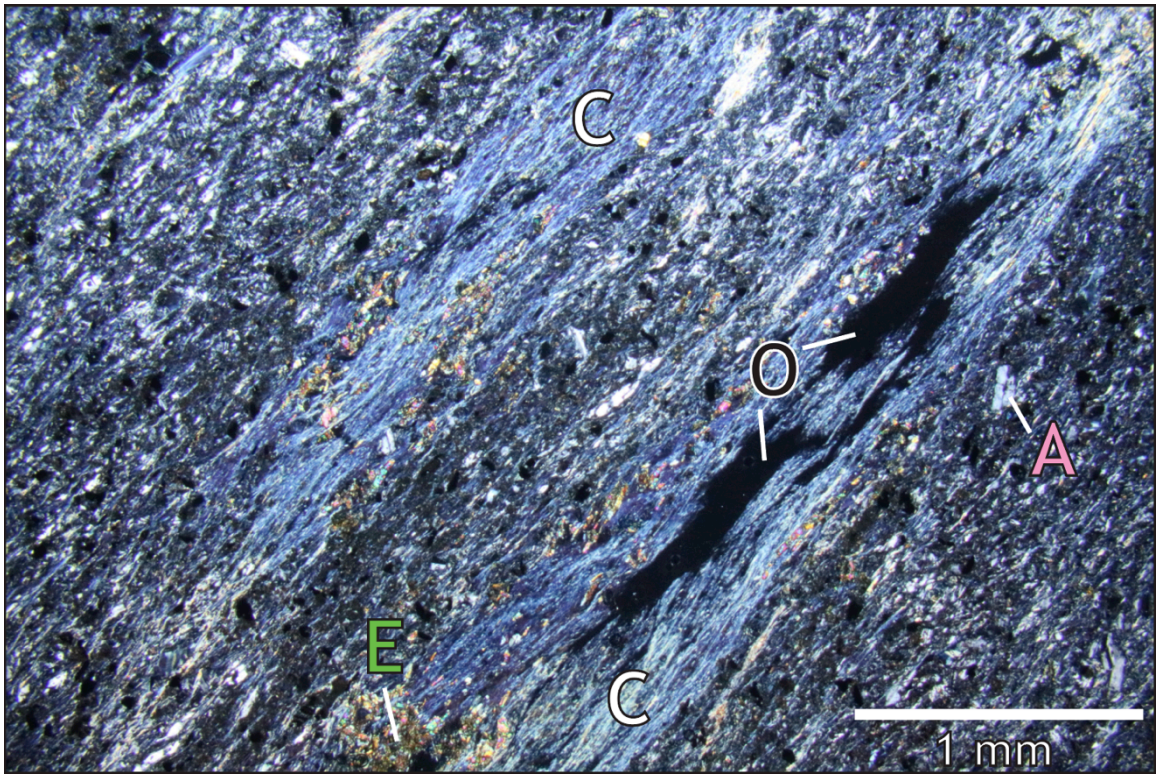

Figure 37b. *Elongated chlorite (C) and opaque grains (O) in the finer grained matrix.*

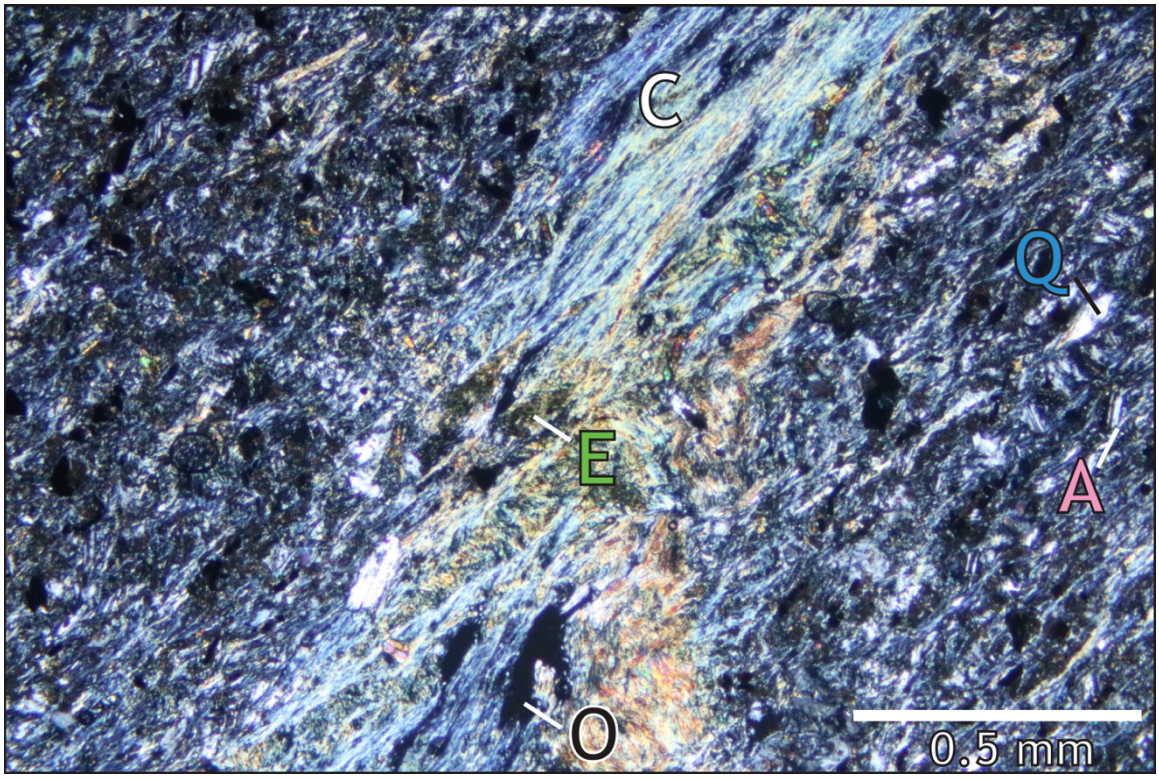

Figure 37c. *Epidote (E) within an elongated chlorite (C) bleb.*

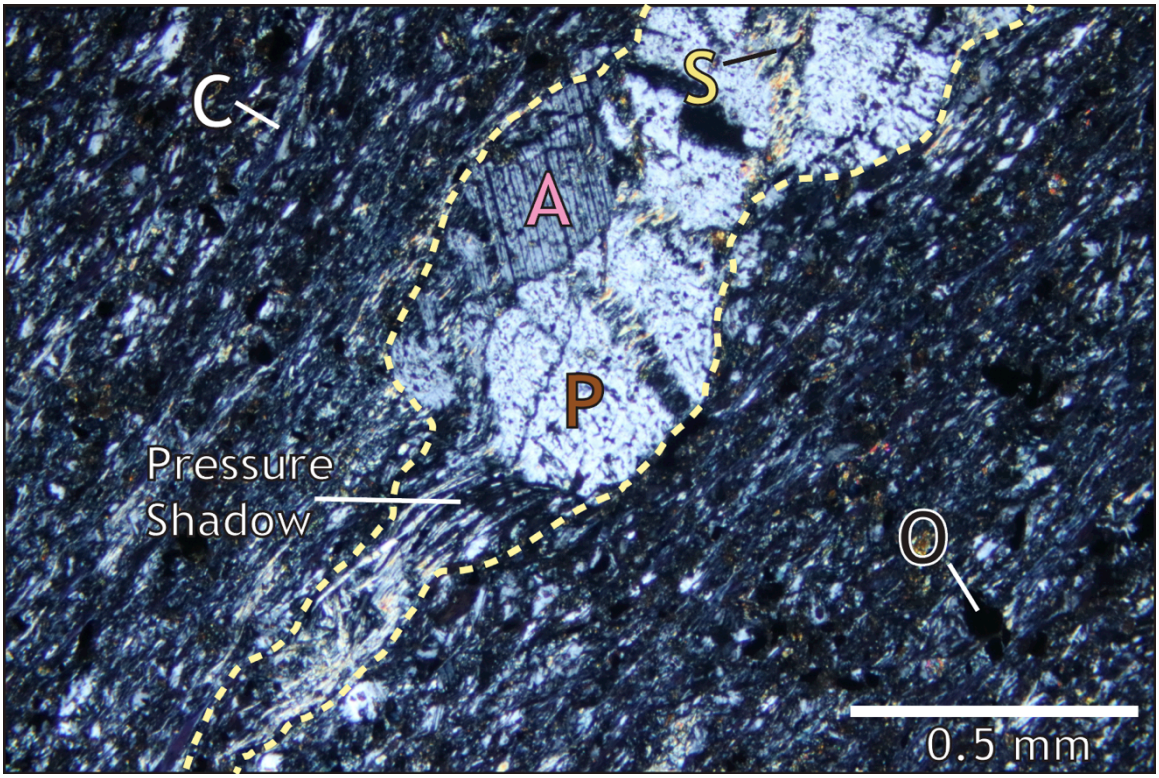

Figure 37d. *Pressure shadow around the large perthite (P) and albite (A) grain.*

Discussion (4)

Rocks (4.1)

The greenstones and metasedimentary units of the Catoctin Formation represent a series of flood basalts. Several lava flows were extruded upon the margin of Laurentia during the Ediacaran (570-550 Ma), while some were deposited subaqueously (Badger and Sinha, 1988; Aleinikoff et al., 1995; Southworth et al., 2009). In between the individual flow events, the sedimentary members of this formation were deposited and subsequently buried by other lava flows. Within the BRT and at Rockfish Gap, the rock types range from arkosic wackes, sandstones, conglomerates, phyllites, and metabasalts. Thus, the changing types of sedimentary sequences can lend insights into the development of different depositional environments (Dilliard et al., 1999). The variable differences seen from field observations and petrographic analysis corroborate that the sedimentary units researched in this study are likely dependent upon variations in effusive rate, clastic supply, and subsidence (Dilliard et al., 1999).

Dilliard et al. (1999) characterized the sedimentary members of the Catoctin Formation in one of two ways: channel elements (CE) and sheet elements (SE). The CE proposed by the Dilliard study were formed from the deposition of sediment into incised, isolated, river channels. CE are likely formed from a high rate of lava extrusion, low sediment supply, and higher subsidence rates. In contrast, the SE comprise the sedimentary unit within the Catoctin Formation and illustrates a change to decreasing effusive and subsistence rates with an increase in sediment supply (Dilliard et al., 1999). As such, these sedimentary CE and SE are good indicators of the conditions under which deposition of the sediments occurred. The isolated CE features are probably from short-term drainage systems, and Smith (1988) noted that

drainages can be reduced or moved by kilometers in comparatively short geologic time frames. With increasing subsidence rates, the paleochannels created more of these isolated CE incised into the underlying flood basalts.

For this study, the channel elements and sheet elements are of particular interest in the interpretation of the large asymmetric boudins in the Rockfish Gap area (Figure 28a-f). They are predominantly epidote-rich sandstone lenses in the metabasalts, and are either rather isolated or part of a complex network of boudin elements (Figure 28d). Typical CE data from Dilliard (1999) gives the average length of the channel being from 0.3 m to 1.1 m, whereas the channels discussed in Bartholomew (1977) are on the order of tens of meters. The idea that these boudinage elements started out at as channel or sheet elements is an intriguing one, in large part because it could help explain the convoluted morphology of the boudins that crop out in the BRT and at Rockfish Gap today.

The tectonic processes associated with greenschist facies metamorphism and ductile NW-directed deformation during the Neoacadian Orogeny likely helps explain how the sedimentary members of the Catoctin Formation become boudinaged. If the individual boudins within the BRT and at Rockfish Gap began in an irregular shape, like a CE, the complex geometry of the boudins are more readily explained. However, Dilliard's study did not address the idea that the exact structures they labeled as CE could potentially be the asymmetric boudinage features that are common inside the BRT and at the U.S. 250 road cut. Field observations of the boudins in the Rockfish Gap area confirm that the creation of the asymmetric features were contemporaneous with Neoacadian ductile deformation. The evidence that the epidote-rich sandstone lenses remained more competent than the surrounding greenstone matrix is seen in the outcrop as the main foliation is deflected around the boudins. Thus, the exact factors

that influence the geometry of the boudins remain enigmatic, but they were nonetheless deformed by the ductile, top-to-the-NW deformation.

While the Dilliard study discussed the stratigraphy in several sections at Rockfish Gap and nearby, their study failed to propose a provenance of the sediments. From observations in the field, the conglomerates have large clasts of blue quartz and feldspars. The most likely provenance of these minerals come from the granitic basement complex that was exposed at the surface during the formation of the Catoctin Formation in Ediacaran period (Figure 38).

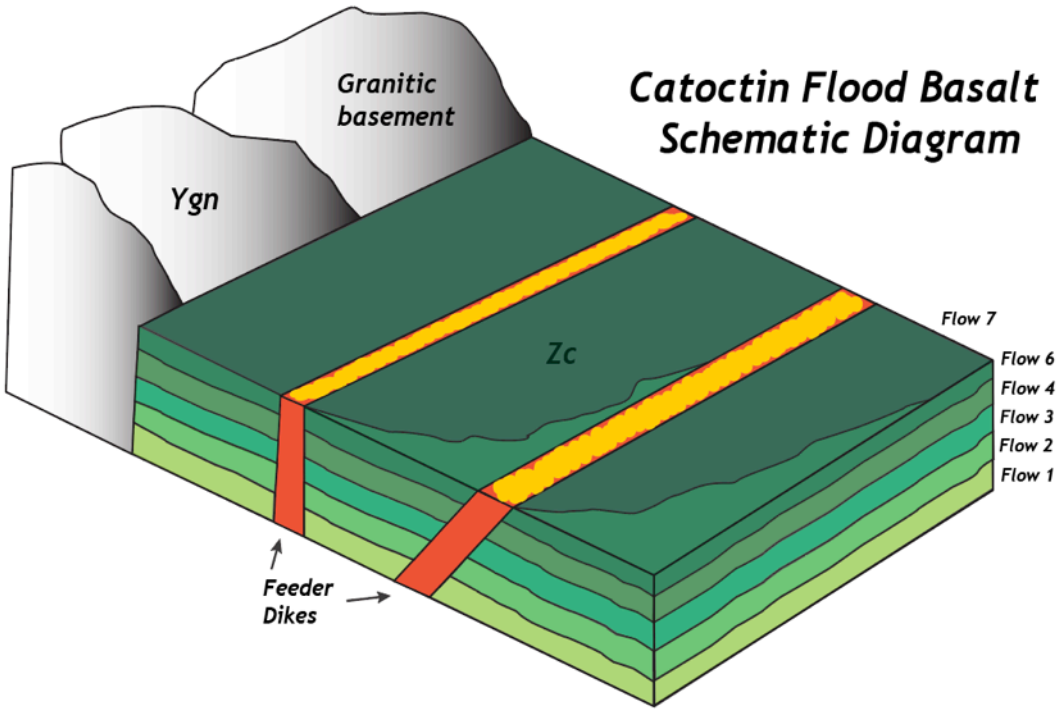

Figure 38. *The schematic block diagram illustrates how the flood basalts were extruded during the Ediacaran period. The red feeder dikes brought up the tholeiitic basalt to the surface and placed them upon the margin of Laurentia. As the granitic basement was eroded, the deposition of channel and sheet elements happened with basalt flow subsidence.*

The other curious sedimentary unit within the Catoctin Formation is the purple phyllite from sample 17KL-05 (Figure 21), which has been interpreted by previous Blue Ridge geologists to be a thin layer of meta-tuff, likely due to its characteristic purple color (Gathright et al., 1977; Dilliard et al., 1999). However, petrographic analysis did not confidently reveal a volcanic texture that a typical tuff displays. While this phyllite is very fine-grained, and purple- to brown in color, this rock has a large amount of hematite staining and opaque minerals. Thus, the presence of the Zct layer is dubious in this area, and deserves to be studied in greater detail to better understand the origin of this layer within the sedimentary sequence of the Catoctin Formation.

Ductile Features (4.2)

The most prominent feature of the Catoctin Formation besides the characteristic dark-green color is the schistose nature of the rock. Foliation dips moderately to the SE from this study and are similar to previous results in the Blue Ridge (Bailey et al., 2007; Mills et al., 2015; Bailey et al., 2017b). This feature was formed during greenschist facies metamorphism and Neoacadian deformation occurring from (345-320 Ma) (Evans, 1994; Wooten et al., 2005; Bailey et al., 2007). Chlorite elongation lineation aspect ratios were utilized to determine that the rocks at Rockfish Gap and in the BRT experienced apparent flattening strain, echoing what previous researchers in the Blue Ridge recorded in mylonites (Bailey et al., 1994; Bailey, 1995; Mills et al., 2015). The low angle shear zones in the metabasalts likely developed during the last stages of this regional metamorphism and deformation, as it differs slightly from the main foliation.

The rocks exposed in the BRT vary from the metabasalts on the eastern portal to the metasedimentary units that characterize the western entrance. The contacts

between the greenstone and the metasedimentary units in the Catoctin Formation are well exposed in the BRT which makes understanding the structure and localized fold pattern much easier to interpret. Modified from Gathright et al. (1977), Figure 39 illustrates the complexly folded nature of the Waynesboro east and west quadrangles. The Rockfish Gap area northwest of Afton is interpreted to be underlain by overturned limbs of the Catoctin Formation, which helps to support the overturned bedding measurements from inside the BRT and at the Rockfish Gap 250 exposure. This exposure illustrates the array of metasedimentary units in detail, allowing this study to interpret the position of the folds relative to stratigraphic indicators. However, the smaller, localized, folds within the Catoctin Formation at Rockfish Gap are dependent on the map's level of detail, and are unable to be mapped in full complexity. The folds verge to the NW and display close to isoclinal fold geometry, and is another record of top-to-the-NW ductile deformation from the Neoacadian orogeny.

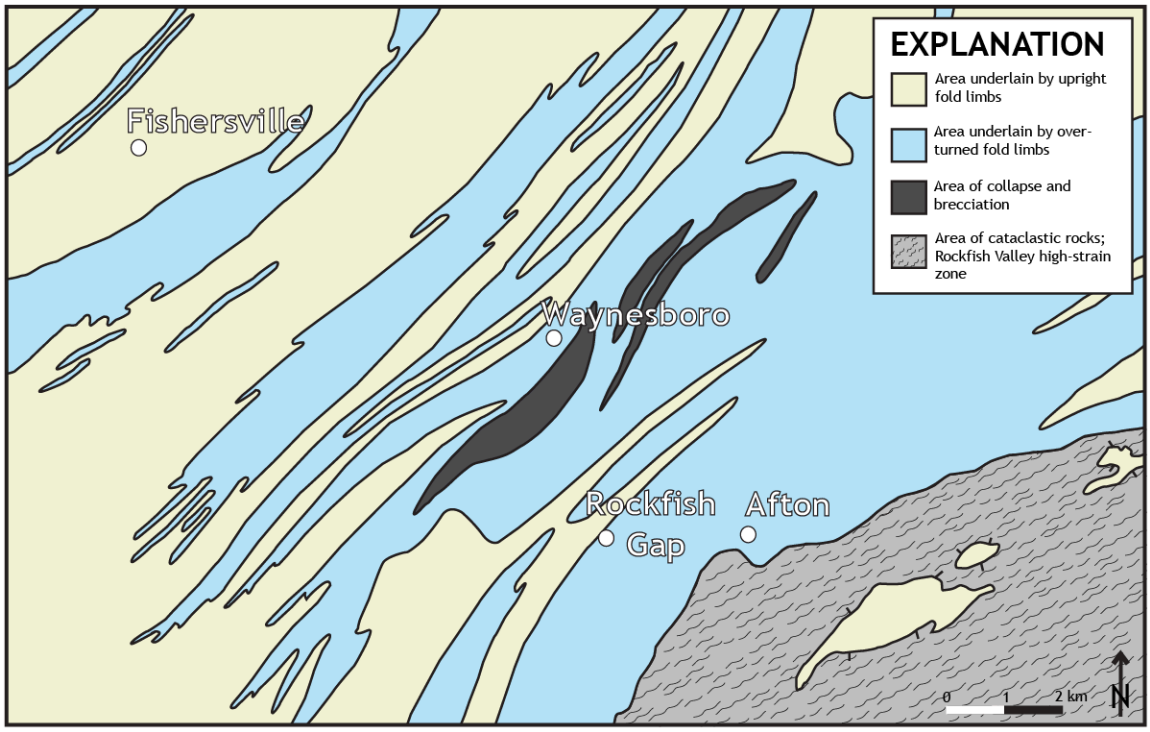

Figure 39. *Generalized structural map of Waynesboro East and Waynesboro West quadrangles illustrating the spatial distribution of overturned and upright fold limbs and areas of collapse and brecciation. Rockfish Gap is directly west of Afton, and is in interpreted to be in the overturned fold limb section. Modified after Gathright et al., (1977).*

Brittle Features (4.3)

When the Blue Ridge and Valley and Ridge province was being created, there was a NW-SE σ_1 oriented shortening during the late Alleghanian (Bailey et al., 2006; Gattuso et al., 2009; Jenkins and Bailey, 2011; Whitmeyer et al., 2015). The fracture measurements from this study strike at an average of 310º, which is at right angles to the fold axes of the Valley and Ridge and Blue Ridge provinces. As extensional fractures develop at right angles to the folds, these fractures from the study can be qualitatively identified as extensional in nature. Fracture measurements collected from Route 250 and near the BRT are associated with Atlantic rifting of Pangaea in the early Mesozoic (Bailey et al., 2006; Whitmeyer et al., 2015). However, the orientation of the dominant set has an approximate 40º range, and potentially could echo what others have suggested to be a record of 40º rotation of the principal stress direction during the late Triassic and Jurassic (Jenkins and Bailey, 2011; Cunningham et al., 2015).

A suite of basaltic magmas intruded the basement complex and the overlying sedimentary cover sequence during the Jurassic. The orientation of the diabase dikes typically strike from 330º-350º (Bailey et al., 2006; Bailey et al., 2017a). The Jurassic diabase dikes strike within a 20º separation to the dominant set of fracture measurements, but the orientations are not close enough to infer that the two features resulted from the same process.

Petrographic Analysis (4.4)

Petrographic analysis allowed this study to gather more details about the temperature, pressure, and metamorphic conditions the Catoctin Formation at Rockfish Gap endured. All four thin sections showed evidence for greenschist facies metamorphism, within 0the mineral assemblage of chlorite, actinolite, albite, epidote, quartz, perthitic feldspars, and opaque minerals (most commonly magnetite). The lack of the index mineral biotite suggests that the Catoctin Formation at Rockfish Gap did not experience temperatures of over 400ºC. Evidence for fluid flow and dissolution were apparent in the microstructures for each sample, illustrated by numerous stylolites and pressure shadows around larger grains. Pressure shadows typically display a top-to-the-NW sense of shear, which is consistent with mesoscale ductile deformation observations. With ductile shearing and fluid movement during metamorphism, the stylolites likely formed due to dissolution processes.

In sample 17BRT-2, the fibrous intrusions that cross cut the sample are antitaxial veins (Figure 37b). The fibers grow from the center outwards and can often include fluid inclusions due to hydrothermal activity within the rock upon formation (Passchier and Trouw, 1998). The fibers normally consist of material other than the "wall rock" or the material directly outside of the vein, which, in this case, would be the sericite matrix. The sharp bends can be attributed to a change in the instantaneous extension direction during progressive deformation or the change in orientation of the instantaneous stretching axes (ISA) with respect to the fabric in the wall rock (Passchier and Trouw, 1998). The veins of 17BRT-2 likely underwent minor changes to the ISA direction, thus resulting in areas of kinking within the veins (Figure 37c).

The development of veins and pressure shadows is closely associated with the circulation of fluids within a rock, and the sericite matrix is a further indication that

the Catoctin greenstones underwent hydrothermal alteration. From the lack of biotite in any of the samples collected for this study and other mineral assemblages characteristic of mid-greenschist facies metamorphism, the rocks did not reach temperatures over 400ºC during metamorphism. Dissolved species of potassium feldspar in aqueous solution must have percolated throughout the feldspathic arkoses during metamorphism and lead to the development of the antitaxial veins (Figure 40).

Bailey et al. (1994), Bailey (1995), and O'Brien and O'Hara (2008) researched the microstructures and variations in quartz and feldspar microstructures in relation to the solution of feldspar. In areas of the western Blue Ridge in North Carolina that experienced thrust and localized shear zones, feldspar undergoes grain-size reduction from cataclasis, followed by a chemical breakdown into sericite, chlorite, and epidote due to infiltration of a hydrothermal fluid. The critical reactions identified are:

1. $3K\text{-feldspar} + 2H^+ = \text{Muscovite} + 2K^+ + 6SiO_2$
2. $\text{K-Spar} + \text{Oligoclase} + 0.5H_2O + 3.5H^+ = \text{Epidote} + \text{Muscovite} + 11SiO_2 + 4Na^+$

Both cases are possible results from the series of deformation, metamorphism, and fluid flow the Catoctin Formation has experienced. Due to the large number of ions in aqueous solution from the feldspathic arkoses and arkosic wackes in the sedimentary units of the Catoctin Formation, the development of antitaxial veins, stylolites, and volume loss is not surprising considering the solution of feldspar.

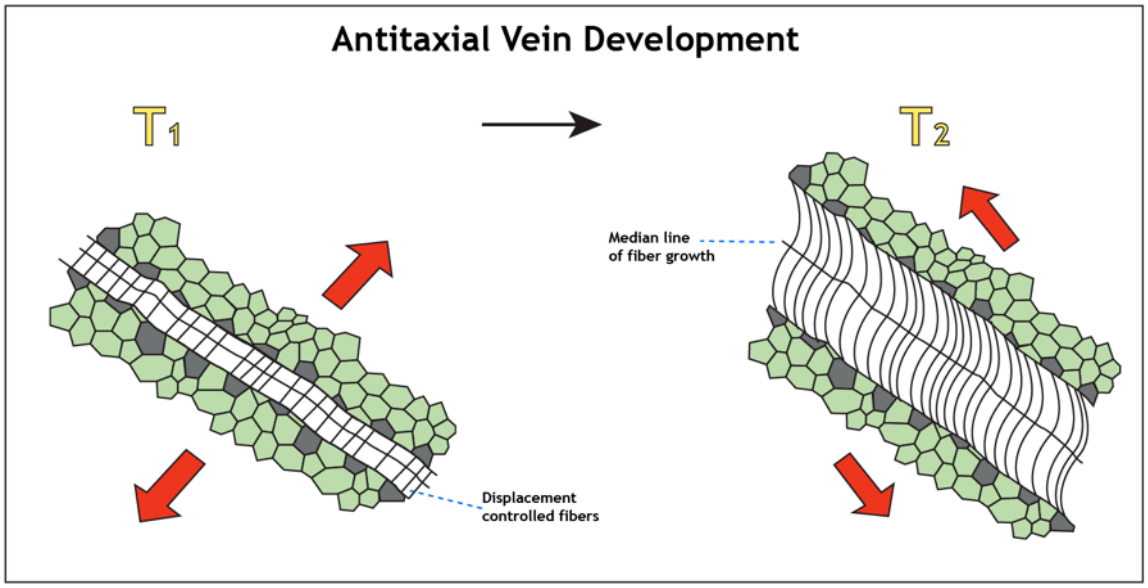

Figure 40. Diagram showing how antitaxial veins are developed. Yellow text and black arrow represents elapsed time, and the red arrows show the relative orientation of the instantaneous stretching axis (ISA) of the flow. The white areas are representative of fibers and the line down the middle illustrates the area from which vein growth begins. Modified from Passchier and Trouw (1998).

Overall Kinematic Interpretations (4.5)

The rocks at Rockfish Gap and the BRT include an array of both brittle and ductile features that record the kinematic history of deformation in the Catoctin Formation in this area. To summarize, the formation was created by the extrusion of the Catoctin basalts and the contemporaneous deposition of the sedimentary units onto the Laurentian margin during the Ediacaran period because of Neoproterozoic rifting of Rodinia. Then, the Catoctin Formation was immediately overlain by the Cambrian Chilhowee-rift to-drift siliciclastic units. The overburden upon the Catoctin Formation forced the rocks to reach depths of 10-12 km. Once buried at this depth, the formation experienced greenschist facies metamorphism and ductile top-to-the-NW directed deformation during the Paleozoic Neoacadian orogeny (Figure 41). This deformation and metamorphism created the penetrative foliation, low-angle shear zones, boudinage, and elongation lineations. A steeply dipping WNW-ESE fracture set developed within the rocks during the late Alleghanian orogeny after the Catoctin

Formation had cooled, and subsequently cut through the pre-existing ductile features. A less steeply dipping NE-SW fracture set developed during Atlantic rifting in the early Mesozoic. Finally, the Catoctin Formation was exhumed and eroded, and now makes up part of a current passive margin (Figure 42).

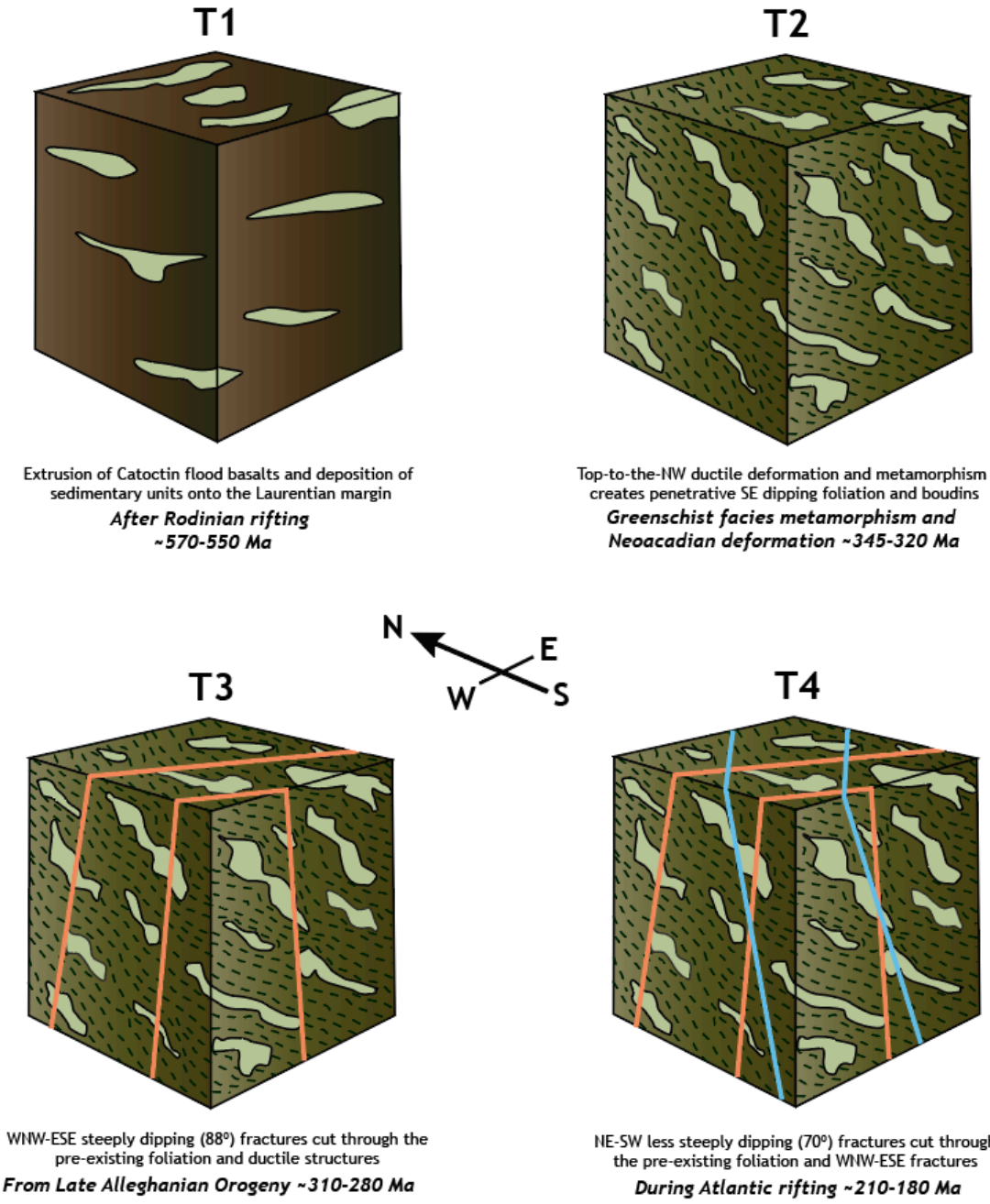

Figure 41. *Schematic block diagram of the Catoctin Formation kinematics in the Rockfish Gap area.*

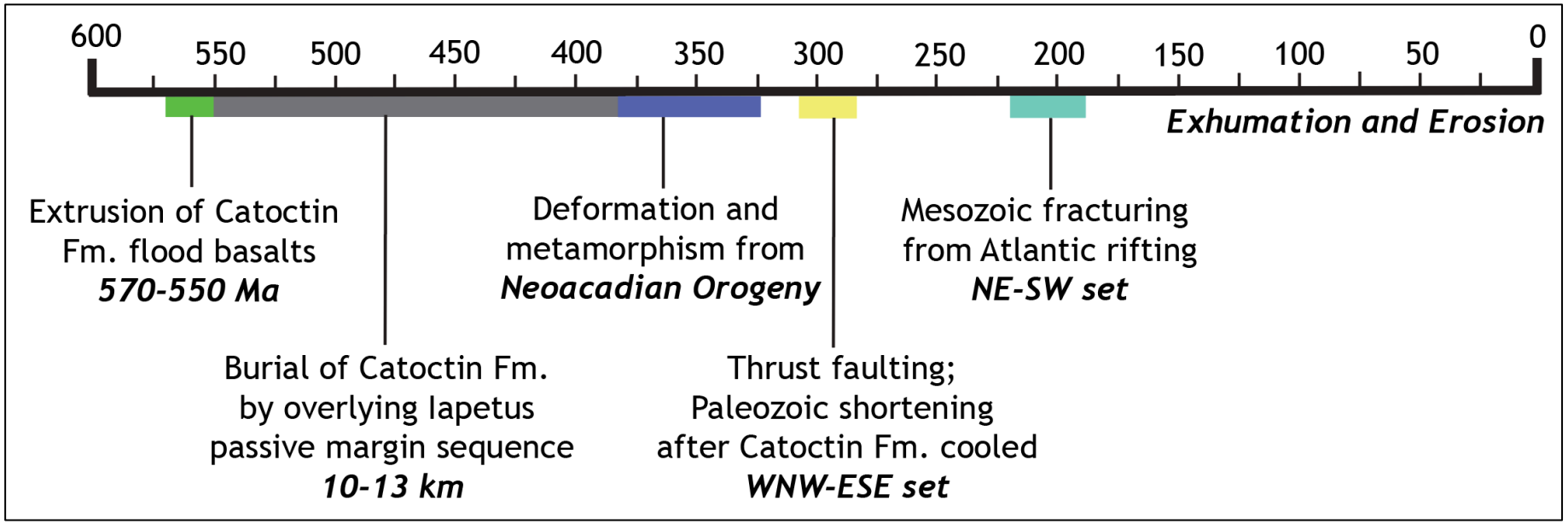

Figure 42. *Timeline of the deformation events of the Catoctin Formation since the extrusion of the unit in the Ediacaran to its exhumation and erosion.*

Structural Integrity and Future of the BRT (4.6)

The BRT's two portals are noticeably different in design, and is a function of the varied geology. The eastern portal is cut from the greenstone bedrock and is not faced or covered with brick (Figure 43). The western portal, on the other hand, is cut into predominantly metasedimentary rocks that are more likely prone to collapse than the denser metabasalts of the eastern portal. Due to this difference in geologic subunits, the rate of tunnel excavation progressed faster from the west than the east (Lyons, 2014). This is plausible as the harder, and more durable greenstone in the east was more difficult to excavate than the metasedimentary rocks in the west.

During construction, Crozet designed a system of brick arches to keep the less stable bedrock in the western part of the tunnel from collapsing. On the eastern portal, a probable test arch was created in order to cover faults and other unstable areas caused by the geology (Figure 44). Additionally, the metasedimentary bedrock of the western portal is faced with blocks of limestone likely quarried in the nearby Shenandoah Valley (Figure 45). Originally, a plinth inscribed with the commencement date and the board of directors' names was placed above the western portal to honor the construction of the BRT; it now resides at Virginia Military Institute.

Although the tunnel is 160 years old, it remains remarkably intact. There is little evidence for rock fall inside the tunnel and only a small percentage of Crozet's original brickwork has collapsed. The structural integrity of the BRT is a function of the durable bedrock of the Catoctin Formation and Crozet's shrewd engineering capabilities. As the BRT is restored, it makes little sense to shotcrete the tunnel interior. By covering the exceptional exposure of rocks within the BRT with a layer of gray concrete, a wealth of geologic information and history will be lost to modern construction. A main goal of this study is to not only advocate for the use of the BRT

in future studies of the Catoctin Formation, but also to preserve the geology within the Blue Ridge Tunnel walls.

Figure 43. *The eastern portal entrance is cut directly into the Catoctin metabasalt bedrock and has little to no evidence of rockfall or structural instability. Note that the tunnel has a roughly elliptical shape, which has lendt itself to remaining intact for about 160 years.*

Figure 44. *The probable test arch from the eastern side of the Blue Ridge Tunnel.*

Figure 45. *Cambrian-Ordovician limestone from the rock facing over the western portal of the BRT.*

Future Work (5)

Due to the impending construction of the BRT into a public trail, future work may prove to be very hard to accomplish. However, if the BRT walls are not covered in concrete and the tunnel is open to the public, a more detailed geologic map of the BRT could be produced. Several other samples from the sedimentary units at Rockfish Gap and the BRT collected from this study were not prepared for thin section analysis due to time constraints, so more petrographic analyses could provide useful information. An in-depth analysis of the intricate kinematics of the boudins could include dilatation measurements, volume loss calculations, and vorticity estimates. More sets of aspect ratios from greenstone samples will further constrain the amount and type of strain the Catoctin Formation experienced. On the eastern portal side, groundwater rapidly gushes out of a fault zone. It would be of value to research the recurrence interval of the water and perform other geochemical tests on groundwater quality. Lastly, the engineering plans of the BRT labels an area close to the western portal as an archaeologically sensitive area; it would thus be useful to conduct an archaeological survey of this area in order to understand the human history of the BRT in addition to the geologic history, as well.

Conclusions (6)

The Catoctin Formation at Rockfish Gap and in the Blue Ridge Tunnel records a detailed history of tectonic kinematics in the region for the past 550 Ma. Although no previous geologic work has utilized the BRT as a study area, the Catoctin Formation near Rockfish Gap has been studied before (Gathright et al., 1977; Dilliard et al., 1999). The structural, kinematic, and petrographic data presented in this thesis

show that the rocks underwent greenschist facies metamorphism and NW-directed ductile deformation during the Neoacadian orogeny, as well as two episodes of brittle deformation. The first is a WNW-ESE set created by NW-SE Paleozoic contraction from the Alleghanian orogeny, likely requiring a 40º rotation of the principal stress direction. The second is a NE-SW set formed by the rifting apart of Pangaea and creation of the Atlantic ocean during the early Mesozoic. Petrographic analysis of the mineral assemblages pinned down that the rocks did not experience temperatures greater than 400ºC, but that feldspar and quartz deformed by cataclastic and crystal plastic mechanisms, respectively, in addition to other microtectonic processes at work. Furthermore, the interplay between geologic history and human history within a study site offers new insights into the coalescence of two distinct academic disciplines. This study argues that the Blue Ridge Tunnel is worth preserving, and covering up the tunnel walls with concrete would not only be disastrous to the structural integrity of the tunnel, but also a loss of an important geologic resource.

Acknowledgements (7)

I would like to start off by thanking my research advisor, Chuck Bailey, without whom I would not have been able to combine my passions for history and geology into a research project. From countless hours of field and laboratory instruction to the advanced structural geology classes, I would not have been able to finish the thesis without his help and dedication. I owe Chuck a thousand thanks for the opportunities he's given to me in the past few years as a geology student and his constant belief that I can do better than I thought possible.

The entirety of this research was funded by the William & Mary Roy R. Charles Center, and for that I owe a great deal of thanks. Undergraduate research is not always a priority at major institutions, and for that, I'm grateful to be in a community where undergraduate research is not only encouraged, but able to be made into a reality.

To the Blue Ridge Tunnel Foundation crew, and especially Bob Dombrowe, who allowed myself and others special access to the tunnel during Phase I and Phase II construction, thanks a million. Bob's wealth of knowledge and passion for the BRT was absolutely essential to my historic understanding of the tunnel, and the tours he led were always a highlight of fieldwork

I also owe a lifetime of thanks towards the William and Mary geology department as well as my fellow geowallies. Many late nights and early mornings have been made all the better knowing that I have a supportive research community to learn and grow in is invaluable. I would particularly like to thank those in the structure research group: Mohini Jodhpurkar, Katie Valery, Lauren Visokay, Cece Hurtado, Mark Simmonds, Aubrey Vaughn, Jason Nykcorzuk, and Richard Watson for field work, lab lectures, and overall encouragement. I'd also like to thank everyone on the

William & Mary campus who supported my love of geology even if they didn't quite understand it. Lastly, I'd like to thank my parents who always believed in me when I didn't, and all of the people I haven't mentioned for taking the time to listen to me talk about "that old tunnel with the boudins."

References

Aleinikoff, J.N., Zartman, R.E., Walter, M., Rankin, D.W., Lyttle, P.T., and Burton, W.C., 1995, U-Pb ages of metarhyolites of the Catoctin and Mount Rogers Formation, Central and Southern Appalachians: evidence for two pulses of Iapetan rifting: American Journal of Science, v. 295, p. 428-454.

Badger, R.L., 1986, Stratigraphy of the Catoctin Volcanic Province, central Appalachians, in Harding, L.E., and Coney, P.J.j eds., A collection of papers honoring Brewster Baldwin: Middlebury College, p. 1-14.

Badger, R.L., and Sinha, A.K., 1988, Age and Sr isotopic signature of the Catoctin volcanic province: Implications for the subcrustal mantle evolution: Geology, v. 16, p. 692-695.

Badger, R.L., and Sinha, A.K., 2004, Geochemical stratigraphy and petrogenesis of the Catoctin volcanic province, central Appalachians, in Tollo, R.P., Corriveau L., McLelland, J., and Bartholomew, M.J., eds., Proterozoic Tectonic Evolution of the Grenville Orogen in North America: Geological Society of America Memoir 197, p. 435–458, doi:10.1130/0-8137-1197 -5.435.

Badger, R. L., Ashley, K. T., and Cousens, B. L., 2010, Stratigraphy and Geochemistry of the Catoctin volcanics: Implications for mantle evolution during the breakup of Rodinia, *in* Tollo, R.P., Bartholomew, M.J., Hibbard, J.P., and Karabinos, P.M., eds., from Rodinia to Pangea: The Lithotectonic Record of the Appalachian Region: Geological Society of America Memoir 206, p. 397-415.

Bailey, C. M. and Simpson, C., 1993, Extensional and contractional deformation in the Blue Ridge Province, Virginia: Geological Society of America Bulletin, v. 105, p. 411-422.

Bailey, C.M., Simpson, C., and De Paor, D.G., 1994, Volume loss and tectonic flattening strain in granitic mylonites from the Blue Ridge Province, central Appalachians: Journal of Structural Geology, v. 16, p. 1403-1416.

Bailey, C.M., 1995, Heterogeneous strain in granitic mylonites from the Rockfish Valley fault zone, central Virginia: Journal of Geodynamics, v. 19, no. 3/4, p. 177-194.

Bailey, C.M., Southworth, S., and Tollo, R.P., 2006, Tectonic History of the Blue Ridge, north-central Virginia: in Pazzaglia, F. J., ed, Excursions in Geology and History: Field Trips in the Middle Atlantic States, Geological Society of America Field Guide 8, p. 113-134.

Bailey, C.M., Kunk, M.J., Southworth, S., and Wooten, K.M., 2007, Late Paleozoic orogenesis in the Virginia Blue Ridge and Piedmont: A view from the South: Geological Society of America Abstracts with Programs, v. 39, no. 1, p. 80.

Bailey, C. M., Spears, A. V., and Marshall, A., 2017a, From Laurentia to Iapetus: Traversing the Blue Ridge–Piedmont terrane boundary in Central Virginia: in Bailey, C.M., and Jaye, S., eds., From the Blue Ridge to the Beach: Geological Field Excursions across Virginia: Geological Society of America Field Guide 47, p. 59–75.

Bailey, C.M., Flansburg, M.E., Lang, K.E., and Biggs, T. H, 2017b, The Geology of Jefferson's Country: A Blue Ridge traverse across Albermarle County, Virginia: Virginia Geological Field Conference Guide, v. 47, 58 p.

Bartholomew, M.J., 1977, Geology of the Greenfield and Sherando Quadrangles, Virginia: Virginia Division of Mineral Resources Publication 4, 43 p.

Blue Ridge Tunnel Foundation, 2017, http://blueridgetunnel.org (accessed November 2017).

Burton, W.C., Kunk, M.J., Bailey, C.M., McAleer, R.J., and Spears, D.B., 2015, Correlating terranes and thermotectonic histories of central Virginia and northern Virginia and Maryland, USA: Geological Society of America Abstracts with Programs, v. 47, no. 7, p. 225.

Cloos, E., 1971, Microtectonics: Johns Hopkins University Press, Baltimore, 234 p.

Cunningham, V.F., Spears, A.V., Mills, C.M., and Bailey, C.M., 2015, Kinematic history of ductile and brittle deformation at the Blue Ridge– Piedmont boundary, central Virginia: Geological Society of America Abstracts with Programs, v. 47, no. 7, p. 146.

Dilliard, K.A., Simpson E.L., Noto R.C., Wizevich M., 1999, Characterization of fluvial deposits interbedded with flood basalts, Neoproterozoic Catoctin Formation, Central Appalachians, USA: Precambrian Research, v. 97, no. 1, p. 115-134.

Espenshade, G. H., 1986, Geology of the Marshall quadrangle, Fauquier County, Virginia: U. S. Geological Survey Bulletin 1560, p. 60.

Evans, M.A., 1989, Structural geometry and evolution of foreland thrust systems, northern Virginia: Geological Society of America Bulletin, v. 101, p. 339-354.

Evans, N.H., 1994, Geology of the Simeon Quadrangle, Virginia: Virginia Division of Mineral Resources Publication 134, scale 1:24,000.

Gathright, T.M., II, 1976, Geology of the Shenandoah National Park, Virginia: Virginia Division of Mineral Resources Bulletin 86, p. 93.

Gathright, T.M., II, Henika, W.S., and Sullivan, J.L., III, 1977, Geology of the Waynesboro East and Waynesboro West Quadrangles, Virginia: Virginia Division of Mineral Resources Publication 3, 53 p.

Gattuso, A.P., Bailey, C.M., and Kunk, M.J., 2009, Stratigraphy, structural geometry, and deformation history of the Neoproterozoic Swift Run Formation, central

Virginia Blue Ridge: Geological Society of America Abstracts with Programs, v. 41, n. 1, p. 20.

Jenkins, C.E., and Bailey, C.M., 2011, Kinematic and temporal history of brittle deformation in Shenandoah National Park, Blue Ridge Province, Virginia: Geological Society of America Abstracts with Programs, v. 43, no. 5, p. 296.

Jenkins, C.E., Bailey, C.M., and Kunk, M., 2012, Argon thermochronology in the central Virginia Blue Ridge and Piedmont: Geological Society of America Abstracts with Programs, v. 44, no. 4, p. 73.

Johnson, T.A., and Bailey, C.M., 2013, Glimpses of the Past: The Catoctin Formation: http://geology.wm.edu/bailey/CatoctinFormation.pdf (accessed November 2017).

Johnson, T. A, Owens, B. E, and Bailey, C.M., 2013, Geology of the Catoctin Formation in the Eastern Blue Ridge, Central Virginia; Stratigraphy, Geochemistry, and Petrogenesis: Geological Society of America Abstracts with Programs, v. 45, no. 2, p. 62.

Johnson, T.A., Bailey, C., Owens, B. E., and Jensen, A., 2014, The geology of the Catoctin Formation and possible associated metagabbros in the Eastern Blue Ridge, Central Virginia: Geological Society of America Abstracts with Programs, v. 46, no. 3, p. 85.

Keith, A., 1894, Geology of the Catoctin Belt: U.S. Geologic Survey, 14th Annual Report, part 2, p. 287-395.

King, P.B., 1950, Geology of the Elkton Area, Virginia: U.S. Geological Survey Professional Paper 230, 82 p.

Laskowski, A., Bailey, C.M., Nicholls, O., Garber, J., Knieser, B., Lederer, G., and Murray, L., 2009, The Sugar Hollow basin: A Neoproterozoic half graben complex in the central Virginia Blue Ridge: Geological Society of America Abstracts with Programs, v. 41, no. 1, p. 55.

Laskowski, A.K., 2010, 3D Restoration of the Sugar Hollow Rift Basin, Blue Ridge, Virginia: Undergraduate Honors Thesis, Paper 592, p. 51.

Lyons, M. E., 2014, The Blue Ridge Tunnel: A Remarkable Engineering Feat in Antebellum Virginia: Charleston, The History Press, 192 p.

Marshall, A.A., Owens, B.E., and Bailey, C.M., 2014, Mineralogy and geochemistry of alkaline ma c dikes in the Blue Ridge province of central Virginia: The product of early Neoproterozoic, pre-Iapetan rifting?: Geological Society of America Abstracts with Programs, v. 46, no. 3, p. 30.

Mills, C.M., Bailey, C.M., and Owens, B.E., 2015, Petrological and structural analysis of metavolcanic rocks in the eastern Blue Ridge and western Piedmont provinces, central Virginia: Geological Society of America Abstracts with Programs, v. 47, no. 2, p. 33.

O'Brien, T. M., and O'Hara, K., 2008, Microstructures and geochemical variations in phyllonites of the Meadow Fork fault Zone, western Blue Ridge, North Carolina: Geological Society of America Abstracts with Programs, v. 40, no. 6, p. 153.

Passchier, C. W., and Trouw, R.A.J., 1998, Microtectonics: Springer Press, Berlin, 289 p.

Ramsay, J.G., and Huber, M.I., 1983, The techniques of modern structural geology, 1: Strain Analysis: Academic Press, London.

Rankin, D.W., 1975, The Continental margin of Eastern North America in the Southern Appalachians: The Opening and Closing of the proto–Atlantic Ocean: American Journal of Science, v. 275-A, p. 298–336.

Reed, J.C., Jr., 1955, Catoctin Formation near Luray, Virginia: Geological Society of America Bulletin, v. 66, p. 871–896.

Reed Jr, J. C, and Clarke, J. W., 1989, Metamorphism and tectonics of Eastern and Central North America; Volume 3, Metabasalts and related rocks of the Blue Ridge Province; traces of Proterozoic rifting in Eastern North America: American Geophysical Union, Field Trip Guidebook T203, v. 3.

Simpson, E.L., and Eriksson, K.A., 1989, Sedimentology of the Unicoi Formation in southern and central Virginia: Evidence for Late Proterozoic to Early Cambrian rift-to-passive margin transition: Geological Society of America Bulletin, v. 101, p. 42–54, doi:10.1130/0016-7 606(1989)101<0042:SOTUFI>2.3.CO;2.

Sinha, A.K., and Zeitz, I., 1982, Geophysical and Geochemical evidence for a Hercynian magmatic arc, Maryland to Georgia: Geology, v. 10, p. 593-596.

Southworth, S., Aleinikoff, J.N., Bailey, C.M., Burton, W.C., Crider, E.A., Hackley, P.C., Smoot, J.P., and Tollo, R.P., 2009, Geologic map of the Shenandoah National Park region Virginia: U.S. Geological Survey Open-File Report 2009–1153, p. 96, 1 plate, scale 1:100,000.

Tollo, R.P., and Aleinikoff, J.N., 1996, Petrology and U-Pb geochronology of the Robertson River Igneous Suite, Blue Ridge province, Virginia: Evidence for multistage magmatism associated with an early episode of Laurentian rifting: American Journal of Science, v. 296, p. 1045–1090, doi:10.2475/ajs.296.9.1045.

Tollo, R.P.,Aleinikoff, J.N., Borduas, E.A., and Hackley, P.C., 2004, Petrologic and geochronologic evolution of the Grenville orogen, northern Blue Ridge province, Virginia, in Tollo, R.P., Corriveau L., McLelland, J., and Bartholomew, M.J., eds., Proterozoic Tectonic Evolution of the Grenville Orogen in North America: Geological Society of America Memoir 197, p 647–677, doi:10.1130/0-8137-1197-5.647.

Virginia Department of Historic Resources, 2016, Jackson's Valley Campaign W-162: http://dhr.virginia.gov/HistoricMarkers/ (accessed December 2017).

Whitmeyer, S.J., Bailey, C.M., and Spears, D.B., 2015, A billion years of deformation in the Central Appalachians; orogenic processes and products: Geological Society of America Field Guide, v. 50, p. 11-33.

Wooton, K.M., Bailey, C.M., and Kunk., M.J., 2005, The nature and timing of deformation in the Blue Ridge Province, Greene County,Virginia, Geological Society of America Abstracts with Programs, v. 37.